Design of Limb Cooling Tourniquet to Prevent Amputation due to Ischemia

Ketan Sunil Mhetre

A thesis

Submitted in partial fulfillment of the

requirements for the degree of

Master of Science in Mechanical Engineering

University of Washington

2019

Committee:

Ashley Emery

John Kramlich

Nathan Sniadecki

Shahram Aarabi

Program Authorized to Offer Degree:

Mechanical Engineering

University of Washington

Abstract

Design of Limb Cooling Tourniquet to Prevent Amputation due to Ischemia

Ketan Sunil Mhetre

Chair of Supervisory Committee:
Professor Ashley Emery,
Department of Mechanical Engineering

During a medevac response, tourniquets are often used as an effective device to mitigate blood loss in incidents involving serious injuries with bleeding. In emergent situations, often involving the transportation of the patient to a medical facility, the prevention of blood loss is prioritized by first responders. Thus, making the use of a tourniquet imperative. Although the device can prevent blood loss from the affected region, the process, however, leads to a deficiency in supplying oxygen which can often result in nerve and tissue damage. Several studies have shown that cooling the limb slows down the metabolism rate and might save a limb from possible amputation. This thesis discusses the process of developing a new limb cooling tourniquet, which consists of a cooling sleeve and an air splint coupled with a conventional tourniquet. To verify the efficiency of the newly developed cooling sleeve, a thermal phantom of a human leg was developed. Its performance was validated with the help of thermal simulation of human limb model. Animal limb cooling experiments were performed at Harborview Medical Center to study the effects of reduced blood flow and oxygen deficiency (ischemia) and the temperature profiles that were obtained as a result of this experiment were compared with the thermal simulation of an animal limb model and the simulations were validated.

Acknowledgments

I am eternally grateful to my advisor, Professor Ashley Emery. Who has been a great mentor, and I had the opportunity to learn a lot under his guidance. I would also like to thank the research group at the University of Washington Medical Center at Harborview, who performed the animal testing experiments. Dr. Shahram Aarabi, the clinical mentor who has been of tremendous help in filling the gap between the engineering and medical side of the project. I would also like to thank the Department of Defence, who sponsored the project under the grant under the name 'Therapeutic Limb Cooling to Prevent Amputation in pDCR ft' (Contract number XWH-17-1-0693), without their sponsorship this project would not be possible. I would like to thank Professor Kramlich and Professor Sniadecki of my committee. Finally, my friends and family who have provided me with their constant support, I am eternally grateful.

Dedication

I dedicate this thesis to my mother, father, and sister

for their constant support, endless encouragement

and for all the sacrifices they have selflessly made to give me the opportunity to achieve my dreams.

List of Figures

List of Tables

Table of Contents

Chapter 1: Introduction

In emergent situations, where blood loss is present, the time of arrival to a medical facility is a critical factor which often determines whether a patient is able to make a complete recovery. The prevention of blood loss is prioritized by first responders in an effort to prevent Hypovolemic Shock [1], often with the use of tourniquets. Hypovolemic shock is a condition categorized by the heart's inability to pump blood due to severe blood loss, often resulting in fatalities. Although the current design of tourniquets is not ideal, they are imperative in preventing hypovolemic shock. Tourniquets are straps that are tightly wound around a limb to stop blood from flowing to the limb, thus preventing blood loss. The concern around the use of tourniquets is often due to the unintended consequences after usage. The prevention of blood flow to a specific limb in an effort to stop blood loss also prevents the oxygen flow from reaching the limb often resulting in Ischemia. Tourniquet induced Ischemia [2] is a fairly common consequence of the use of this device, even short period usage is known to cause nerve damage [3]. Thus, making the arrival time to a medical facility of extreme importance in an effort to minimize the complications often caused by Ischemia and nerve damage. The duration which a tourniquet is applied on a limb is the major deciding factor whether limb will be amputated during recovery [4]. This condition is known as Acute Limb Ischemia (ALI). ALI is also induced by blood clots in major arteries and veins, causing a cut-off of blood flow to a limb. In both cases, lactate levels in the limb increase which accelerates the degradation of nerves and tissues as time passes. If nerve damage crosses a threshold, the need for an amputation becomes inevitable. Around 20,000 ALI caused amputations are reported in the USA alone every year[3]. Currently, the only known treatment for ALI is the restoration of blood flow by vascular surgeons. Consequently, making the reduction of damage before surgery crucial. Currently, there is no formal treatment plan to control damage caused by ALI [5].

However, there has been an informal consensus amongst medical professionals that Ischemic damage in the tissues can be contained by decreasing the temperature of tissues, this is essentially funded under the same principles that organ preservation is done. During transportation, organs are fully preserved until they reach their destination by cooling them. Similarly, several studies have proven that cooling can slow down the progression of ischemia including nerve damage in animals [6], [7]. However, applying freezing temperatures on human skin may leave frostbites [8]. Thus, cooling the limb would have to be done at a balanced temperature, optimized in such a way that it is not too cold to damage the skin, but cold enough to cool down the limb rapidly. A possible solution for this is to maximize the heat transfer between the skin and a cooling sleeve in an effort to cool the limb rapidly. Therefore, the development of a Limb Cooling Tourniquet (LCT) is necessary. The LCT can cut off the blood flow to prevent blood loss while preventing Acute Limb Ischemia therefore, decreasing the number of unnecessary amputations.

Chapter 2: Background

2.1 Arteries, Veins, and Nerves

Our body is a complex system composed of countless individual organ systems working in symphony to perform day to day functions. The blood flow through the body provides the necessary oxygen, nutrients and food, and energy source to the organs. The blood flow starts from the heart, where it is pumped and the blood pressure that is generated in the heart allows blood to travel to all parts of the body. The arteries are the blood vessels which carry oxygenated blood and veins are the blood vessels which carry deoxygenated blood. The flow of blood is a cycle that starts from the heart. Through arteries, the oxygenated blood is supplied to the various organs. The organs utilize oxygen and the blood which has no oxygen, and which carries carbon-di-oxide (CO_2) starts traveling back through the veins. The blood then goes to the lungs where CO_2 is released to and oxygen is absorbed from the air that is taken in by respiration. This fresh oxygenated blood goes back to the heart to be pumped again to the body. This cycle continues and it is very important that our body gets a constant blood supply to maintain the normal working of each organ. Any deviation from this cycle causes disorders and the need for immediate medical attention.

Similar to blood flow system, the nervous system is an important part of the body. The nervous system carries information to and from the brain. The central nervous system is located in the head, which includes the brain, eyes, and brainstem. The peripheral nervous system extends all over the body. The spinal cord runs all the way until the end of the torso and a network of nerves originates from the spinal cord.

The peripheral nervous system is consisting of two kinds of nerves, Somatic and Autonomic systems. Somatic nerves help us control voluntary organs. On the other hand, Autonomic nerves control involuntary systems like heart, digestive system, reproductive system. The peripheral

nervous system is roughly divided into 4 parts. Cervical nerves cover shoulder and hands. Thoracic nerves cover region starting from lungs and heart. Lumber nerves cover the region from digestive system till the end of the back. Sacral nerves start around the end of the back and they go all the way till the end of toes in legs.

Typically nerves running through limbs are centrally located in the cross-section, along with major blood vessels. Specifically, in legs and lower extremities, the sciatic nerve is a major nerve that innervates the region. It primarily connects calf muscles, knees and toes, and feet. The sciatic nerve runs quite closely and parallels to bones like the tibia in the lower extremity.

2.2 Energy cycles and Ischemia

Our body needs a constant supply of oxygen to be provided to each organ. With a continuous supply of oxygen from bloodstream, organs can perform a normal course through which they convert the energy obtained from food sources into *ATP*, *Adenosine Triphosphate* to provide energy to cells [9]. In the absence of oxygen, this cycle is operated in a slightly different pattern which generates *lactic acid* as a by-product. So, whenever we exercise or sprint and we need an extra boost in energy part of that energy comes from aerobic respiration where normal *ATP-ADP* cycle takes the place of utilizing the supply of oxygen, the extra energy is generated from the Cory cycle, characteristic of anaerobic respiration. In this process, *Glucose* gets converted into *Pyruvate* to give out *ATP*s and later it is converted to *lactate*. This process is efficient to give a sudden burst of energy, but downsides are that the *lactate* that is generated has to be removed from the site immediately [10]. After an intense workout, while we take rest, the *lactate* goes to the liver where it gets converted back to *glucose* [11]. The threshold of *lactate* level in blood is 4 mmol/liter and if it is exceeded the nerve and tissue damage accelerates [12], [13]. The condition where we do not get enough oxygen to an organ is termed “Ischemia”. In the ischemic condition, the organ performs anaerobic respiration for a longer duration and the recirculation of *lactate* does not happen. Thus, levels of *lactate* do exceed the threshold and start to cause tissue damage. There have been several studies which show how the concentration of various chemicals like *lactate* and *pyruvate* vary with time in an ischemic limb. A group of researchers from the Surgery department in Harbourview Medical Centre at the University of Washington is performing animal experiments (swine model) to understand the progression of ischemia in a limb of an animal. They are performing a series of experiments which will give us an idea of the effect of cooling on ALI as well. Thus, the development of this device goes hand in hand with the testing and updated design specifications that are provided from the medicine side of the project.

2.3 Acute Limb Ischemia

Acute Limb Ischemia (ALI) is a case where the blood perfusion to a specific limb suddenly decreases and causes permanent limb damage. Every year about 3 in 20,000 people suffer from this condition in united states alone [14]. Blood supply and nutrition to limb are suddenly cut off, due to Ischemia. The symptoms of ALI develop over the first few hours. The main symptoms are a pain, muscle weakness or paralysis, pale skin and even absence of a pulse in a limb. The main reason ALI causes damages is that it happens all of a sudden and the development of new blood vessels to compensate for decreased blood flow is not possible in such a short time. Often vascular surgeries are necessary to restore the blood flow in order to start the recovery of the limb or an organ. Depending on the time since the blood flow is cut off, this may or may not help recovery, because after it reaches a certain threshold of time the damage that takes place is permanent. Death rates and amputations caused by ALI are thus high. About 10-15% of patients undergo amputation after hospitalization even if surgeries are performed in an emergency situation and vascular structures are re-established. About 15-20% of patients die within one year after ALI inception because of conditions resulting from ALI and recovery [15], [16]. Thus, treatment of ALI is very critical and the first response to emergency plays a major role in deciding the wellbeing of the patient.

ALI can initiate because of various conditions. An acute thrombosis in an artery of a limb or embolism can induce ALI. It usually starts with previous vascular diseases. Usually, plaque starts building around major arteries and if this occurs, it suddenly triggers ALI [17]. The bypass grafts in previous surgeries can lead to thrombosis if clotting occurs at the surface of grafts [18]. On the other hand, an embolism can occur out of nowhere. It starts with some material flowing through the bloodstream like a blood clot traveling through blood vessels and it obstructs the flow. Patients with myocardial diseases can have embolisms that originate in the heart arteries, called arterial

embolisms. These can result in mild heart attacks if trapped in an artery, or cause ischemia if embolisms travel down to organs and blocks the blood vessels [17].

2.4 Tourniquet: Everything we need to know

The medivac response team responds to accidents and their primary aim is to make arrangements for transfer to the hospital and to minimize any effects of traumatic injuries. In accidents where patients are severely wounded, the first order of function is to stop the blood loss. If the wound is small, the natural clotting process starts immediately. But in the case where the wound is quite big, the bleeding does not stop on its own. If the bleeding continues the loss of blood may affect blood circulation and heart rhythm. Due to the loss in blood pressure and blood loss the heart has a problem pumping blood. This condition is known as Hypovolemic shock [1]. This condition definitely needs to be avoided and thus a tourniquet is applied to cut off blood flow towards the limb. The time is of extreme importance after the placement of the device. The blood loss is almost stopped with the tourniquet. But due to a disruption in oxygen flow, the limb starts to experience symptoms of ischemia.

Figure 1: Tourniquet attached on a limb [19]

There are several steps to put on tourniquet [20]. The first step is to remove the clothing and clean the part where a tourniquet is to be applied. Then, the tourniquet is to be placed on the limb at least 2 inches above the wound, and it is also made sure that it is not on a joint because applying a

tourniquet on joints may damage joint. The tourniquet is slid over the limb and placed in one place. Its strap is pulled tight and Velcro strap is strapped on. The next step is tightening the twist handle. It allows various levels of pressure and it is recommended to twist it until blood flow from wound stops. Then handle the is locked and the time is noted on the tourniquet [21]. Figure 1 depicts the application of tourniquet on a limb [19].

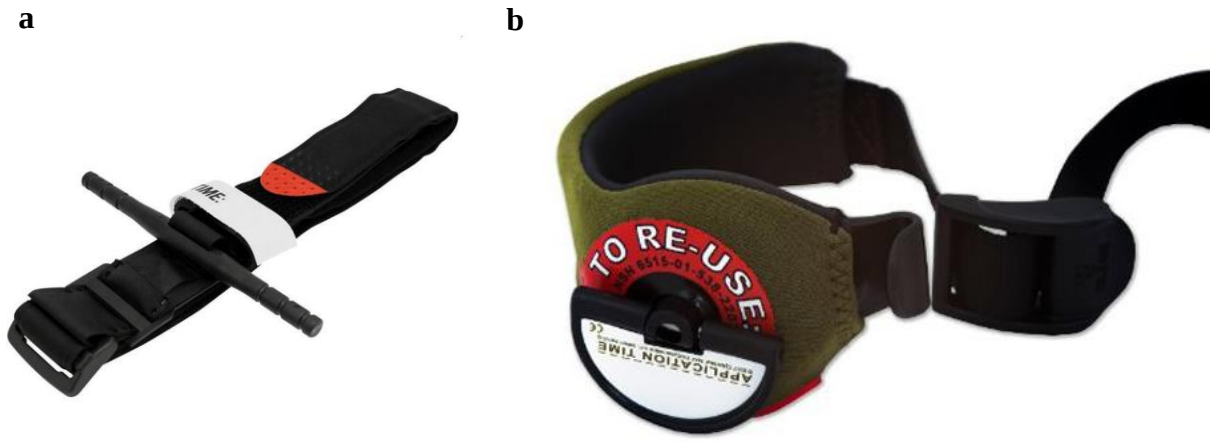

Figure 2: Pictures of: (a) CAT tourniquet; (b) MAT tourniquet [22]

Tourniquets come in various sizes and types [22], [23]. Military Emergency Tourniquet (MET) is lightweight and open-loop and has an aluminum windlass and comes with two breadth options. Second and most utilized type is Combat Application Tourniquet (CAT). (Figure 2a) It is closed-looped and it has one locking point for the windlass. We have Special Operations Force Tourniquets (SOF-T) which come with an alligator clip and metal windlass. Mechanical Advantage Tourniquet (MAT) consists of a C shaped cup which can be easily attached and removed. We need to fasten the strap properly before we tighten it. See Figure 2b. Apart from

these, we have Ratcheting Medical Tourniquet and Emergency Medical Tourniquet which has a pneumatic tightening mechanism.

Figure 3: Abdominal Tourniquet

Recently Abdominal Tourniquets [24] (Figure 3) have been developed. In the case of pelvic injuries, these can be effective because previously there was no way to stop bleeding in the pelvic region. For the Army personnel deployed in the field, they usually have tourniquets attached to their limbs and if wounding happens all they have to do is tighten the windlass. (Figure 4) [25]

Figure 4: CAT Tourniquet being used on field operation [25]

The main focus of this project is to design a device for personnel deployed in the field. And since CAT is used widely across various branches of an army, the device is designed with CAT as an integral part of it.

2.5 Tourniquet Induced Ischemia

It is a known fact that tourniquets are efficient at minimizing blood loss by preventing blood from going towards a limb. consequently, as soon as the blood is cut off the oxygen supply stops, and the limb starts progressing towards ischemia. Even if a tourniquet is used for a relatively short amount of time, the nerve and tissue damage is observed in the limb [3]. In emergent cases where treatment is received immediate the damage is minimal. In contrast, in most cases where the transportation time to a medical facility exceeds the one-hour mark, the patient suffers from some sort of nerve or muscle damage, which increases recovery time. Figure 5 depicts the effect of time on the health of the limb.

Figure 5: Timeline after the tourniquet is applied

As pictured above, 4 hours of tourniquet use causes permanent disability and 6 hours of tourniquet use will cause amputation of the limb. Thus, making the time of critical importance. Consider a soldier deployed in Afghanistan. If he gets wounded severely in the field, a tourniquet is put on him. The primary and secondary care inspect the condition of the limb and decide he needs surgery, but the tertiary care center where surgeries can be performed is in Germany. Even he is airlifted immediately and taken to Germany, the flight time is 6 hours and including his checkup and time

required for preparing the patient for flight total time reaches to 9-10 hours. So, this means saving a limb is very difficult as we can not reduce the time required for travel by any means. Thus, slowing down the progression of ischemia is the only way we can possibly save the limb.

2.6 The solution: Limb Cooling Tourniquet

Traditionally organs that are used for transplants are cooled for preservation at the time of transportation. It is a known fact that cooling slows down the metabolism rate in organs [26]. Even in the circumstances of toes cut accidentally from a limb are kept in icepack so that can be surgically be attached back to the limb. Using the above situations where cooling is used to keep an organ or part of the limb viable for hours, medical professional hypothesized about the use of cooling to prevent ischemia induced by the use of tourniquets. A group of researchers at Harborview Medical Center studying ischemia, are focused on its progression over time with various constraints on an animal limb model. The desired result of using animal experiments is to understand the effect of cooling on ischemia. It is theorized that if the core temperature of the limb reaches 5-10 °C, the symptoms of Ischemia will be prolonged and roughly doubling the time frame before amputation is necessary.

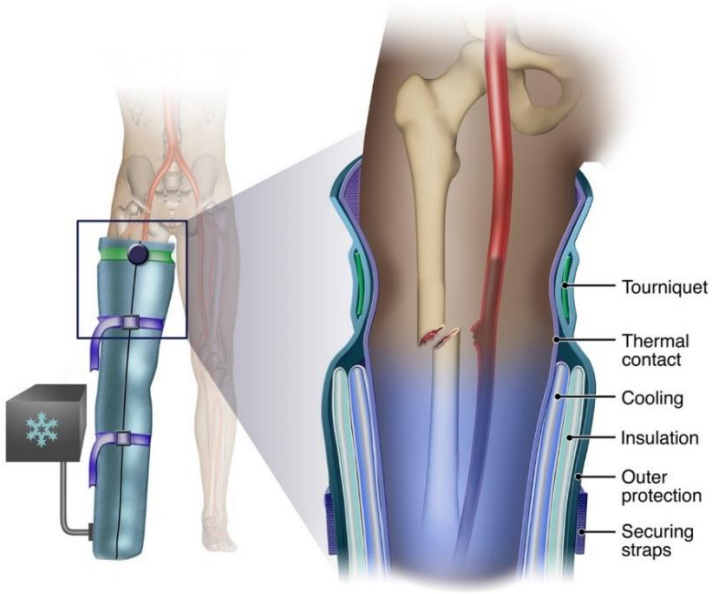

Figure 6: Limb Cooling Tourniquet

Figure 6 depicts the assembly of a Limb Cooling Tourniquet. The limb is first covered with a cooling sleeve which has a thermal gel which provides better adhesion between the skin to the

cooling pad surface it also serves to remove any air bubbles thus enhancing heat transfer. Outside the cooling sleeve, an air splint is located, which is crucial in case of compound fractures in order to keep the limb intact. Outside the whole assembly, there is nylon covering which serves to protect the air splint and the cooling sleeve from punctures. The cooling sleeve and air splint are attached to a chiller-cum air pressure regulation system. The umbilical cord has 3 tubes, coolant inlet, outlet, and air inlet. The chiller will continuously supply coolant which is cooled all the way to 0 °C and try to maintain the surface temperature at the skin-gel junction at the freezing point. The air pressure regulation system will be essential in maintaining constant pressure in the air splint accommodating to changes in temperature and elevation in the case a patient needs to be transported via air.

2.7 Scope of the thesis

The problem statement is broadly defined as to design a device that will prevent severe bleeding using tourniquet but will mitigate the unintended consequences. The device assembly is designed with components which take into consideration the need for maximum heat transfer between the limb and give structural support to the fractured limb.

The research done is mainly focused on the initial design of the product. involving, validating animal limb cooling experiments, and testing of the cooling sleeve with the help of thermal phantom. Also, guidelines about the power requirement of the chiller can be derived from simulations.

To test the heat transfer capacity of the cooling sleeve the thermal phantom of the human limb is designed which will mimic the thermal conductivity and the heat holding capacity of the limb. The thermal simulation model of a human limb is generated and compared with the results with a phantom to understand the loss of efficiencies and measure the efficacy of the phantom. The thermal simulation model of an animal limb was generated, and its results were compared with cooling experiments in Harborview Medical center.

2.7.1 Plan of work

The animal experiments were carried out at Harborview Medical Center. For developing the simulation model, it was planned to obtain the CT scan of an animal limb after the experiment.

To develop the human limb simulation model, it was planned to obtain human limb CTs from anonymized datasets from the University of Washington Medical Center.

For the development of human limb thermal phantom, the thermal conductivity tests were planned to establish a relationship between carbon percentage and thermal conductivity of silicone. After that experiment phantom was designed and manufactured.

2.8 Outline

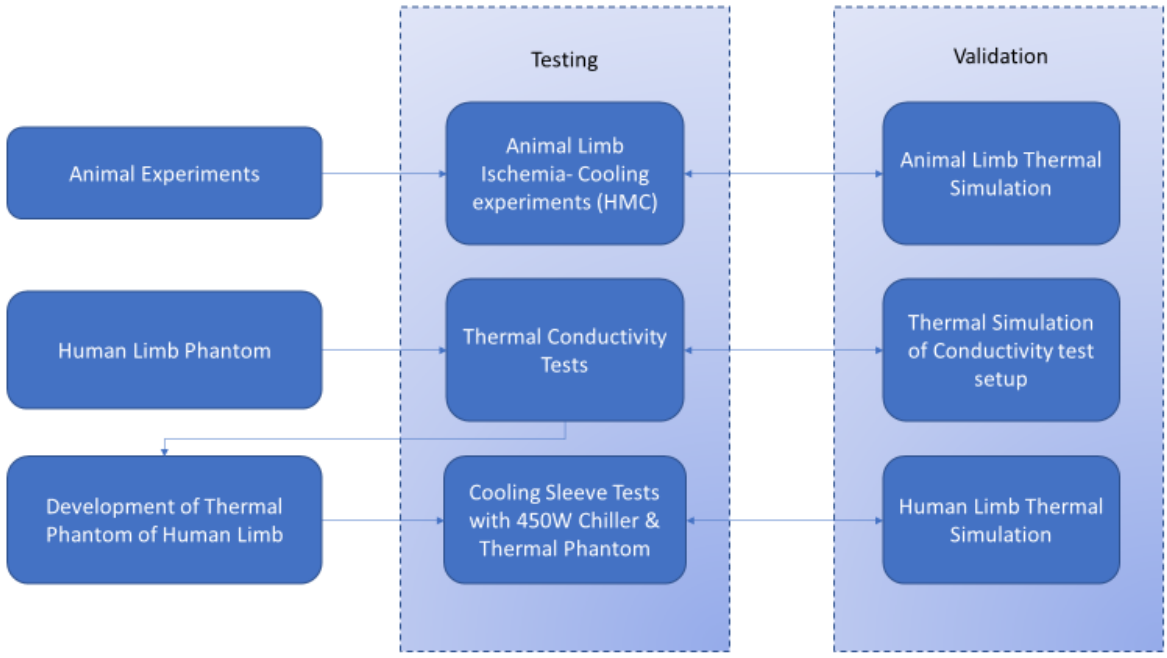

Figure 7: Outline of the Thesis

The Introduction and Background give an idea about the existing problem of induced Acute Limb Ischemia (ALI) because of tourniquet use. It also discusses the idea of limb cooling tourniquet.

The project can briefly be divided into two parts, animal testing, and human phantom and testing. Animal testing experiments are performing at Harborview Medical Center (HMC) which will give proof of concept that cooling affects Ischemic Progression. The animal limb simulation was performed to validate the cooling performance in animal limb cooled with an icepack. Animal limb simulation, animal experiments and the comparison between the two are further discussed in Chapter 3.

In Chapter 4, the human limb simulations are discussed, and it resulting in theoretical computations about temperature histories that can be obtained with various boundary conditions. It also discusses the power requirements of the chiller as guidelines to design chiller for the specific application.

Chapter 5 discusses the development of the human limb phantom. The thermal conductivity tests which helped to determine thermal properties of materials to be used in phantom are discussed in the same chapter. It also discusses tests performed to asses efficiency of the cooling sleeve and chiller using thermal phantom. It then compares the human limb simulation results with the thermal phantom.

Chapter 6 is a summary of the project itself along with recommendations regarding further work that needs to be done to consolidate this design further.

Chapter 3: Thermal Simulation of Animal Limb Model

3.1 Finite Element Method

The Finite Element Method (FEM) is an effective computational method to numerically solve problems which are governed by equations. It is versatile and can be used for problems of structural mechanics, heat transfer and fluid dynamics. Some problems that can be fit into given boundary conditions and theoretical solutions can be obtained by solving governing equations can be solved easily. But the problems involving abstract boundary conditions, problems which involve intricate geometries are hard to solve theoretically. In such conditions, a numerical method is the only way to go. Numerical methods approximate governing equations using schemes like Galerkin's method and the weighted residual method [27], [28]. These schemes convert differential equations into approximate numerical equations which are quite easy to compute. The Finite element method divides complex geometries into small elements which can be squares or triangles (2-D analysis) and cubes and tetrahedrons (3-D analysis). The numerical solutions are calculated for each of those small elements. This process can be computationally expensive, but with the significant increase in the capabilities of computers over the past few decades, FEM methods are becoming a more viable option for simulation of physical phenomena. Initially, it was used for validation of process but now FEM is an integral part of the design cycle as it allows us to predict the behavior of a particular component and cuts down multiple iterations of actual manufacturing. Thus, FEM methods are quite popular in industries.

The FEM method has few steps to solve a given problem. It is grouped into 3 main stages, called Pre-processing, Solution, and Post-Processing.

3.1.1 Pre-processing**:** Pre-processing is mainly defining the problem and setting the boundary conditions. The solid model is generated and is divided into elements, which is known as meshing.

The shape of the elements and the positions of nodes for each element are decided in this step. Once the elements are well defined, their properties are defined, e.g. stiffness for structural analysis, thermal properties for thermal of heat transfer analysis. Boundary conditions of a problem are defined at the end of this step.

3.1.2 Solution: In this step, the numerical method is chosen which will give the most accurate results while keeping computational demands as low as possible. The numerical equation as an approximation of the governing equation is formed using numerical schemes like Galerkin, weak-form Galerkin, least-squares, subdomain, collocation, etc. The stiffness matrix is generated which later can be solved for the quantity that is to be computed with given constraints and boundary conditions.

3.1.3 Post-processing: Once the computation is done, we have values of quantities of interest like temperature, displacement in each element and at each node. So, we can calculate remaining quantities of interest like forces, heat flux across each element. Once all the quantities are computed, we come to the visualization part. The computed quantities are displayed and plots such as contour plots, plots showing transient behaviors of quantities, such as temperature history of a particular point of interest. And later conclusions are drawn from these visualizations.

Usually, commercially available software suits like ANSYS come with the integration of all three stages, but we can also choose to treat each step separately. Commercial software like Hyperworks gives more control over meshing in terms of mesh region refinements. COMSOL is a good solver and provides Multiphysics capabilities where we can integrate thermal and structural problems. So, depending on the type of problem we have and various constraints, we can choose one option over another.

3.2 Governing Equation for Heat Transfer

Consider an object with transient temperature distribution π(x,y,z,t). Assuming isotropic conductivity, the heat equation can be written in 3-D coordinates as shown in

$$\left[\frac{\partial}{\partial x}\left(k\frac{\partial T}{\partial x}\right)+\frac{\partial}{\partial y}\left(k\frac{\partial T}{\partial y}\right)+\frac{\partial}{\partial z}\left(k\frac{\partial T}{\partial z}\right)\right]=-Q+\rho C_p\frac{\partial T}{\partial t} \qquad \textit{Equation 1}$$

Where k is isotropic conductivity and Q is the internal heat generation per unit volume.

In vector form, it can be written as

$$\nabla.(k\nabla T)=-Q+\rho C_p\frac{\partial T}{\partial t} \qquad \textit{Equation 2}$$

Where $\nabla=\hat{\imath}\frac{\partial}{\partial x}+\hat{\jmath}\frac{\partial}{\partial y}+\hat{k}\frac{\partial}{\partial z}$

Depending on boundary conditions, we can add heat flux on each face to the equation.

$$\nabla.(k\nabla T)+q_x+q_y+q_z=-Q+\rho C_p\frac{\partial T}{\partial t} \qquad \textit{Equation 3}$$

If the boundary is convective, we can modify the equation 4

$$\nabla.(k\nabla T)+q_c=-Q+\rho C_p\frac{\partial T}{\partial t} \qquad \textit{Equation 4}$$

Where $q_c=h_c(T-T_c)$,h_c is heat transfer coefficient, T_c is ambient temperature

The FEM method approximates these equations, and the process of approximation is known as discretization. It simply converts complex differential equations into algebraic equations. Usually, across multiple points, it is written down as a stiffness matrix and a vector which has boundary conditions. By solving the matrix equation, we get the values for the quantity of interest at each point.

3.3 Animal Limb Simulation

The group of researchers at Harborview Medical center are performing Ischemia study on swine. Animal studies will allow us to test the effect of cooling on ischemia. The cooling sleeve specifically designed for swine limbs will be tested in these tests. Cooling experiments have already been performed where ice packs have been used for cooling and temperature histories have been recorded. Thus, the FEM model of the animal limb can be used to perform thermal simulation where similar conditions can be imparted, and test results will be validated. Power requirements can be calculated from the thermal simulation.

3.3.1 Model Preparation

For an accurate representation of tissues in animal limb, e.g. muscle, bone, we need to have precise data about the composition of a limb. And since we can not know the percentages and locations of various tissues, we need medical imaging data. CT scan or MRI scan can be used for such purpose. MRI does a good job to identify soft tissues since it works on excitation of the water molecule. But it does not retain the bone structure well. On the other hand, the CT scan does a good job with bones. CT scan does give you 2-D slices made with each X-ray scans. Multiple X-rays are stacked and render a 3-D model. Each slice is stored in a way similar to the way a monochromatic picture will be stored. The image is divided into pixels and each pixel has grayscale value, which is set according to the density of tissue at a particular point from CT scan. Thus, when these slices stack up, each element is a cube, i.e. a volumetric pixel, also known as a voxel.

3.3.2 Simpleware [29]

All medical image viewers work with voxels to visualize the image that is captured from organs [30]. Simpleware is a commercial software suite, which is a voxel modeler. The medical images are usually stored in standard format also known as DICOM format. Simpleware takes all kinds of medical images, from CT scan to MRI images as input. It then generates a 3-D voxel model with each voxel having particular density value. Since different tissues have different density values on a CT scan, we can easily separate bones from muscles, fats, and skin. Using various density thresholds, we can generate various masks on the 3-D model which will then represent tissues like bones and skin. Simpleware can output STL files which can be 3-D printed.

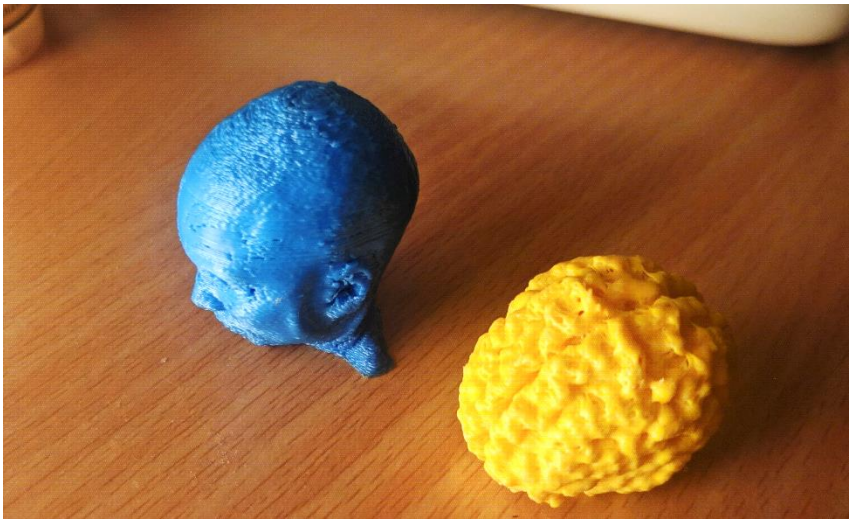

Figure 8: 3-D printed head and brain recovered from CT scan

Figure 8 depicts the 3-D printed objects that were recovered from the CT scan of a fetus. In such a way, we can recover any kind of information about the internal structure of any organ of a body from a CT scan. Simpleware also gives the option to export a mesh refined to our requirement for finite element programs like ANSYS, COMSOL or Abaqus. Since different masks like skin, bone, the muscle ware used when generating a Simpleware model, when the mesh file is imported to Ansys it generates different a part for each mask. Thus, we can assign different properties to each

of these parts, and the simulation model becomes quite accurate and behaves similarly to the actual animal limb.

Figure 9: Imported animal limb CT into simpleware

Figure 9 depicts an imported CT scan of an animal limb into Simpleware. Bones are highlighted as they have maximum density amongst all tissues in the CT scan. Five different masks named Bones, Fats, Nerve, Muscle, and Skin are generated in the model. Figure 10 shows a finished model with 5 masks which is ready to be exported to ANSYS input file in Simpleware interface.

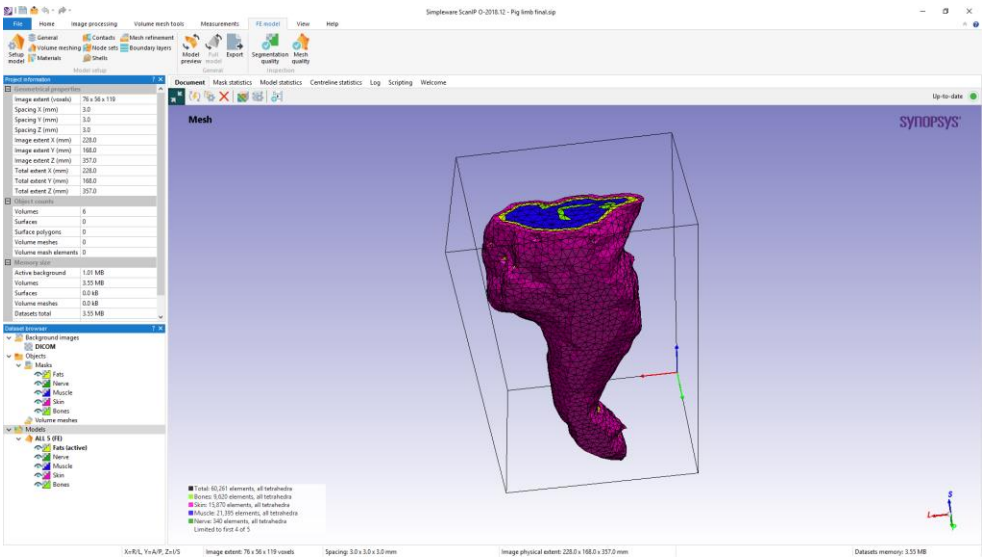

Figure 10: FEM mesh for a pig leg from 5 masks in Simpleware

When the mesh is finer, we tend to get more accurate results. But also, as we decrease element size and increase the number of nodes and elements the computation becomes more expensive. Thus, finding a balance between a fine enough mesh for an acceptable solution and still to be able to carry out the simulation the computational resources available is important. There are a total of 60,261 elements in the simulation model of the animal limb. Table 1 shows the number of elements in each mask.

Sr. no.	Mask	Number of elements
1	Bones	9,620
2	Fats	13,036
3	Muscle	21,395
4	Nerve	340
5	Skin	15,870
	Total	60,261

Table 1: Number of elements in masks

All elements are tetrahedral and linear. Export type is ANSYS Workbench Volume. It generates *.*inp* file which can be imported via external model option in ANSYS workbench. Each mask is given different thermal properties, i.e. specific heat, thermal conductivity and density[31], [32]. Table 2 shows the thermal properties used for each mask in the simulation.

Sr. no.	Mask	Density kg/m^3	Thermal Conductivity W/m.K	Specific Heat J/kg.K
1	Bones	1908	0.41	1313
2	Fats	911	0.317	2348
3	Muscle	1090	0.518	3421
4	Nerve	1075	0.49	3613
5	Skin	1109	0.209	3391

Table 2: Thermal properties for various tissues

Pre-processing and mesh generation is the same for all animal limb simulations. The boundary conditions and other settings will be discussed in detail in each simulation.

3.4 Steps for Simulation using Ansys

1. Model preparation: Generate input file for given model geometry from Simpleware.
2. Import the model into Ansys as an external model.
3. Share external model data with Ansys Thermal tab.
4. Add thermal data for various tissues to Engineering materials tab.
5. Open the Setup tab under Ansys Thermal.
6. Assign the material properties to various parts of the model.
7. Set the initial temperature.
8. Set the boundary conditions; for example, constant temperature boundaries, fixed heat flux or adiabatic boundaries.
9. Set the parameters for analysis, i.e. time steps, total physical time for simulation.
10. Check all the settings and solve.
11. After the solution, use post-processing tools provided in Ansys thermal to extract data like maximum and minimum temperatures at any points at a given time and heat fluxes of a given surface.
12. The extracted data can be exported into *.txt files which can be imported into programs like Matlab for visualization.

3.5 Animal limb simulation 1

Simulations are performed in ANSYS thermal transient analysis. Since we are dealing with thermal analysis, Ansys thermal is a better way to go with the simulation. If fluid flow is involved in the problem, Ansys Fluent is necessary. Figure 11a shows the imported mesh used by Ansys thermal.

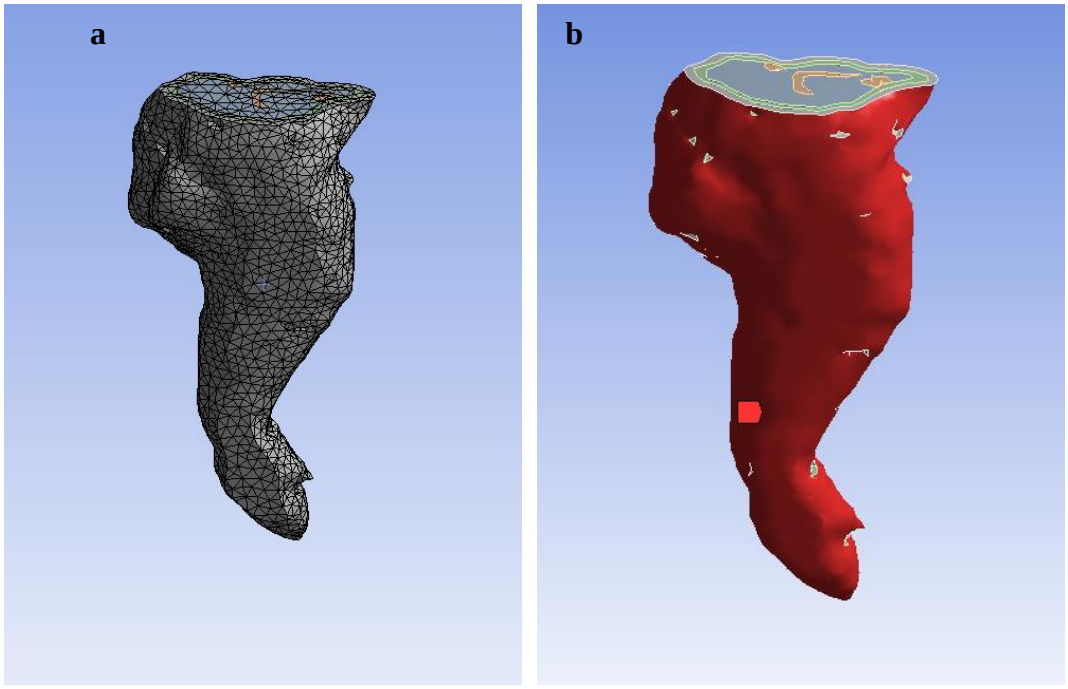

Figure 11: (a) Mesh imported to Ansys Thermal (b) Boundary conditions

In the first simulation, the limb is treated as an isolated entity. Thus, we have boundary condition near the thigh region as a no heat flow boundary, i.e. perfect insulation or an adiabatic boundary. The surface of the leg where the icepack was applied and the cooling sleeve will be in contact with has been given a constant temperature boundary condition of 0°C as depicted in Figure 11b. The simulation was carried out for 18,000 seconds (5 hrs) of physical time. The initial temperature of the limb was set to 35°C. Auto time-stepping, where substeps are chosen according to the requirement of the simulation was enabled and was program-controlled. There were total time steps specified where the calculation of temperatures was necessary. Initially, the size of the user-

defined time steps was small and it was increased gradually. The rest of the simulation settings are as given in Table 3.

Parameter	Setting
Simulation length	18000 s
Minimum time step	3.6 s
Maximum time step	360 s
Time Integration	On
Solver type	Program Controlled
Flux Convergence	0.0001
Maximum Iterations	1000
Solver Tolerance	0.1 W/m^2
Over Relaxation factor	0.1
Number of Physical Cores	4

Table 3: Simulation solver settings

The time elapsed for total simulation and post-processing the results requested was 1104 seconds. The result files were stored on local disk and the resulting file size was 8.9725 GB.

3.5.1 Results and Discussions

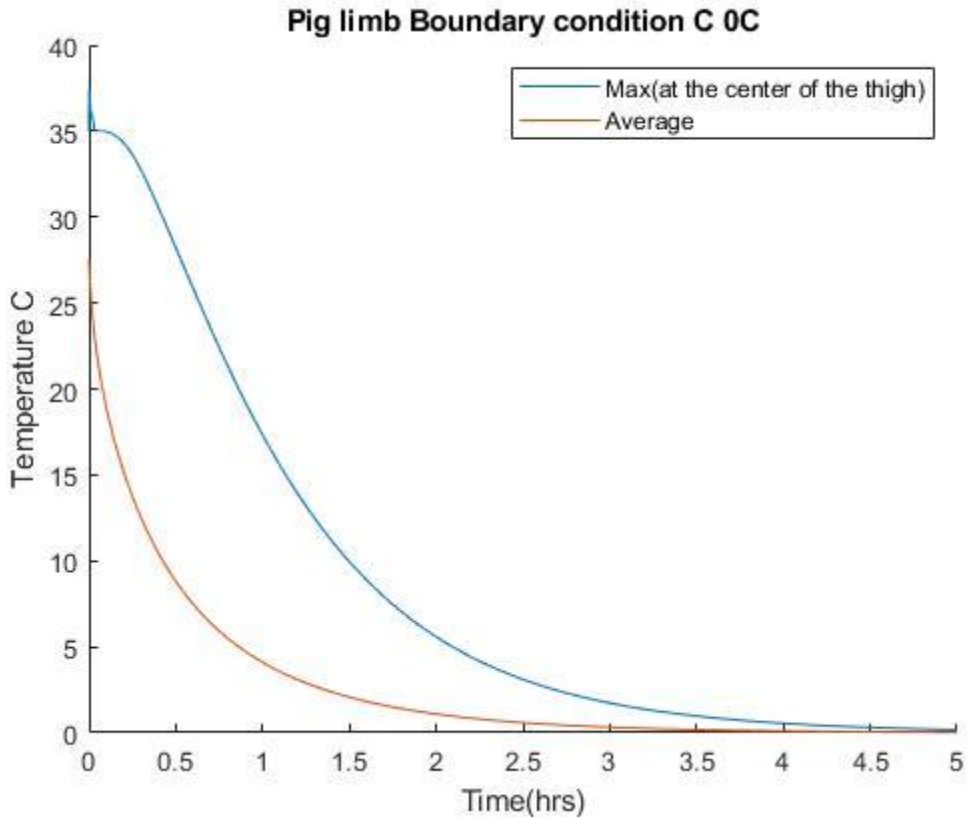

Figure 12: Average and maximum temperatures (at the center of the thigh) across time

Figure 12 depicts temperature histories from the first animal limb simulation. It plots average temperature across time and maximum local temperature of any point on the limb across time. The average temperature drops rapidly in the first half an hour, and later the variation becomes much lower than the initial temperature. The reason can be explained by varying heat transfer rates at the limb skin-cooling sleeve surface. Assuming the temperature of coolant remains constant at 0°C with a sufficiently powerful chiller unit, the surface temperature at the skin will be constant at 0°C. Initially, the temperature of the whole limb was 35°C and as time progresses, the limb starts cooling from the skin, slowly pulling heat from inside. As time passes an outer portion of the limb starts cooling, followed by inner portion at the limb. As visible from Figure 13 which shows temperature contours at t=837 s the elements next to the skin have reached temperature in a range

of 0-5°C while the temperature at core is still about 34°C. Thus, the outer surface of the limb cools down faster than the inner portion. But the heat transfer rate at the surface is driven by the temperature difference between the surface of the cooling sleeve and the temperature on the skin. So, as time passes, the rate of heat transfer decreases exponentially.

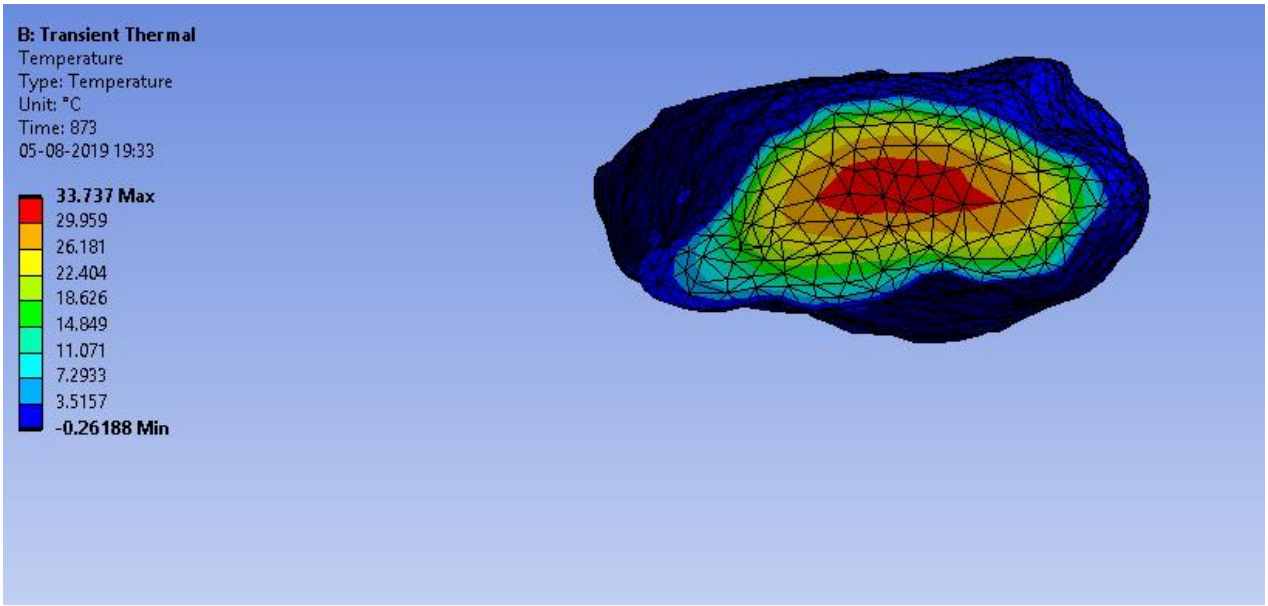

Figure 13: Temperature contours on the thigh cut of the limb at t=873s

It can be observed from the maximum temperature curve in Figure 12, for the initial few seconds, the maximum temperature in the limb does not change. It takes the time required for the heat to flow from the point of maximum temperature towards the surface. Thus, the maximum temperature curve has an initial plateau. The recommended cooling temperature range is 10-15°C. Maximum temperature reaches 15°C in 70 minutes from start. It reaches to 10 and 5°C in 90 and 125 minutes respectively. The average temperature reaches 15°C quite early in 12 minutes. It takes 26 and 52 minutes to reach 10 and 5°C respectively. About after 2 hours the gap between average and maximum temperature becomes sufficiently small, less than 5°C.

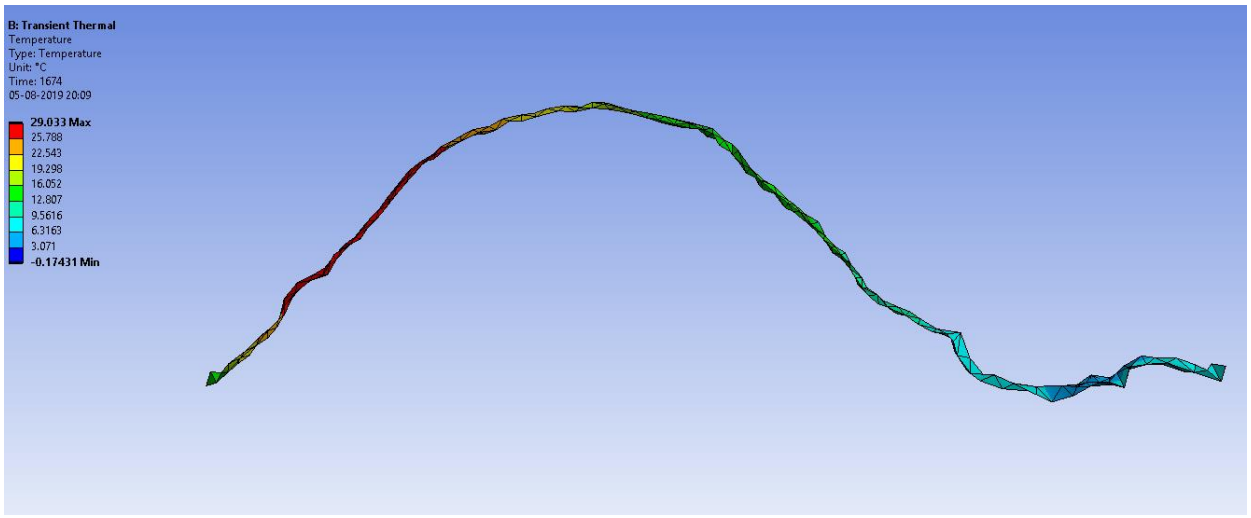

Figure 14: Temperature profile across nerve

Figure 14 depicts the temperature profile on the nerve at t=1674 seconds. The left side of the figure is towards the thigh, proximal to the cut near thigh and the right end is the distal part of the nerve. It can be observed that the nerve gets colder faster on the distal end and it takes more time to cool the proximal part. In fact, since the nerve is roughly located at the center of the limb, usually the point of the maximum temperature lies very close proximity to nerve if not on the nerve and is in the proximal region. It can be observed that the red region is at 29°C which is the maximum temperature at that time. And since preserving the nerve is the main objective of designing limb cooling device, studying nerve temperatures and in turn, studying maximum temperature regions is important.

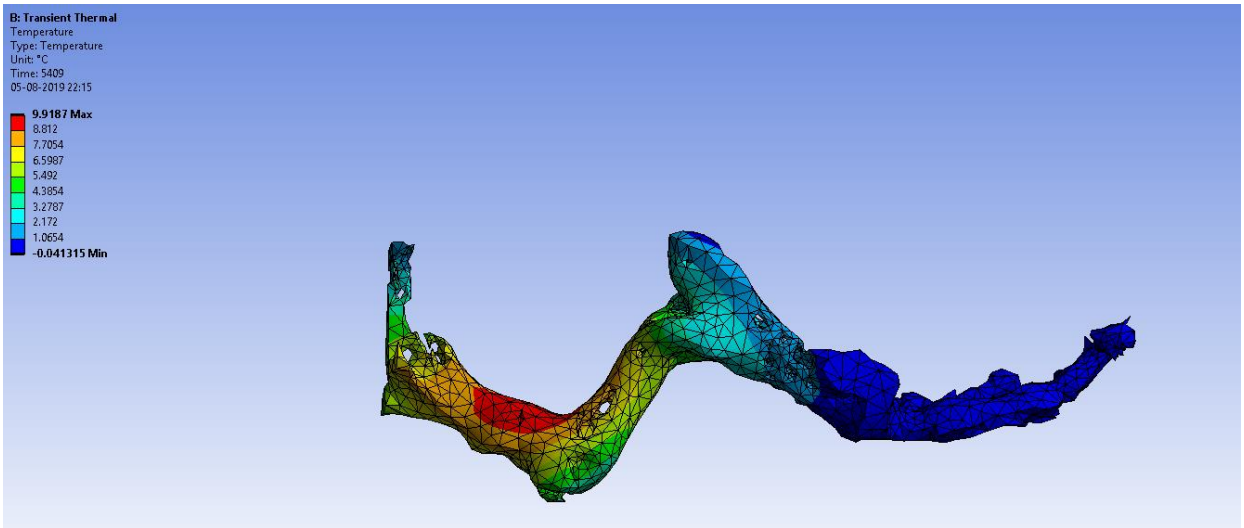

Figure 15: Temperature profile on bone after 90 minutes

Figure 15 depicts the temperature profile in the bones at t=5409 seconds (approximately 90 minutes). It can be observed that part of the limb below knee gets cooled almost up to freezing temperature (0°C) and the part above the knee is hotter since it is part of the thigh. This is the same time where the maximum temperature drops below 10°C. The reason that this part of the limb cools slower is that the thighs are thicker and have more muscle mass and fat mass, and this increases the heat holding capacity of the part of the limb above the knee.

3.6 Animal limb simulation 2

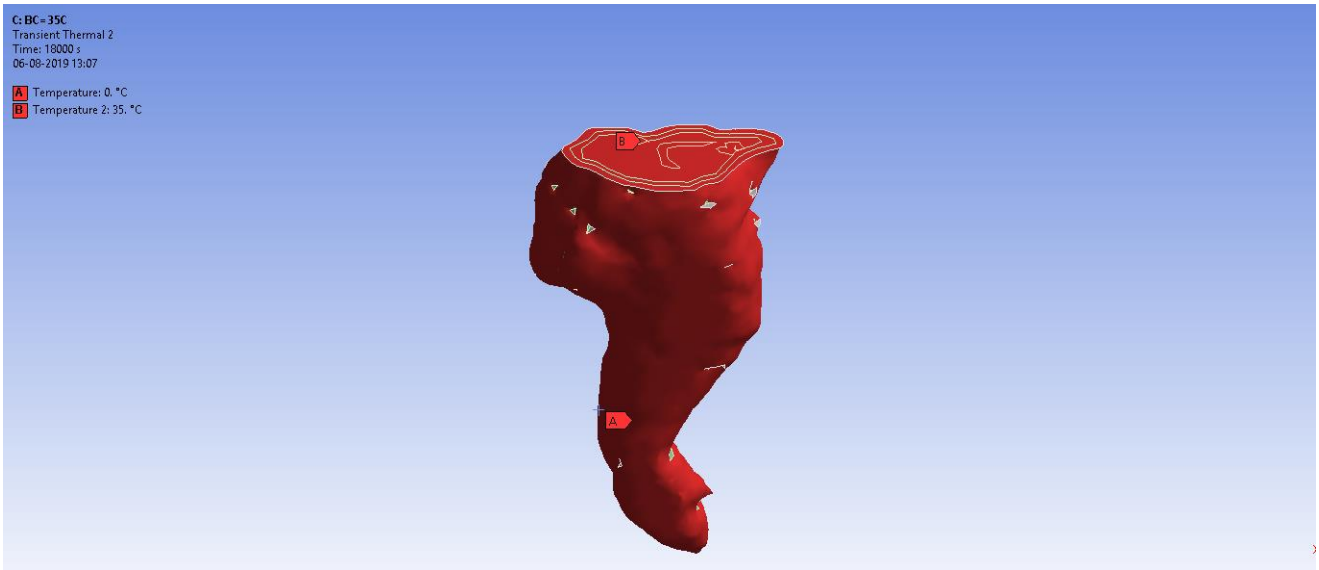

Figure 16: Boundary conditions for animal limb simulation 2

Figure 16 depicts the boundary conditions for Animal limb simulation 2. The added boundary condition near the thigh region makes this simulation closer to the actual working condition. It was assumed that the limb is isolated from the body, but in reality, it will be in contact with the body, attached with the torso. Since the body temperature of swine is 35°C, the constant temperature boundary of 35°C has been assigned to the plane. In simulation 1, there was no heat source and the surface was adiabatic. Here there is a heat source which will give out more heat as heat transfer rates are driven by temperature difference. All other settings are the same as for the previous simulation. Auto sub stepping was program-controlled, only big steps were given by the user. There were a total of 19 user-defined steps and sub-steps were program defined. Solver type was chosen to be direct type because it converges faster than iterative solver. Total time elapsed needed for computation was 18 minutes 24 seconds. The result file took 8.97 GB on the disk.

3.6.1 Results and Discussions

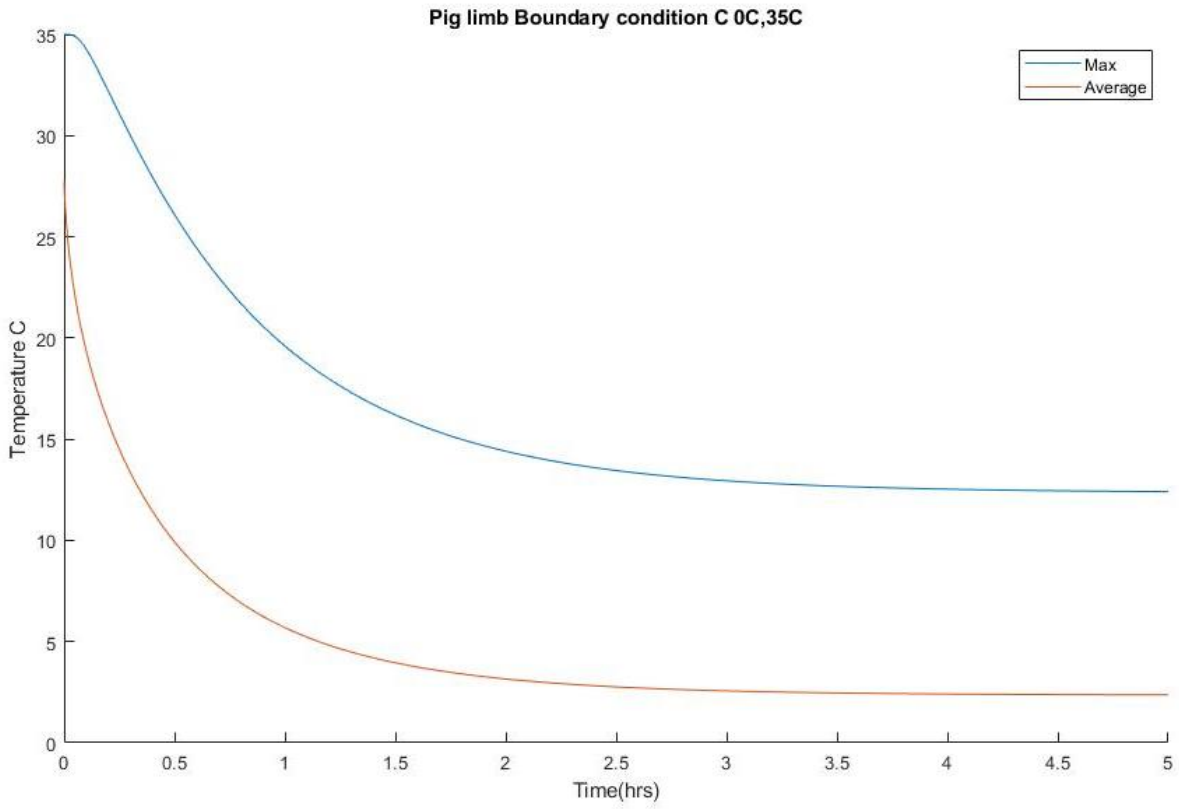

Figure 17: Minimum and average temperatures over time

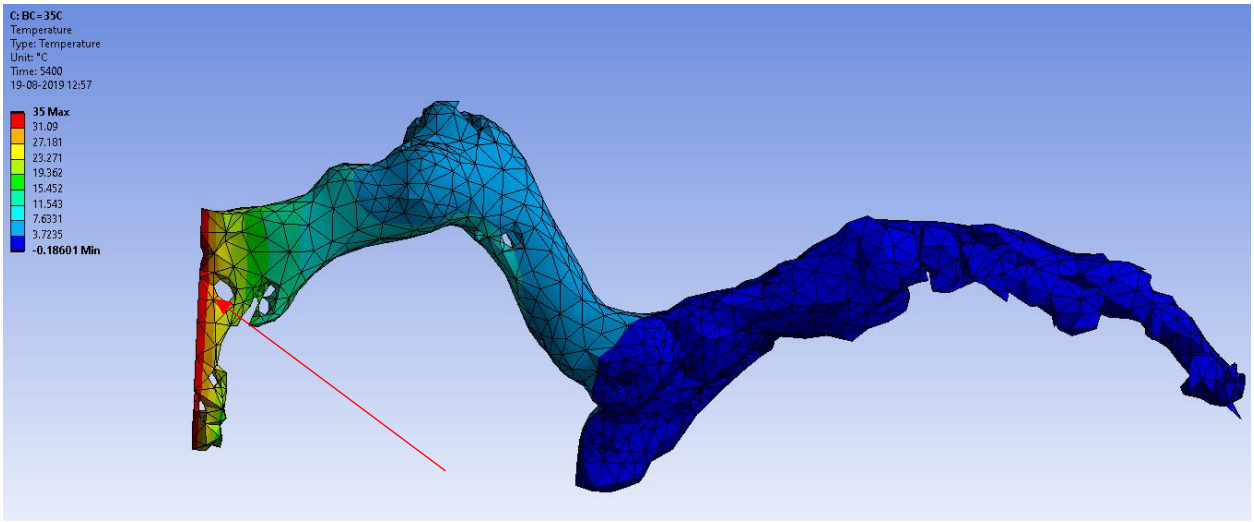

Figure 18: Point of maximum temperature (arrowhead)

Figure 17 depicts temperature histories in the animal limb model over time for simulation 2. We observe similar trends in maximum and average temperature curves. Maximum temperature drops after a few minutes of initial stable temperature. Here we need to that the maximum temperature curve represents the point just below the cut plane of the limb near the thigh (Figure 18) since it is applied with the boundary of the constant temperature of 35°C. The maximum temperature drops down in similar fashion as in simulation 1, but it can be observed that there is plateau towards the end, after 2.5 hrs mark. This can be explained by heat source flowing in from a constant temperature boundary of 35°C. The heat flow increases as time progresses. Figure 19 depicts the variation of the heat flux across the constant temperature boundary of 35°C. As we can see, it also becomes almost constant at 2.5-hour mark. Since maximum temperature curve also stabilizes at some point, we can say at this point system nearly reaches thermal steady state.

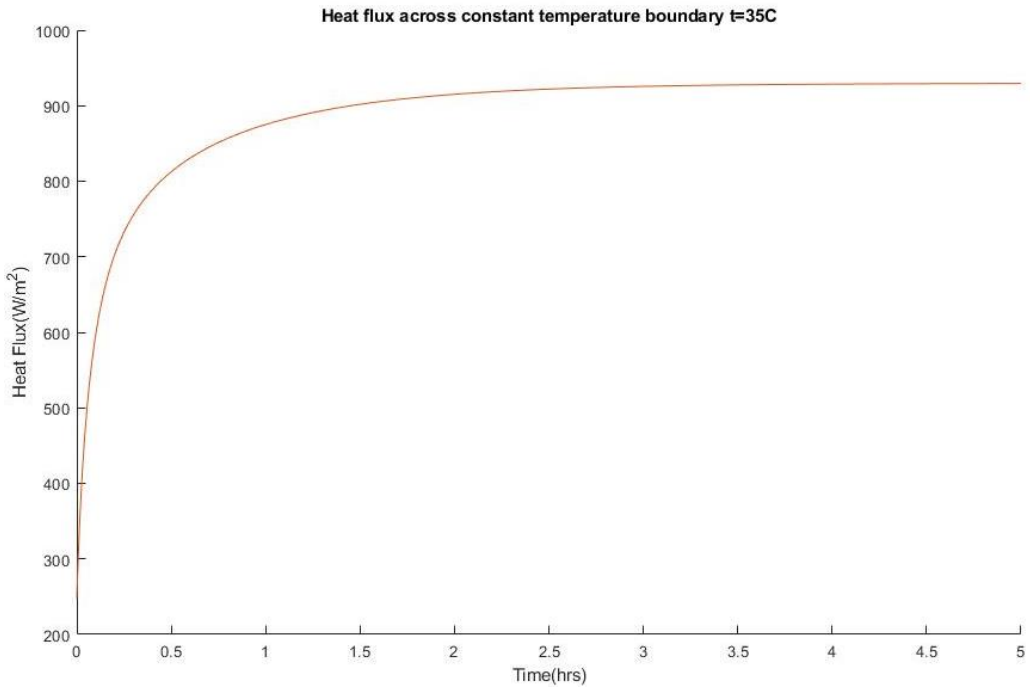

Figure 19: Heat flux across a constant temperature boundary of 35°C

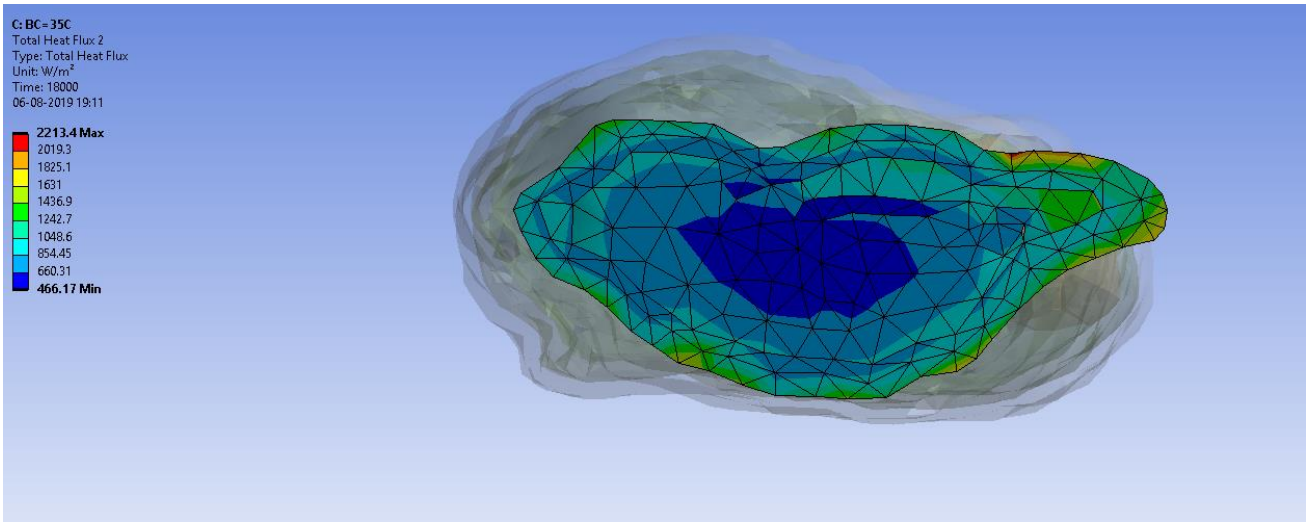

Figure 20: Flux distribution on constant temperature boundary of 35°C at t=5 hrs

We can observe in Figure 20 at steady state, the heat flux is higher near the edges where cooling is applied and lower in the inner parts of the limb.

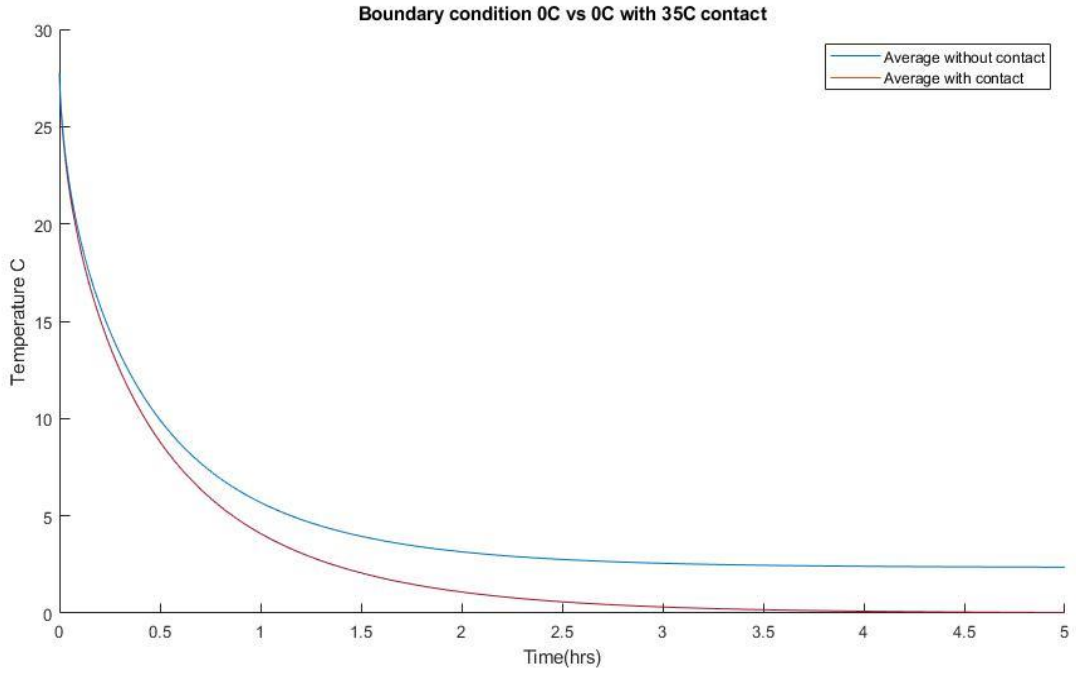

Figure 21: Comparison between average temperature in simulation 1 and simulation 2

The average temperature follows a similar trend in simulation 1. It goes down rapidly and gradually the rate of decreases in the average temperature decreases. It also stabilizes around 2.5 hours. It can be seen in Figure 21 the average temperature curves for both simulations follow closely with an isolated limb with slightly lower temperature. Isolated limb reaches steady-state around 4 hours and it reaches nearly 0°C. On the other hand, the limb with thermal contact with the torso reaches steady-state around 2.5 hours and the steady-state average temperature is nearly 3°C. Thus it can be deduced that with a limb in contact with the body, the temperature can not drop below 3°C, even if we employ a constant temperature boundary of 0°C.

3.6.1.1 Chiller power requirements for pig limb experiment

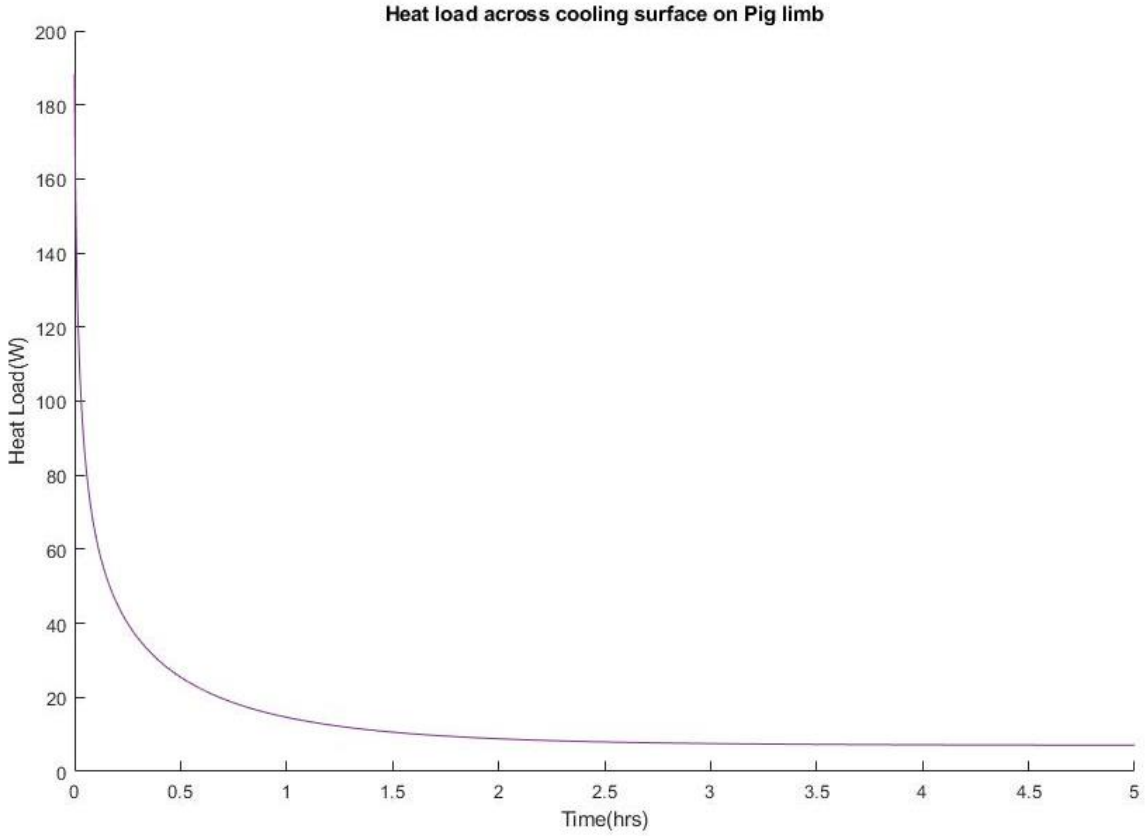

Figure 22: Heat load across the cooling surface

Figure 22 depicts the heat extracted vs time from the cooling surface. Initially, the heat load is about 190W and it decreases rapidly as the temperature drops down rapidly. And as we have talked earlier, the heat transfer rate is driven by the temperature difference between the cooling surface and an average temperature of the body. The current chiller is manufactured by company "Coolance" and its capacity is 450W. Thus, if make sure there are minimum heat losses from cooling sleeve tubes, from the backside of the cooling sleeve, then 450W chiller can be effectively used to cool the swine limb effectively.

3.7 Animal testing protocol

Figure 23: ALI studies on an animal model

Animal research is being carried out at Harborview Medical Center and the swine limb model is used to study ischemia. The primary objective of the experimentation is establishing swine limb model of Acute Limb Ischemia (ALI). The effects of limb cooling on metabolism rates are being studied by keeping track of blood levels chemicals like lactate and pyruvate. By the end of this experimental protocol, the relation between cooling and metabolism rates will be defined and thus will bolster the idea of prevention of limb amputation with the Limb Cooling Tourniquet. Along with embolic and traumatic ischemia, there will be an experiment which simulates hemorrhagic shock which is reduced perfusion to limb resulting in the deficiency of oxygen. Figure 23 depicts the ALI studies taking place on a swine limb model. Usually, blood contents are monitored at regular intervals.

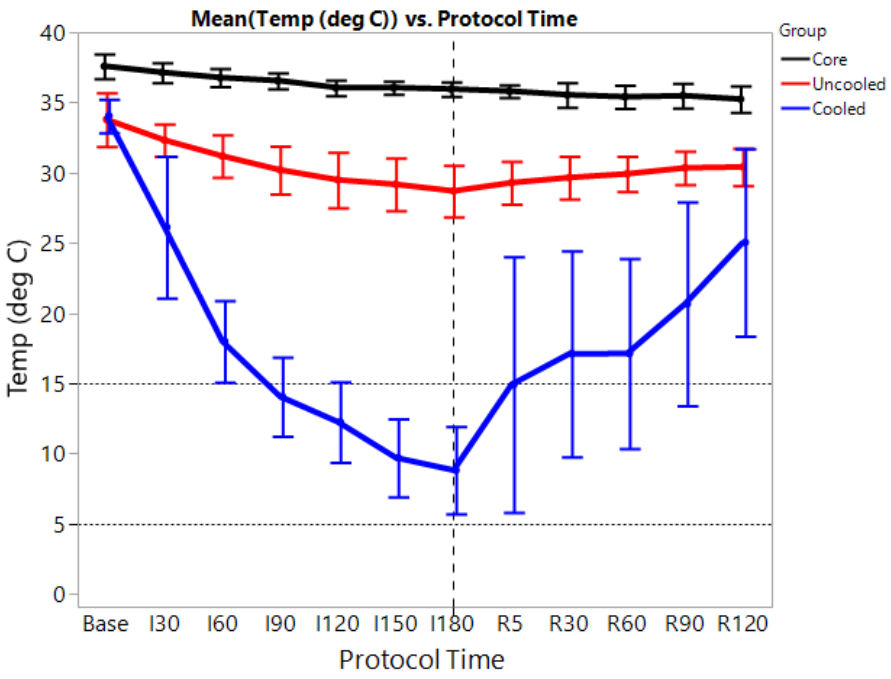

Figure 24: Temperature histories in pig limb cooling experiment

As a part of the experiment design using a tourniquet, the cooling experiment was performed. The ischemic condition was simulated, and the limb was cooled using icepacks on its surface. It was hypothesized that cooling the limb to 5-15°C will help with ischemia. In this experiment, one limb was cooled and the other limb was not cooled. The experiment was performed on hind limbs. The temperature histories of both limbs and core temperature of bodies were constantly tracked.

Figure 24 shows temperature histories of both limbs and the core body temperature is also plotted on the same plot. I is ischemia and R is reperfusion on timeline. The experiment was performed with the help of icepack. Both limbs started at 35°C. Limbs were cooled about for 3 hours where the limb temperature dropped below 10°C. After that cooling was stopped and blood reperfusion is allowed in both limbs. We can observe that the uncooled limb also experiences a slight drop in temperature. This can be explained that because of ischemia the normal metabolism is disturbed. After reperfusion, both limbs increase their temperatures as the core is able to supply blood.

3.7.1 Comparison with simulations

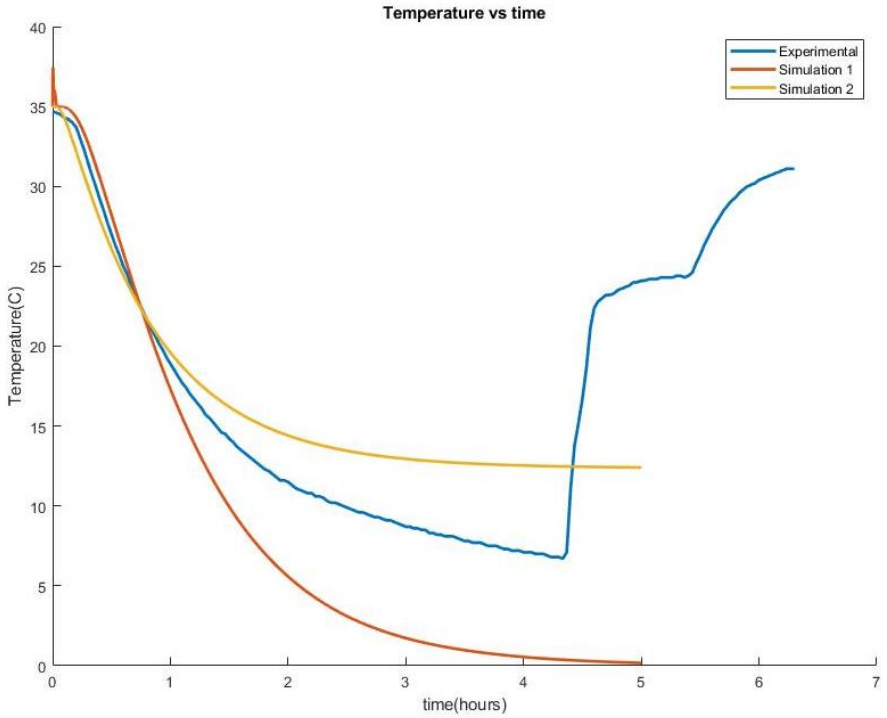

Figure 25: Comparison between an animal limb icepack cooling experiment and simulations

Figure 25 shows the comparison between temperatures from animal limb experiment with ice cooling and maximum temperature curves attained from simulations. Initially, the curves start at 35°C and go pretty closely and after 20°C, they start parting. Isolated limb simulation cools fastest and simulation which assumes 35°C at the contact with body cools slowest. The actual experiment shows a temperature curve which is in between these two curves, roughly goes in such fashion that it bisects region between both curves. We can infer from this fact that the actual heat flow is different from the assumption of both simulations. Thus, a few more simulations were performed with varying temperature boundaries at the thigh. Figure 26 depicts comparisons with various temperature boundaries with experimental data.

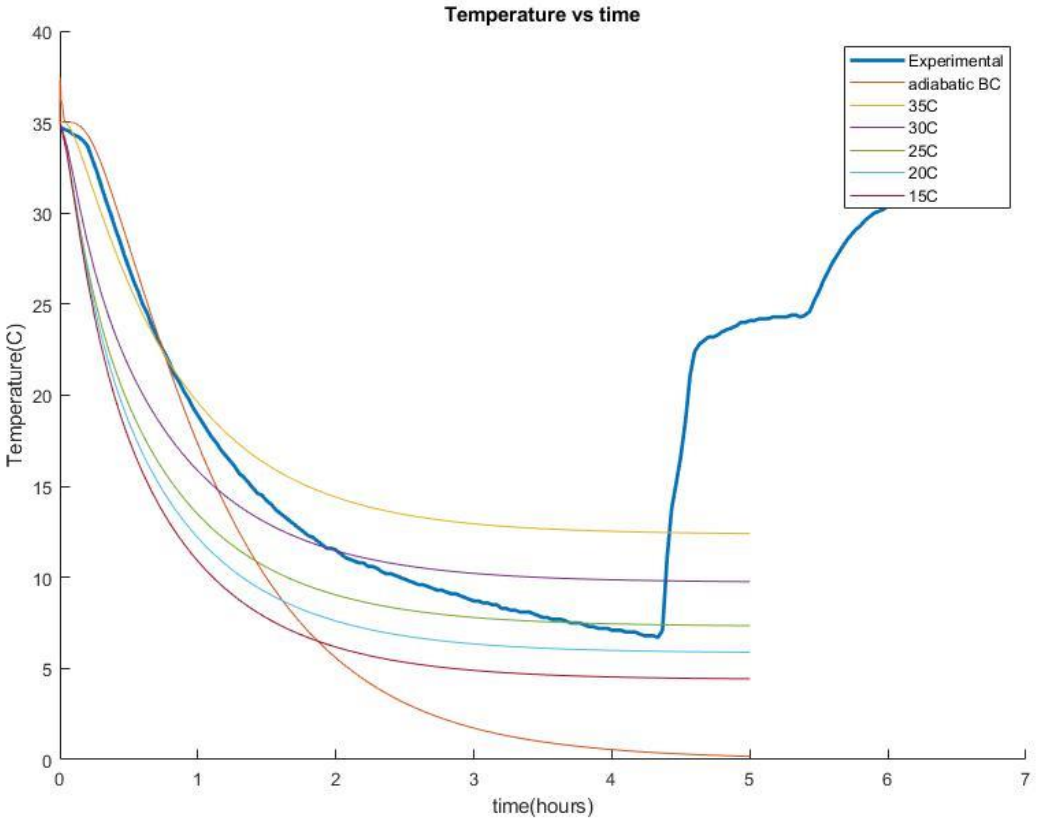

Figure 26: Comparison between an animal limb icepack cooling experiment and simulations with various boundary condition

The limb is not insulated from the body and will have some heat flowing in. But the junction is not exactly at constant temperature boundary of 35°C either. As we can see, the experimental curve is very similar to the simulation curve of 35°C until 22 °C, but after that point heat coming in from the torso to the thigh does not keep up with increased heat flow towards the cooling surface. Thus the actual thermal regulation in the body with trauma is a very complex process. And it is quite difficult to replicate the thermal regulation in simulation with assumptions made. So further cooling experiments might give a better idea about the exact mechanism of heat generation in particular condition so that more precise boundary conditions can be set for simulations.

Chapter 4: Thermal Simulation of Human Limb Model

In the development of any medical device, testing the device is a crucial part. Some devices are easy to test because they are relatively simple. Class-I devices do not require human testing for the Food and Drug Administration (FDA) approval, which is also known as 510k- exempt. But devices that claim to save lives and are more complex, (Class II and Class III) require human testing before they get approved by the FDA. In the design cycle of the device, the device is not always ready to be tested on a human subject. Thus, the design of experiments may employ phantoms which will replicate physical properties of the particular biological environment. FEM simulations are important since we can simulate the environment without actually putting any subject to risks which might arise because of an underdeveloped device. So, throughout the design cycle, each updated design is first tested with the help of numerical methods such as simulations, then they are prototyped and tested on phantoms and then the design is improved.

In the case of developing limb cooling tourniquet, it was important to generate a simulation model which will replicate the thermal properties of a human limb accurately. Specific heat, thermal conductivities, and densities of various tissues need to be identified correctly in order to represent the human limb. Also, knowing details about the distribution of different tissues in the limb was necessary to make a realistic model for the thermal simulation of a human limb. This methodology helped to visualize how the limb will behave undercooling. Calculating heat flows on the surface was also possible, which helped us find heat loads across cooling surfaces at different instants of time. The simulation model gave theoretical limits of how fast a limb can be cooled without damaging the skin since the temperature on the cooling surface can not go below freezing temperatures in order to save it from frostbites.

4.1 Model preparation

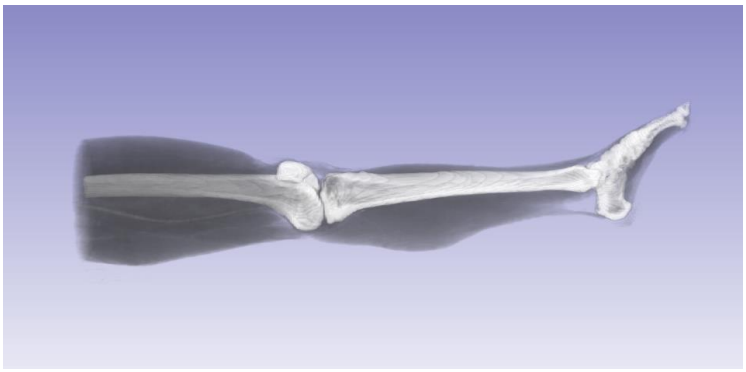

Figure 27: 3-D reconstruction of human limb CT scan

To generate tissue composition data, a similar approach to testing the animal limb was followed. Anonymized data of a healthy 29-year-old male was obtained from the Radiology department at the University of Washington Medical Center. CT scan data was stored in native DICOM format and imported into Simpleware software suit. Figure 27 shows the 3-D reconstruction of a human limb from CT scan data that was imported into Simpleware. The five masks developed for separating the tissue layers were Bones, Muscle, Fats, Skin, and Nerve. The finite element model was made using these 5 masks. The meshing algorithm used was FE free which lets the program choose the shape of elements as opposed to the FE grid algorithm, and all the elements were tetrahedral and linear. The type of export was Ansys Workbench Volume, which generated a standard input file for Ansys workbench, file with *.inp format. Figure 28 shows the FEM model ready to be exported.

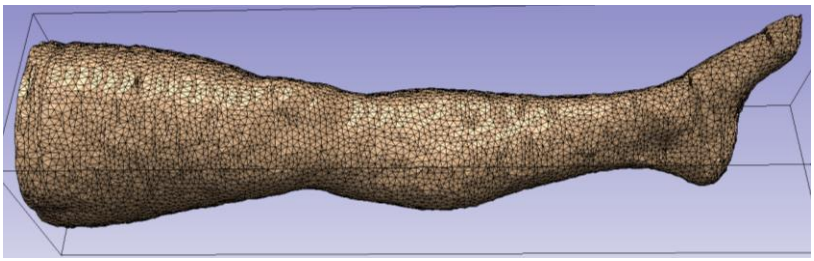

Figure 28: Model ready to be exported as FEM mesh

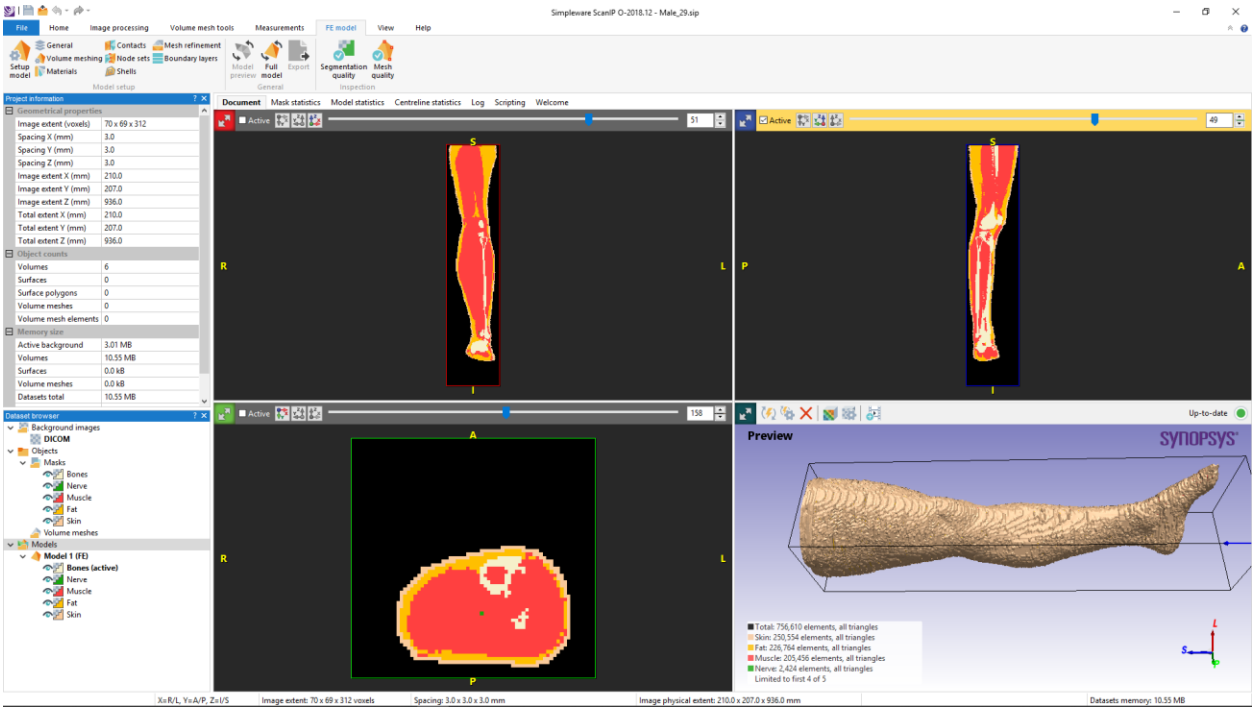

Figure 29: Simpleware, 3 views and rendered assembly of 5 masks

Figure 29 depicts the Simpleware suite showing 3 views and rendered assembly of 5 masks. The bottom right window shows model preview while other 3 windows are X, Y and Z planes of voxel modeler.

There was a total of 302,539 elements used in this model. Five masks were generated and were assigned different thermal properties. Table 4 shows the number of elements and thermal properties corresponding to each mask.

Sr. no.	Mask	Number of elements	Density kg/m^3	Thermal Conductivity W/m.K	Specific Heat J/kg.K
1	Bones	35,403	1908	0.41	1313
2	Fats	74,025	911	0.317	2348
3	Muscle	132,458	1090	0.518	3421
4	Nerve	1600	1075	0.49	3613
5	Skin	59,053	1109	0.315	3391

Table 4: Thermal properties and the number of elements for each mask

4.2 Human limb simulation 1

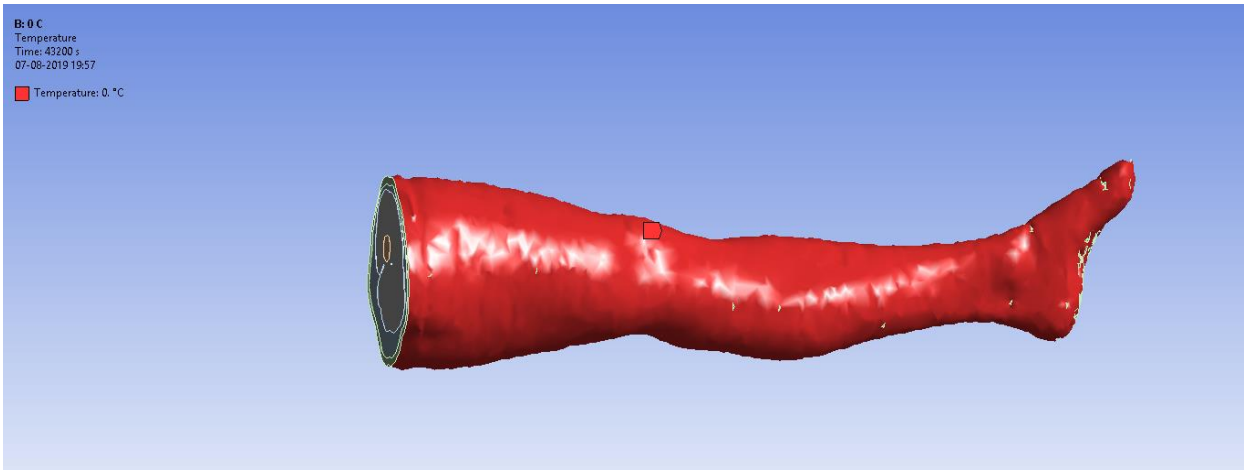

Figure 30: Boundary conditions for simulation 1

The simulations were performed in Ansys thermal transient analysis. Figure 30 shows boundary conditions for the first simulation. The limb was considered to be isolated in the first simulation. The cut near the thigh contact was assigned with a perfectly insulated adiabatic boundary. The surface of the leg where the icepack was applied and cooling sleeve will be in contact has a given constant temperature boundary condition of 0°C as can be seen in the red highlighted part in Figure 30. The simulation was carried out for 43,200 seconds (12 hours) of physical time. A typical tourniquet causes amputations in about 6 hours, although for long-distance transports it can be used for as long as 12 hours. The initial temperature of the limb was set to normal body temperature, 37°C. Auto sub stepping was enabled, and it was program-controlled. There was a total of 19 user-defined steps and length between steps was increased gradually and made constant at 1800 seconds. The last few time steps were as big as 3600 seconds. The remaining simulation settings can be found in Table 5.

Time elapsed for total simulation and post-processing was 1 hour and 42 minutes. The resulting file was 53.08 GB.

Parameter	Setting
Simulation length	43,200 s
Minimum time step	3.6 s
Maximum time step	360 s
Time Integration	On
Solver type	Program Controlled
Flux Convergence	0.0001
Maximum Iterations	1000
Solver Tolerance	0.1 W/m^2
Over Relaxation factor	0.1
Number of Physical Cores	4

Table 5: Simulation parameters

4.2.1 Results and Discussions

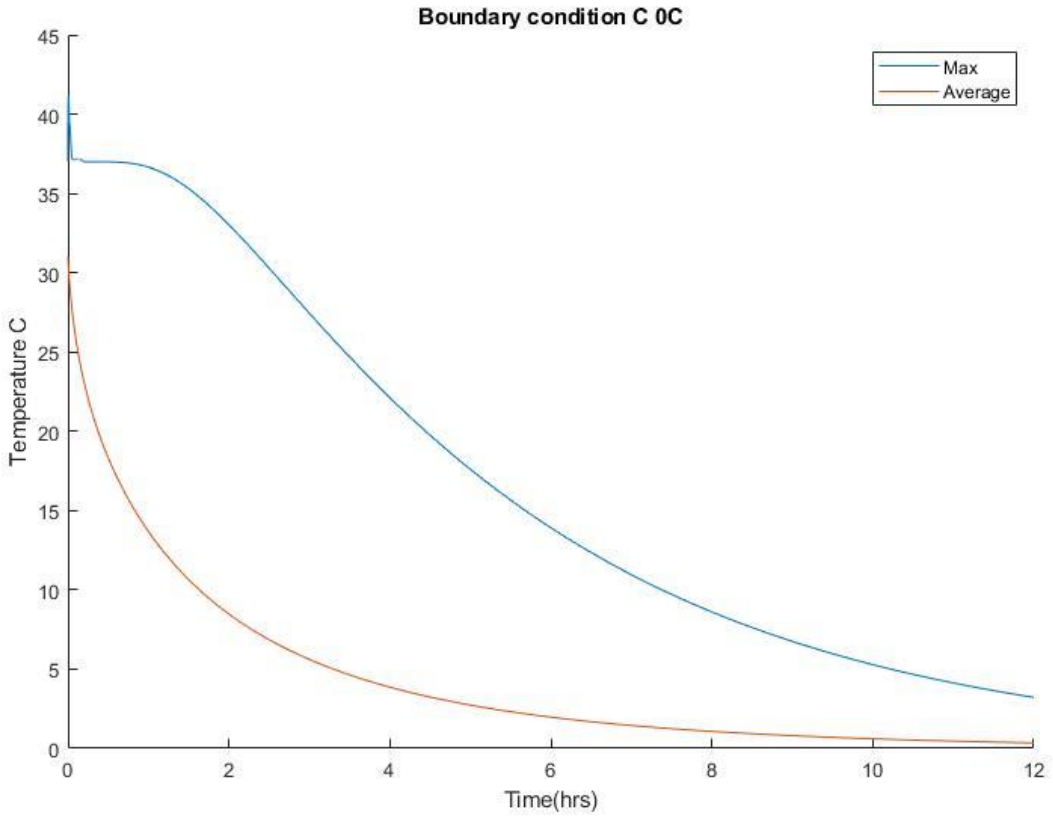

Figure 31: Average and maximum temperatures across time in simulation 1

Figure 31 depicts the temperature histories from the first human limb simulation. It plots two curves. Maximum temperature curve plots temperature of the point which has maximum temperature across the limb at any given instance, which is roughly at the centerline of the thigh. The average temperature drops rapidly for the first 2 hours and then the rate of temperature drop decreases. This curve follows an exponential law which is typical in case of bulk mean temperature drop across the isothermal boundary. The varying heat transfer rates are because of dropping temperature. The heat transfer rate is always proportional to the temperature difference across the boundary. As time passes, the temperature difference goes on decreasing and cooling the limb further becomes slower.

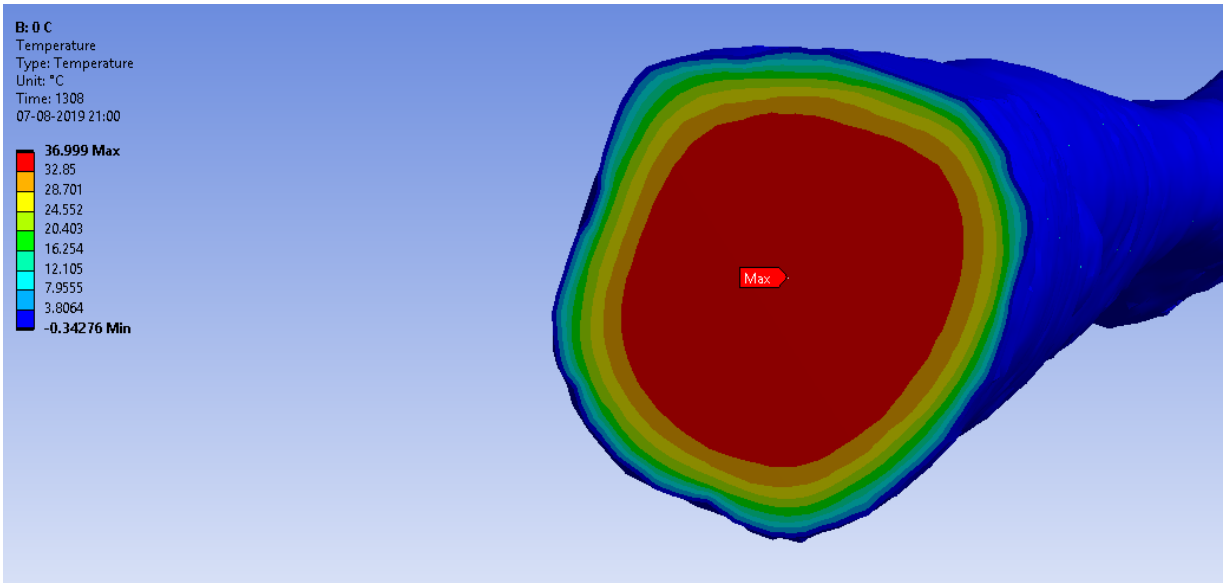

Figure 32: Temperature distribution across thigh contact plane

The maximum temperature curve does not change for the first few 20 minutes. This is because that much of time is required for heat to flow outside since thermal conductivity of tissues is very low. Thus, there is an initial plateau in maximum temperature curve.

Figure 32 shows temperature distribution across the cut on the thigh where we have an adiabatic boundary at t=1308 seconds. At this time the maximum temperature starts dropping below 37°C. We can see that most of the limb is still hot while some layers inside skin have started cooling slowly. After this point, the maximum temperature starts dropping.

The recommended cooling range is 10-15°C for prevention of the effects of ischemia. The average temperature drops down to 15°C in about 50 minutes from the start. And it reaches 10°C in 100 minutes from the start. But it takes about 5 hours and 42 minutes to drop the maximum temperature to 15°C. And at the point of maximum temperature, it does not come below 10°C until 7 hours and 25 minutes. It can be observed in Figure 33 that at t=8 hours, the maximum temperature reaches 8.61°C and the point of maximum temperature is always at the adiabatic boundary since all other points are closer to heat sink than the center of thigh cut.

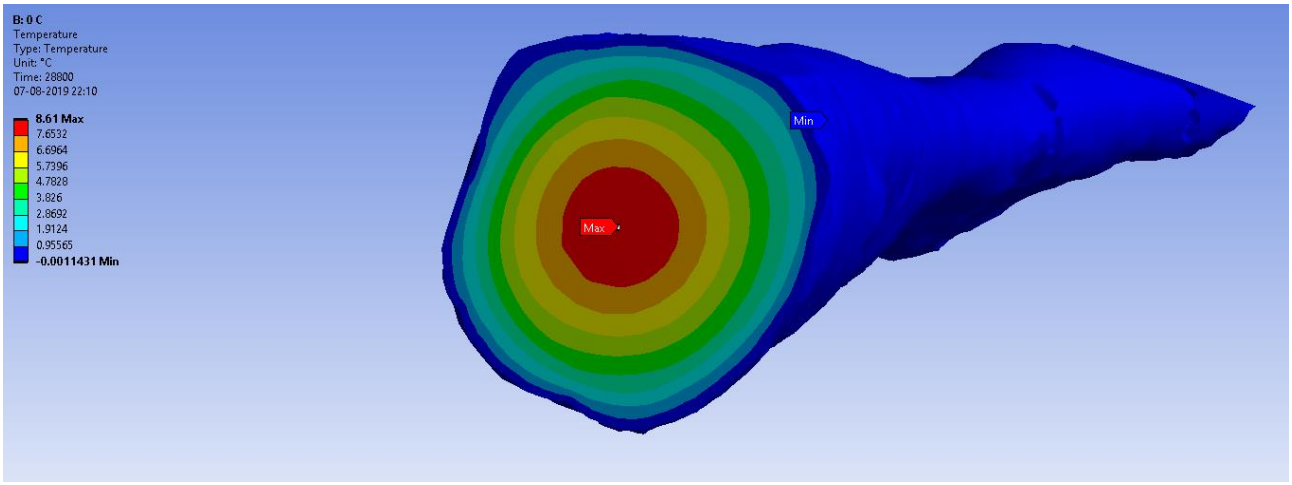

Figure 33: Temperature distribution at t=8 hours

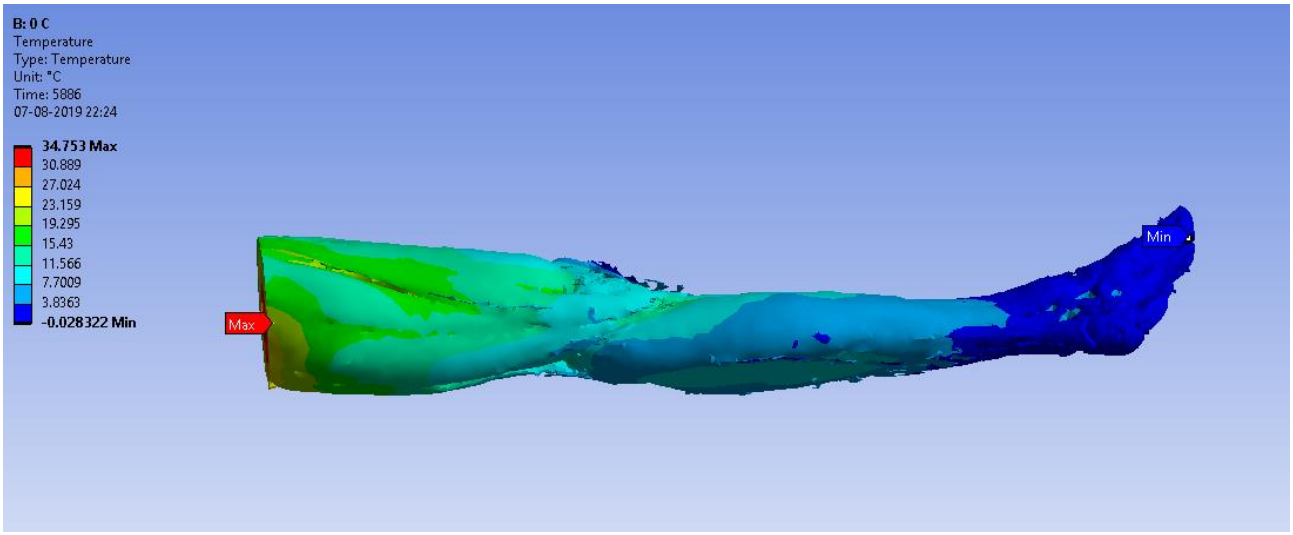

Figure 34: Temperature distribution inside the fat layer

Figure 34 shows temperature distribution inside the fat layer. We can see that lower limb cools significantly faster than the thigh. The Lower limb injuries are more common than wounds above the knee. Thus, studying what time does it take to cool the lower limb can be important since sometimes tourniquets are applied just above the knee and hence the bottom part of the limb will be cooled. We can insert temperature probes in the simulation model at calf muscle and find out the temperature histories for the lower limb.

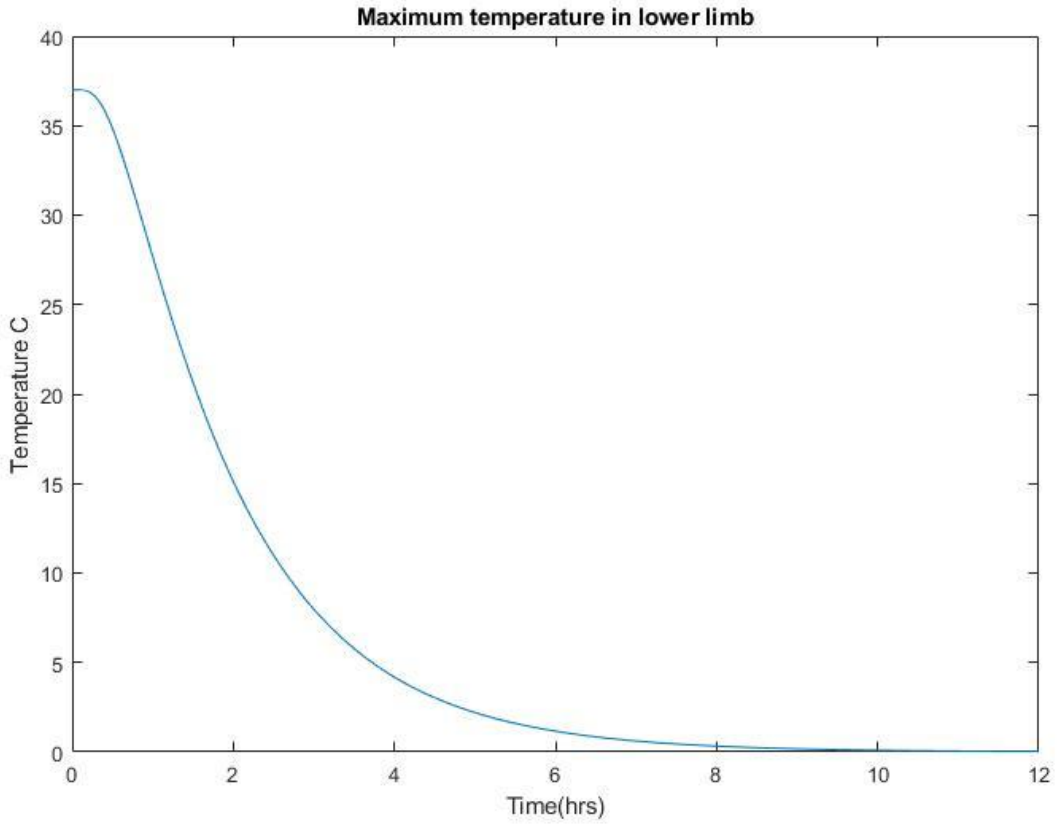

Figure 35: Temperature curve in lower limb

Figure 35 depicts the temperature curve at the point in the lower limb at the center of calf muscle which has maximum temperature in the lower limb. It takes roughly 2 hours to achieve a temperature of 15°C and it takes about 2 hours 40 minutes to reach 10°C. Thus, cooling is way more effective if we are considering injuries in the lower leg.

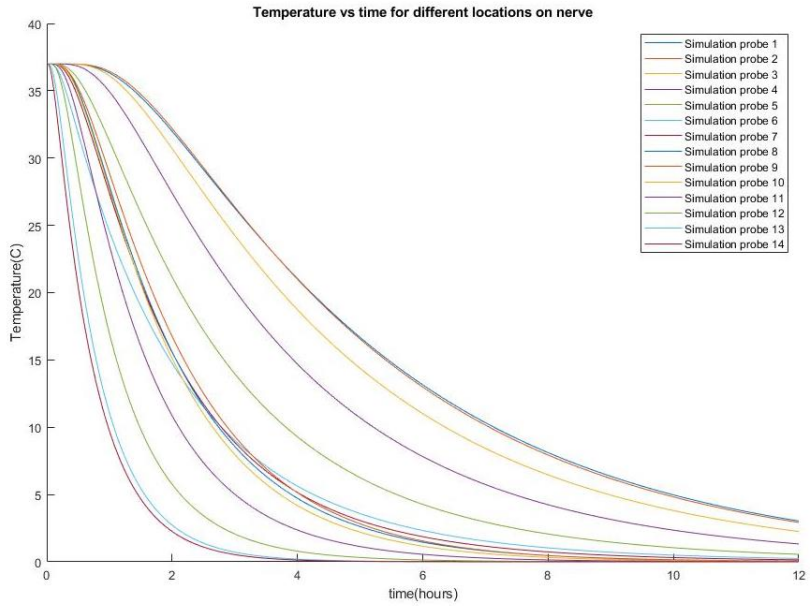

Figure 36: Temperature vs time on different locations on the nerve

Figure 36 depicts the temperature profiles of 14 different points on a nerve. Point 1 is at thigh and as we go up to point 14, we reach the end of the calf muscle. As we go towards the lower extremity, the limb cools faster. Figure 37 depicts the position of all points from the end of the thigh.

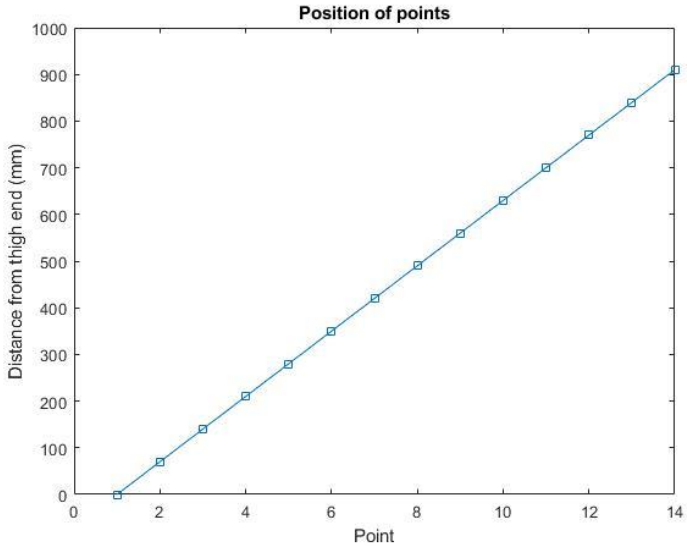

Figure 37: Position of points on the nerve

4.3 Human limb simulation 2

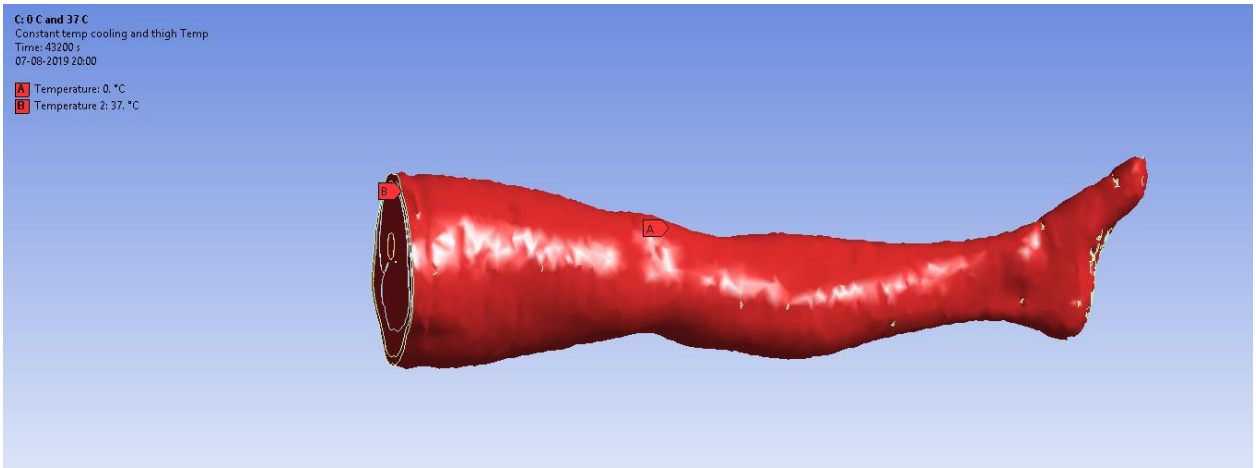

Figure 38: Boundary condition for human limb simulation 2

Figure 38 shows the boundary conditions used for human limb simulation 2. In this simulation, all other settings and conditions are the same as previous simulation, except one boundary condition. In the first simulation, it is assumed that the limb is isolated from surrounding and even from the body. Thus, the boundary condition at cut near the thigh is set as no heat flow or adiabatic boundary. So, simulation 1 gave a good idea about how much heat is stored in the limb and how much time is required to draw that heat from the limb. But in reality, the limb is attached to a torso and it will have some temperature and there will be some sort of heat flow in from the contact surface. Thus, to make the simulation more realistic, a constant temperature boundary of 37°C is added to the contact surface. Thermal regulation in the wounded and ischemic body is a very complicated process, but this simulation assumes that part of the body above tourniquet is fully functional and the core temperature is maintained at 37°C.

The time elapsed to compute the results and post-processing was 1 hour and 40 minutes. Result file took 51.92GB space.

4.3.1 Results and Discussions

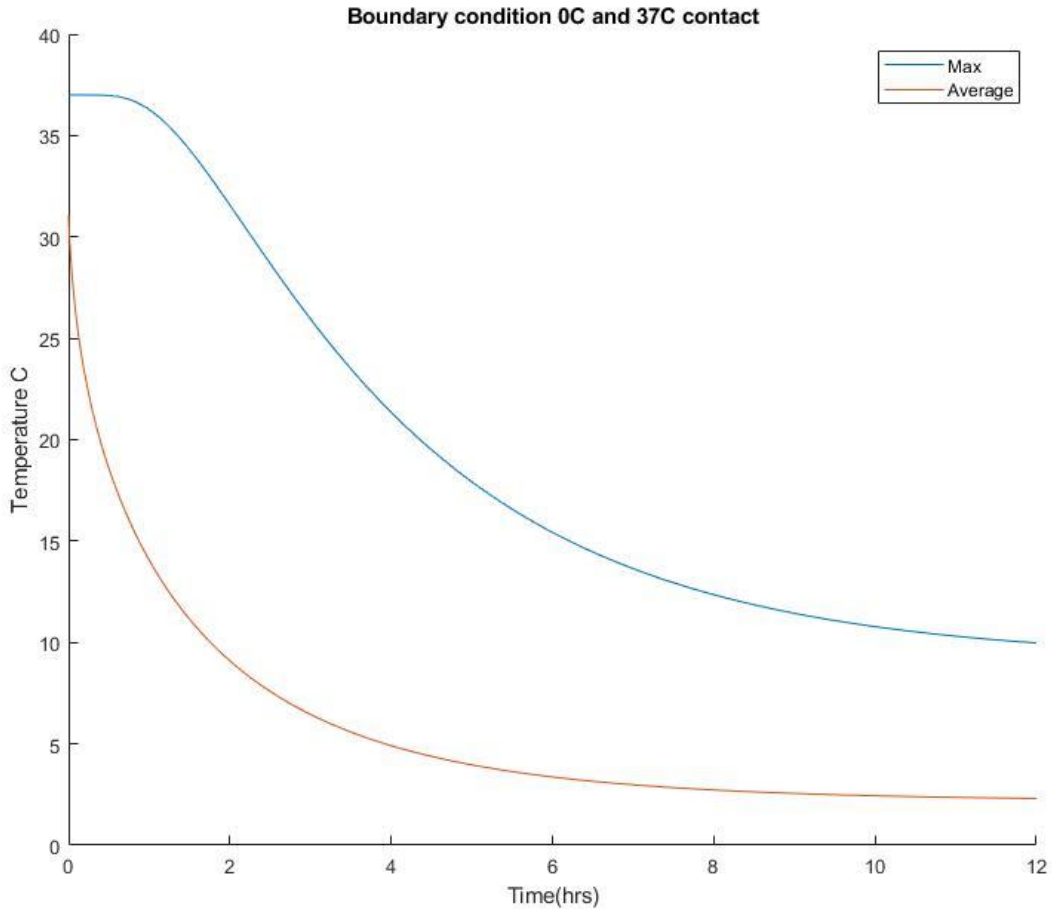

Figure 39: Average and maximum temperatures across time in simulation 2

Figure 39 depicts temperature histories in human limb model over time in simulation 2. The average temperature curve follows a similar trend as in simulation 1. However, after about 8 hours it stabilizes around 3°C. Unlike the previous simulation, this simulation has a steady-state solution since there are one heat source and one heat sink. The simulation would cool down infinitely until everything cools down to 0°C. But this model will have some positive nonzero temperature as a steady-state temperature for both average and maximum temperature.

Before discussing the maximum temperature, it should be noted that in this simulation the point just inside the contact surface near the thigh has a maximum temperature. Because we have applied 37°C as constant temperature boundary, the boundary itself will be at maximum temperature all the times.

Following trends from the previous simulation, the maximum temperature starts dropping down after the initial plateau. The temperature starts stabilizing at around 10 hours. It can be anticipated that the maximum temperature point will stabilize around 10°C by observing the slope of the curve. In steady-state this is possibly the lowest temperature we can achieve for maximum temperature. It can be seen in Figure 40 that heat flowing in from contact surface goes on increasing as temperature drops.

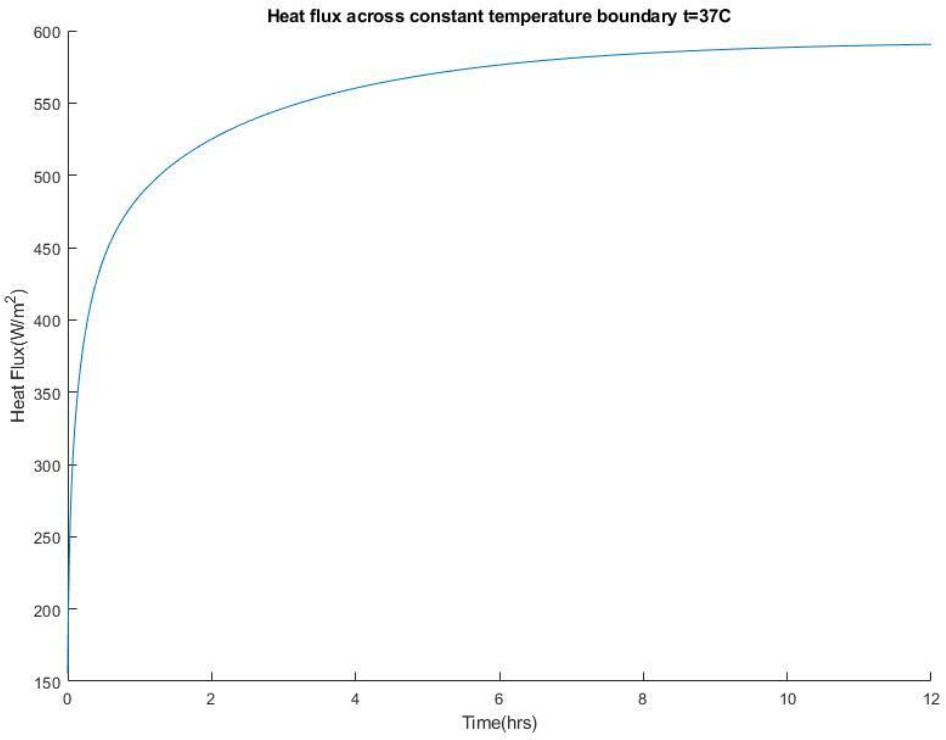

Figure 40: Heat flux across the contact surface

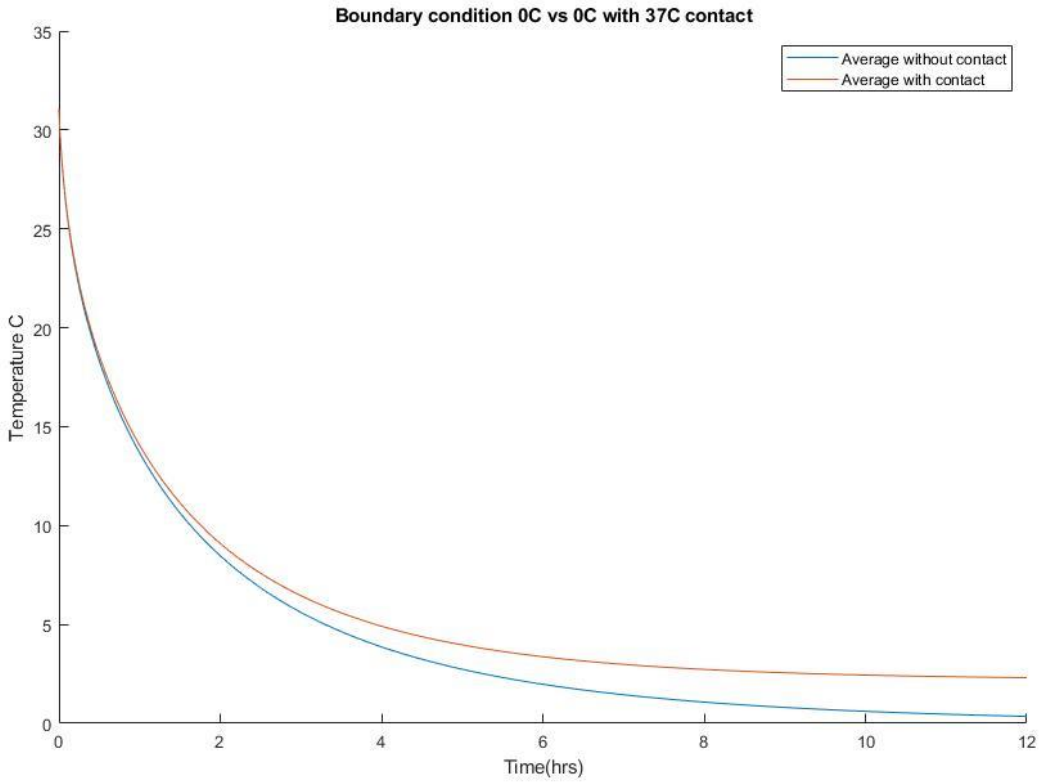

Figure 41: Comparison between average temperatures from both simulation

Figure 41 compares average temperatures from simulation 1 and simulation 2. Both results follow the same trend until 2 hours mark with isolated limb having a slightly lower average temperature after that. The actual heat transfer across contact could be more complicated than these boundary conditions, but heat transfer will not be absent like simulation 1 and it will be less that of 37°C contact boundary. So, it can be anticipated that average temperature curve we will be getting will be somewhere between these two curves.

This simulation predicts that to reach an average temperature of 15°C it takes 52 minutes and to drop the average temperature down to 10°C it takes 108 minutes. On the other hand, to drop the maximum temperature to 15°C it needs cooling for 6 hours and 15 minutes and it takes almost 12 hours to reach it around 10°C.

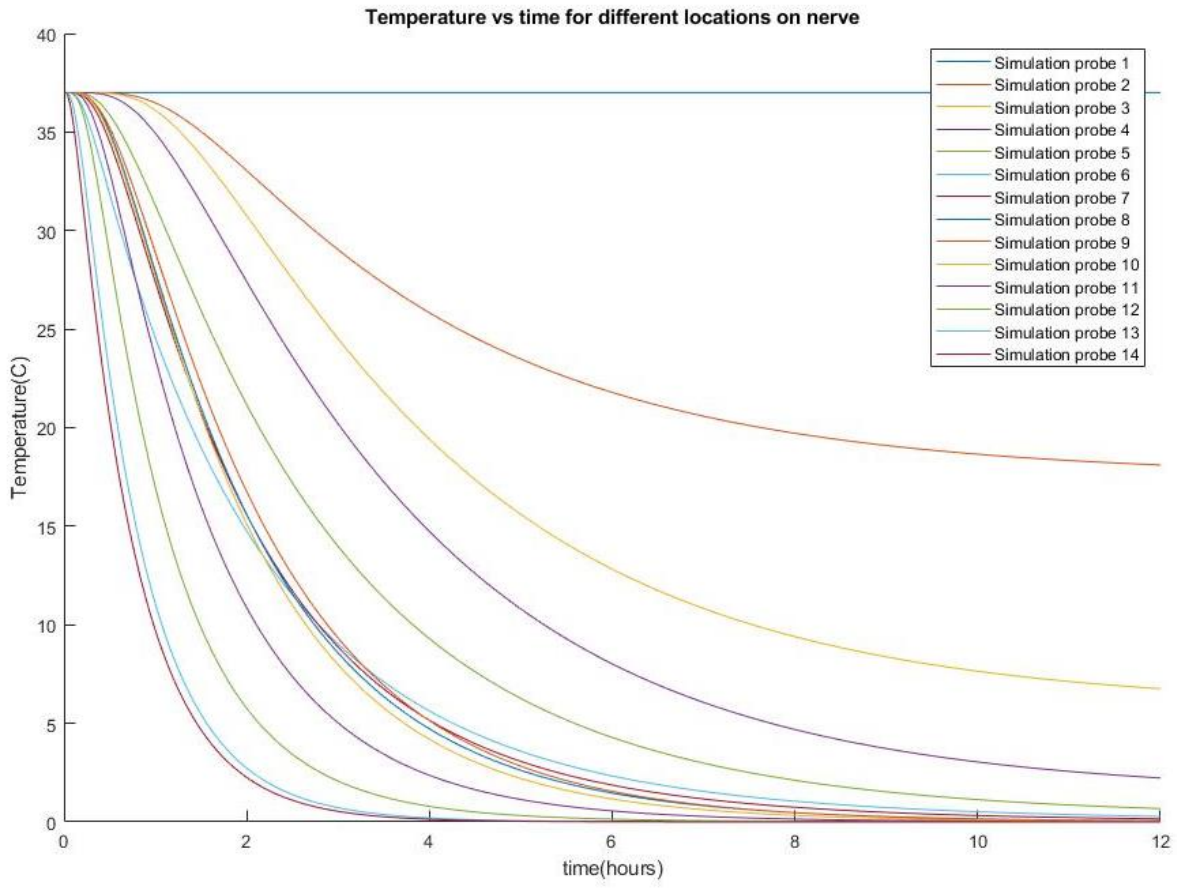

Figure 42: Temperature vs time on different locations on the nerve

Figure 42 depicts the temperature profiles of 14 different points on a nerve. Point 1 is at thigh and as we go up to point 14, we reach the end of the calf muscle. As we go towards the lower extremity, the limb cools faster. An interesting difference from simulation 1 is probe 1 which is at the constant temperature boundary of 37°C remains constant at a given temperature. With the heat source, the

temperature difference between lower extremity and thigh becomes more pronounced as time passes. Figure 43 depicts the position of all points from the end of the thigh.

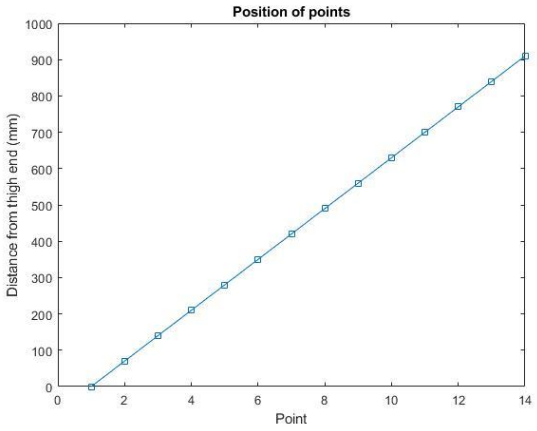

Figure 43: Position of points on the nerve

4.3.1.1 Chiller power requirements for human limb cooling experiment

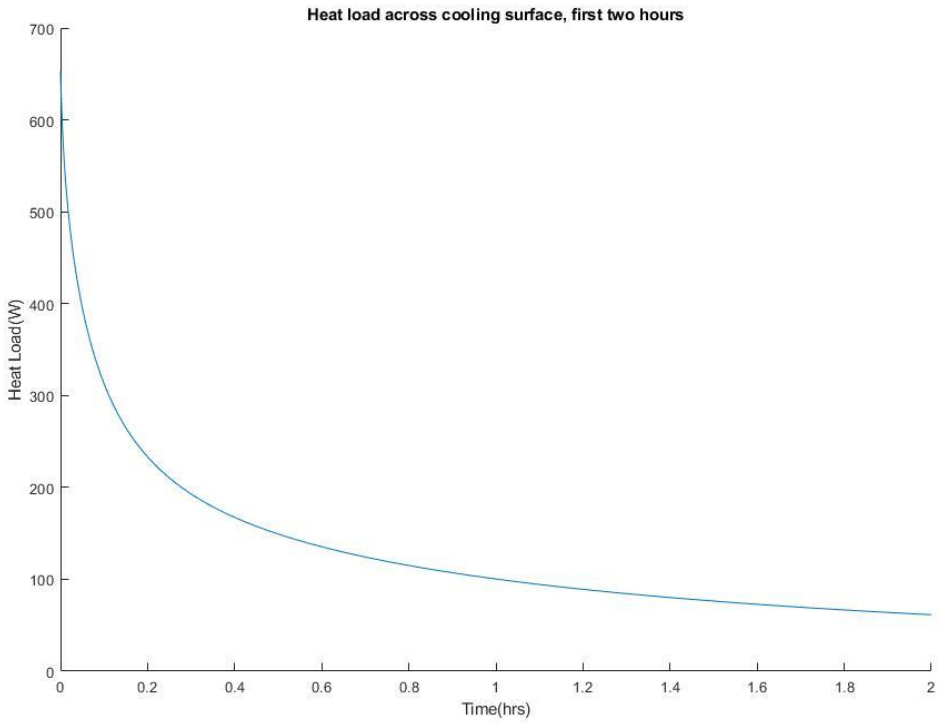

Figure 44: Heat transfer rate across the cooling surface

Figure 44 depicts heat transfer across the cooling surface. It can be observed that the initial heat transfer rate is as high as 650W. It drops rapidly as time progresses. The initial heat loss rate is high because the temperature difference between the skin and cooling surface is high. Since heat transfer rate is dependent on the temperature difference between two surfaces where heat transfer is occurring.

But this highlights that keeping the coolant temperature at a constant temperature of 0°C is difficult initially. So, if the chiller unit is not sufficiently powerful or if the heat losses are more than we expected them to be, then the initial cooling rate will be quite slow. Because enough cooling is not provided, the temperature of coolant will not drop to 0°C and that will decrease the heat transfer rate. Thus 450W chiller may not be enough for human limb cooling, and design of custom chiller with given requirements will be necessary.

Chapter 5: Thermal Phantom of Human Limb

In the previous chapter, we discussed a way to analyze the cooling performance of the human limbs under controlled cooling environment using simulations. Simulations help us getting analytical results under ideal conditions. But in the actual scenario, the working conditions are far from ideal. There are many inefficiencies which are not factored into the ideal case. It is assumed that the chiller is powerful enough to maintain the coolant temperature at 0°C and the surface of the cooling sleeve is maintained at that temperature. In practice, there are many heat losses which occur from coolant circulation, starting from the storage tank, coolant-carrying pipes, and even from the back of the cooling sleeve. That is why it is important to study the performance of chiller and cooling sleeve in actual testing conditions.

Since we can not perform tests in realistic condition with all variables because human testing is not an option at this stage of development, we need to design something which will help us simulate the testing condition. We need a thermal phantom of a human limb, which will have the similar conductivity as does the human limb and has similar heat holding capacity so that we can perform transient analysis and understand how much time it might take to extract a given amount of heat using the designed device.

This chapter describes materials and devices that are used to test and build a thermal phantom which will mimic the thermal properties of a human limb. The materials that are used, ways to manipulate thermal conductivity of materials, and ways to manipulate specific heat, and heat holding capacity of the phantom in effect will be discussed. Based on tests conducted, the first version of the phantom is developed. Results from the tests of the current version of limb cooling device with phantom will be discussed and the direction to improve the next version of a phantom will be decided.

5.1 Silicone Rubber

Silicone Rubber was used as the main material for the phantom. Silicone rubber is polymer made up of carbon, silicon, hydrogen, and oxygen. It can come with several variants, different additives which gives it different physical properties. It is an elastomer and can be easily shaped while curing. It is used for prototyping, sealing and it is widely used in many areas such as automotive parts, storage products, apparels and even in medical devices.

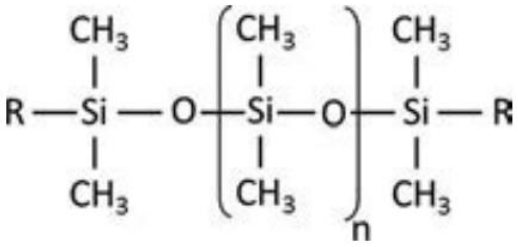

Figure 45: Chemical structure of silicone rubber polymer [33]

Figure 45 depicts the chemical structure of silicone rubber. (CH_3-SiO-CH_3) is a repeating unit of the polymer which forms long chains and (R-Si(CH_3)-O-) is the terminating end where R can be any alkyl group. Because of this unique structure silicone has flexible properties, thus comes it in the category of elastomer. Important physical properties of silicone are listed in Table 6.

Density	950-1200 kg/m^3
Tensile strength	4-13 MPa
Thermal conductivity	0.2-0.4 W/m-K
Specific Heat	1050-1300 J/kg-K

Table 6: Properties of Silicone [34], [35]

Thermal conductivity of silicone can be increased from 0.2 W/m-K to 1.3 W/m-K with help of inorganic additives [36]. Thus, we can manipulate the thermal conductivity of silicone using doping with high conductivity materials.

For increasing the thermal conductivity of silicone, carbon (graphite) was added. Carbon is thermally conductive and is available in powdered form as a graphite powder. It is very cost-effective as it is widely manufactured and used for various purposes including lubrication. It is readily miscible in silicone polymerization mixture and hence we can get a homogeneous mixture of curing mixture. Thermal properties of graphite are mentioned in Table 7.

Density	1888 kg/m^3
Thermal conductivity	130 W/m-K
Specific Heat	725 J/kg-K

Table 7: Thermal Properties of Graphite

Thus, the conductivity of silicone can be increased by mixing graphite, which has very high conductivity compared to silicone. It is important to understand the relationship between the percentage of graphite in silicone and thermal conductivity.

To establish the relationship between the percentage of graphite in silicone and its thermal conductivity tests were performed. Thermocouple wires and data acquisition system used in the experiment to determine the thermal conductivity of samples will be described in Appendix A3 and A4 respectively.

5.2 Thermal Conductivity Tests

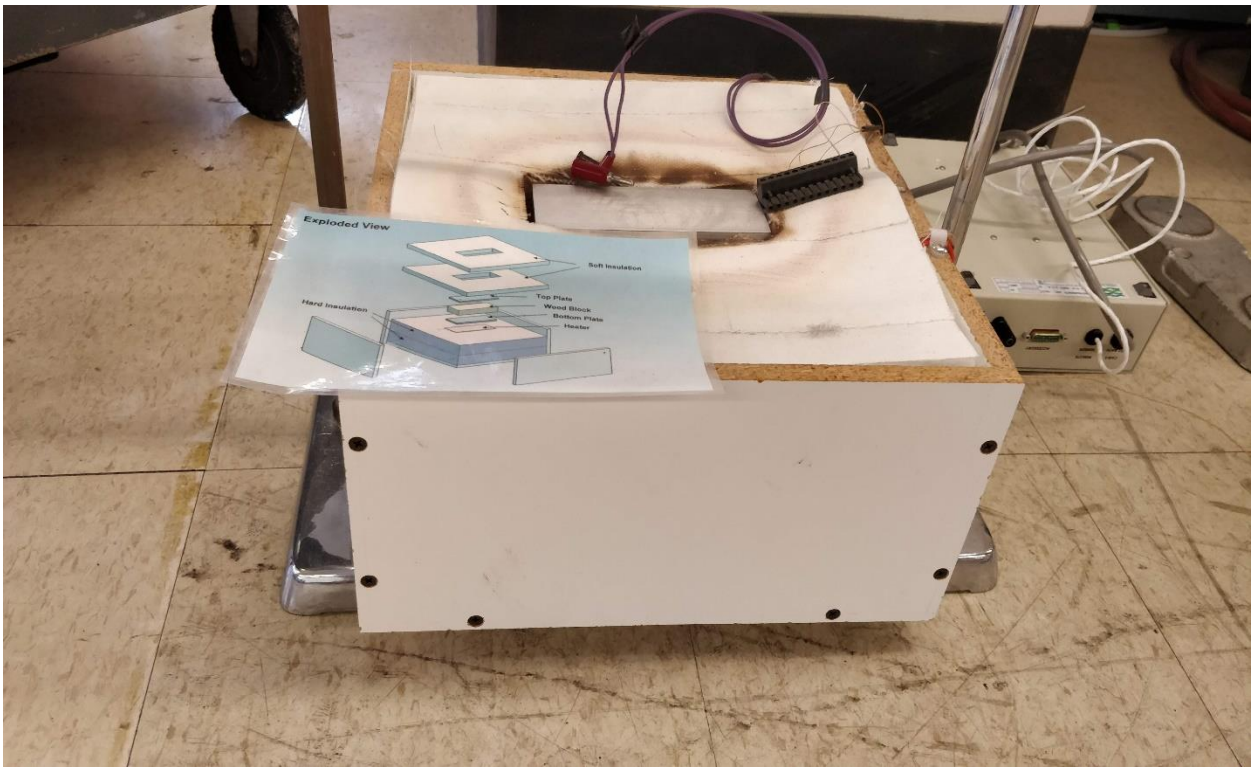

Figure 46: Old thermal conductivity test setup

Figure 46 depicts the test setup for thermal conductivity involving a 3-plate assembly. It has two aluminum plates, one on top and one on the bottom, with the sample between the two plates. At the bottom of the aluminum plate, there is a heater and on top of the top plate, there is a heat flux sensor. Temperature probes were attached at several heights. The glass wool surrounds the three-plate assembly and works as thermal insulation from the atmospheric air. The experiment is run until the steady-state is achieved. The thermal simulation for this experiment was carried out in Ansys.

The simulation can be found in Appendix A1. The boundary conditions of the simulation were set as the bottom plate was assigned as constant temperature boundary of 50°C and the top surface of the top plate was assigned a boundary of free convection in the air.

The heat flowing from all sides of the sample were calculated. In total 0.60753 W of heat flows in from the bottom surface of the sample. Out of that, 0.1925 W of heat flows from the sides (direction other than measurement of thermal conductivity). The remaining 0.4111 W of heat flows up to the top of aluminum plate. It means that out of 100% heat that gets in, 31.68% heat is lost through the insulating wool to the surrounding. Less than 70% heat passes through the top plate, i.e. the direction in which we are measuring thermal conductivity.

This brings significant uncertainty in heat conductivity that is being measured because the heat loss through surrounding can vary according to a number of factors.

So, it was decided to change the design of the experiment so that we will eliminate this uncertainty. If we consider a cylindrical heater, there will not be any side surfaces (top and bottom areas of cylinders have small surfaces) which will lose heat. Thus, the idea of a cylindrical setup was thought of, which has a heater in center and test specimen surrounding the heater. Initial setup was thought to be a cylinder with outer diameter of the shell as 50 mm with a heater of diameter ¼'' (6.35 mm) at the center. The thermal simulations were carried out to determine the heater power required.

5.2.1 Thermal simulation of the cylindrical test setup

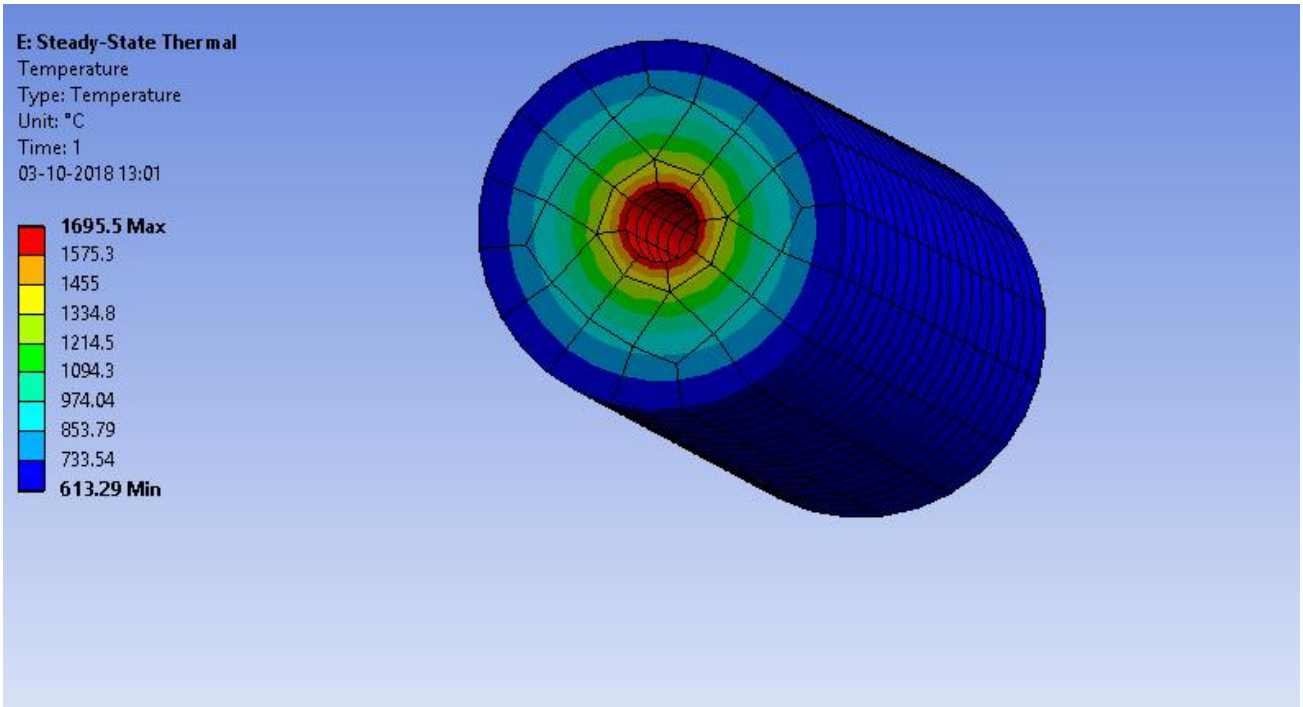

Figure 47: Heat distribution for the sample with a cylindrical heater of 150 W

For initial simulation, we used a heater of power 150 W. The temperatures as shown in Figure 47 were very high compared to the melting point of silicon rubber. Hence, the power of the heater needs to be a lot less than 150W.

Determination of heater power

Since a lot less power was needed than produced by available electric heaters, we had to find out the power of heater using simulations. The temperature of silicon rubber at any point should not exceed 300 °C which is the melting point of silicone rubber. Thus, at the start simulations were carried out at a lower power level. The powers for which simulations were run were 0.5W, 1W and 2W respectively. The temperature distribution in simulations can be seen in Figure 48, Figure 49 and Figure 50.

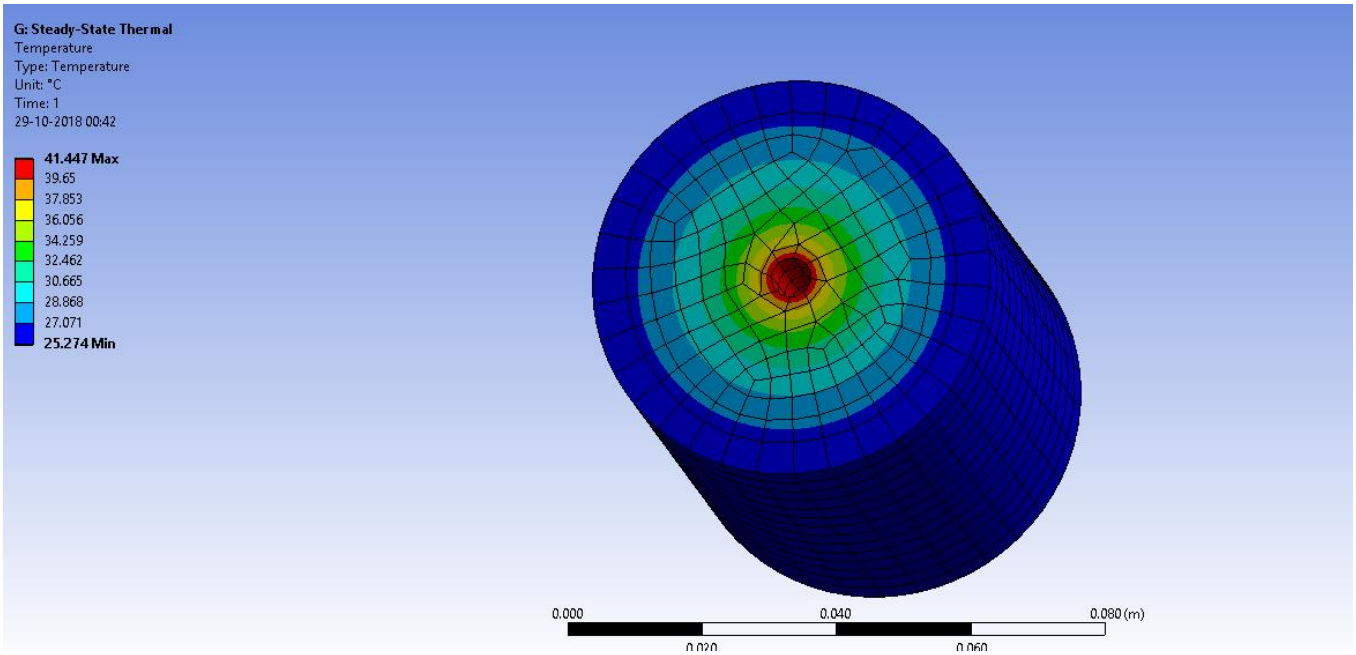

Figure 48: Heat distribution in silicon rubber for test setup at heater Power 0.5W

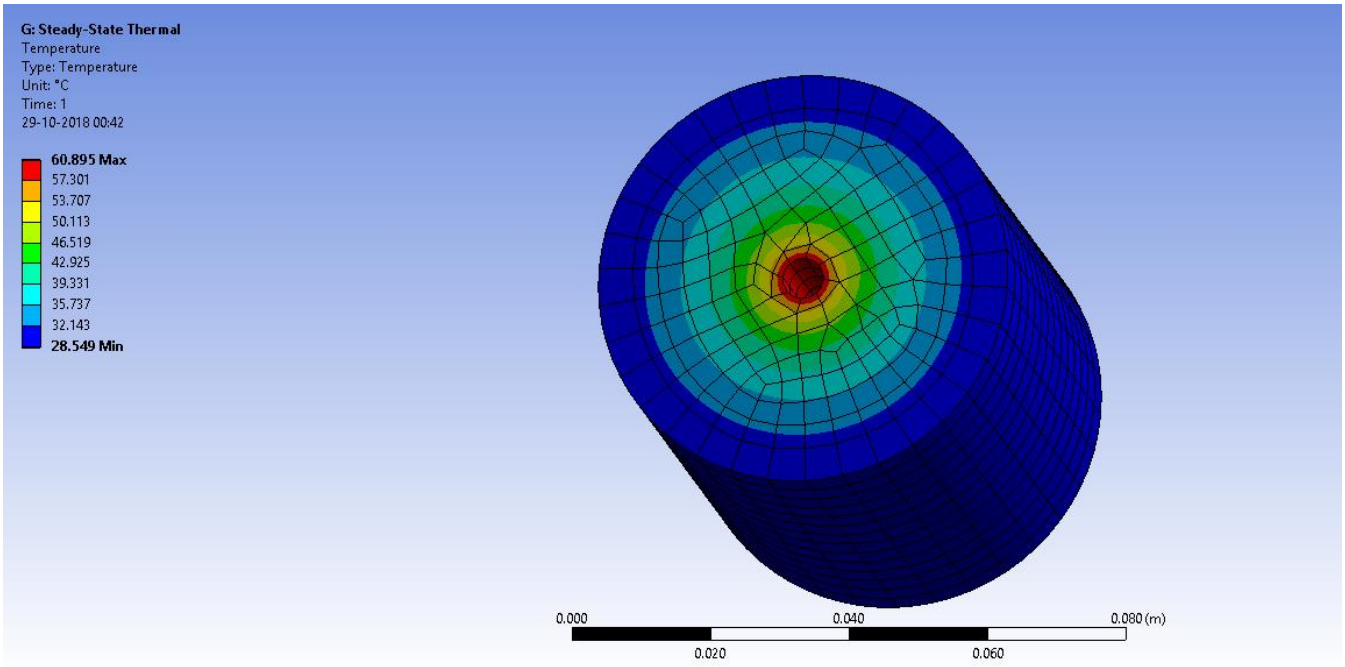

Figure 49: Heat distribution in silicon rubber for test setup at heater Power 1W

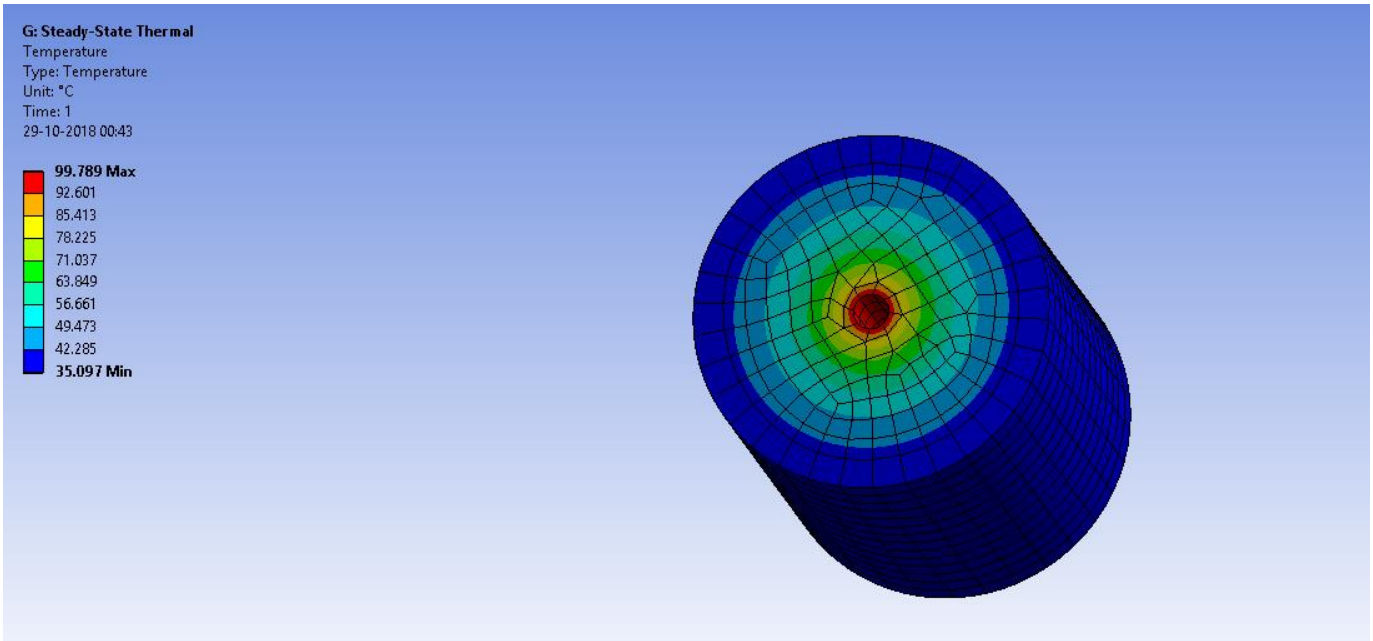

Figure 50: Heat distribution in silicon rubber for test setup at heater Power 2W

From the simulations, it is safe to assume that the heating power of 4W or less is appropriate for the given setup. To achieve lower powers using 150W heater cascading of two variable voltage transformers was tried on. The lowest power available with given dimensions was 32W. The power to the heater was adjusted using a variable voltage transformer.

5.2.2 Thermal conductivity tests: Experimental setup

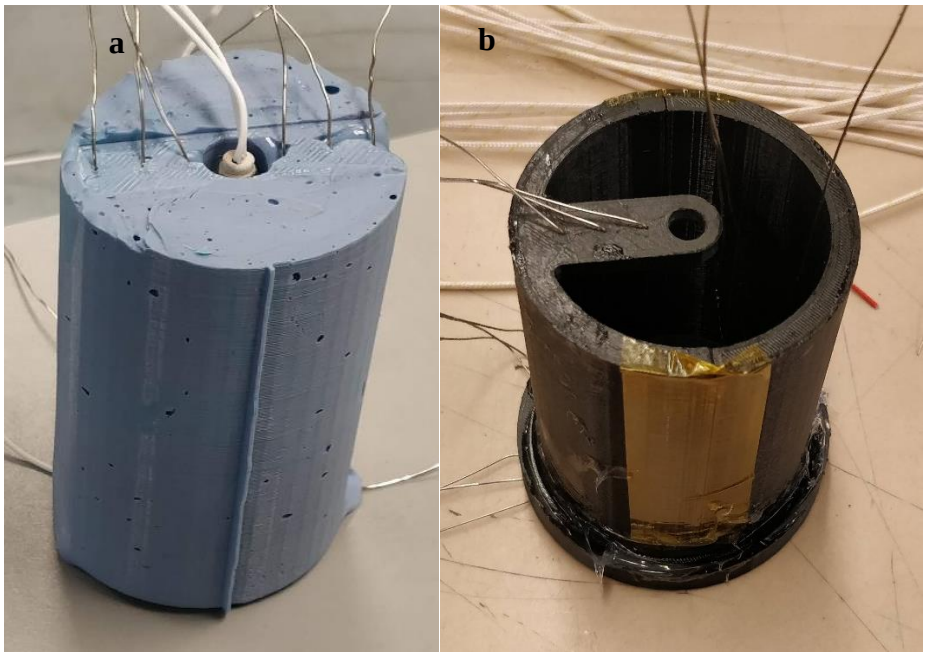

Figure 51: (a)Molded specimen ready for a test (b)3-D printed mold

Figure 52: Experimental setup

The test setup involves a heater surrounded by silicone rubber. The diameter of heater was ¼'' (6.35 mm) and length of the heater was 3.5'' (about 90 mm). The heater power was 32 W. It was

coupled with a variable voltage transformer. The power delivered to the heater is directly proportional to the square of the voltage. The conductivity experiment was carried out for four levels of power, 1-4 W with an increment of 1W. The voltages used for each level of the test can be found in Table 8.

Power (W)	Voltage (V)
1	21.21
2	30.00
3	36.74
4	42.43

Table 8: Voltages applied to the heater for each level of power

The 3-D printed mold was made for molding the silicone into a particular shape. Figure 51(b) shows the mold used to make the sample. It also had accommodation for holding the thermocouples. Thus a total of 6 thermocouples were on each side of the heater. The 3 thermocouples on either side of the heater were at a fixed distance, 7mm, 15mm and 22 mm radially from the center. The samples were made by adding different proportions of graphite to silicon rubber and molding. Figure 51(a) shows the sample taken out from the mold and ready to be tested. Once it was taken out from the mold, a layer of silicone was applied on top and bottom surface in order to increase the insulation from the surrounding. The temperatures were recorded using the DAQ system and the experiment was carried out until the temperatures stabilize for each level of power, i.e. attain steady state. The steady-state temperature readings were recorded and were used for calculation of conductivity.

5.2.2.1 Analytical Background

At steady state,

Consider any two points in the cylindrical shell,

The expression for thermal conductivity is given as follows:

$$k = \frac{P \ln\left(\frac{r_1}{r_2}\right)}{2\pi l(T_1 - T_2)}$$

This expression allows us to calculate conductivity using all other known quantities.

In the experimental procedures, there are 3 points on either side of the heater where we have thermocouples and we will get 3 values of conductivity from them, thus each level of power will give us 6 values and we have 4 power levels, thus total 24 readings per sample.

The least-squares fitting routine was used to calculate the average value of conductivity from these readings. The code for least-square fitting can be found in Appendix A2.

5.2.2.2 Results of the thermal conductivity test

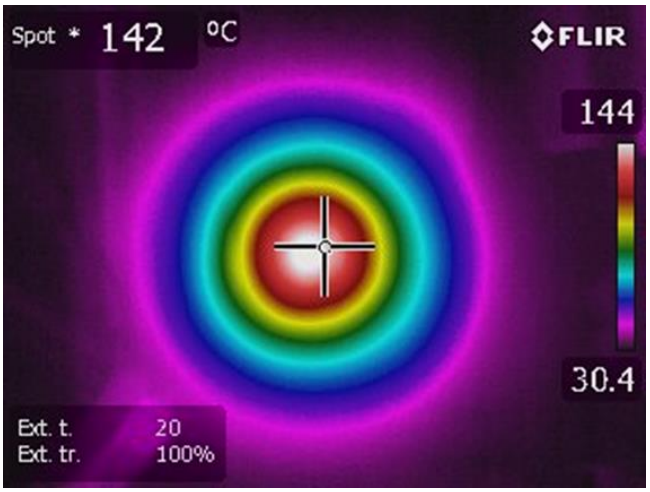

Figure 53: Thermal image of the top surface of a sample taken using an IR camera

The tests were performed with 5 samples, and varying levels of graphite. The sample mass was fixed at 216 grams. The 0,5,10, and 15 grams of carbon were added to silicone respectively.

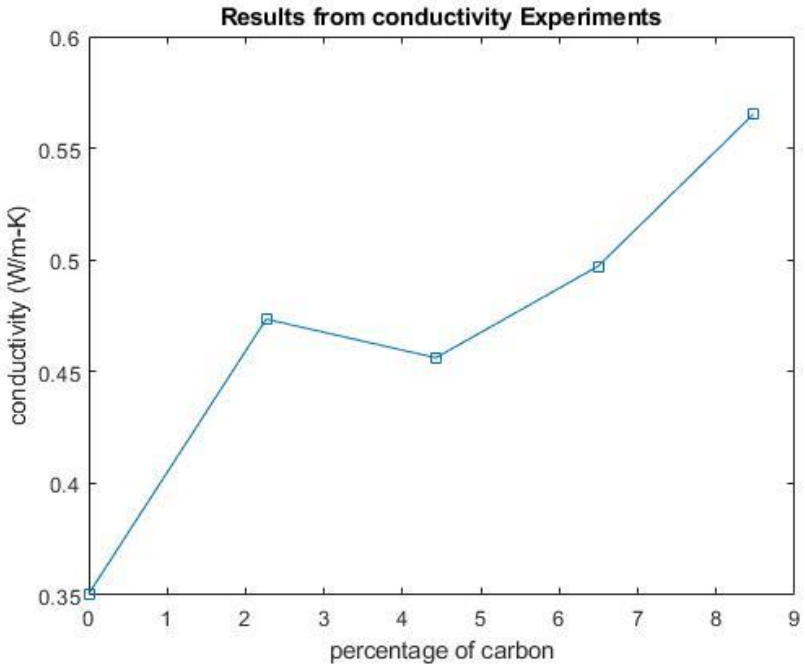

Figure 54: Results from thermal conductivity experiment

Figure 54 depicts results from the conductivity tests performed. We can see a lot of variation from a linear trend. Thus, we can use a curve fitted version for getting the relationship between the percentage of carbon and thermal conductivity. Figure 55 depicts the extrapolated curve.

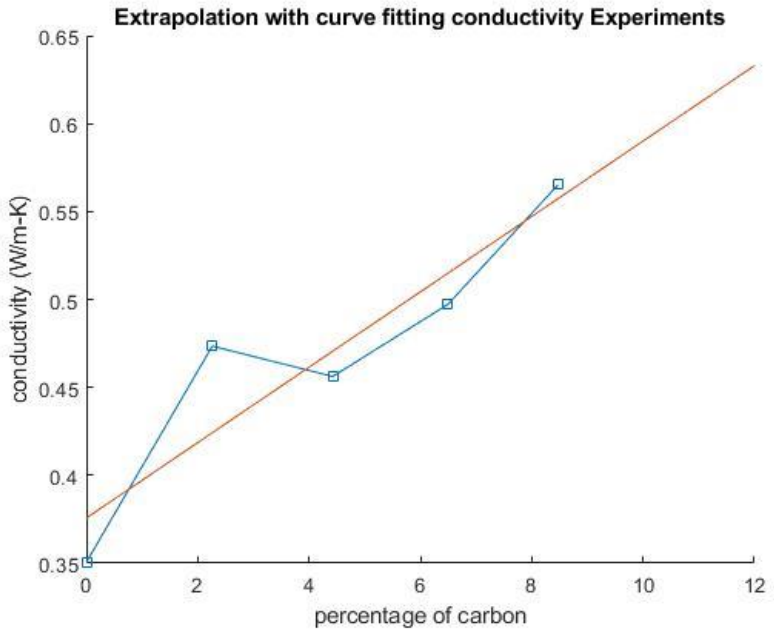

Figure 55: Curve fitted relation between conductivity and percentage of carbon

But we can easily see that actual test results vary from the fitted curve at couple points. It is because of uncertainty in the measurement of the thermocouple location. While molding the thermocouples can be misplaced slightly and this may lead to changes in the computing of conductivity.

The sensitivity of radius on thermal conductivity can be given as follows:

$$\frac{dk}{dr} = \frac{P}{2\pi l \Delta T} x \frac{1}{r}$$

Thus if there is the uncertainty of 0.1 mm in the measurement of radius, the conductivity readings can vary by almost 0.1 W/m-K, which is about 50% of the conductivity of pure silicone.

Therefore, testing conductivity with more sophisticated means was necessary. The firm in Canada named ‘Thermtest’ [37] does test the conductivities of samples. So, a total of 7 samples were sent to measure the conductivity. Results from Thermtest are depicted in Figure 56.

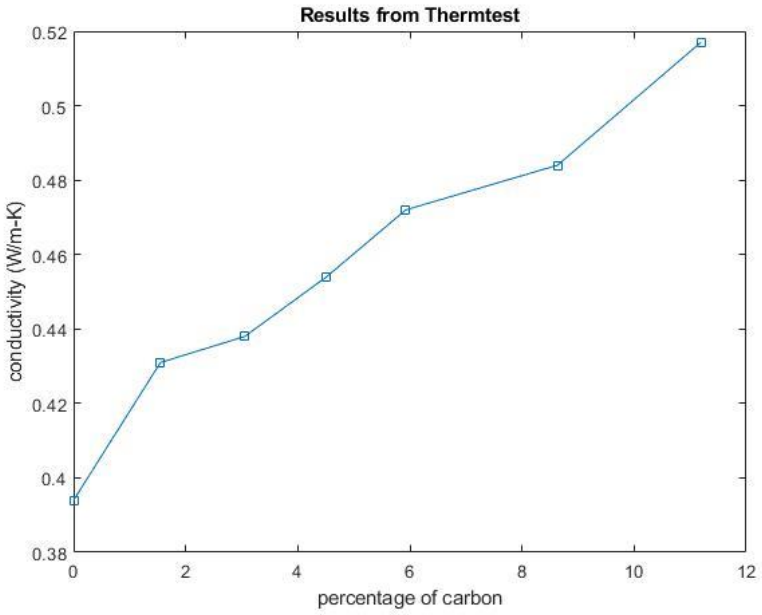

Figure 56: Results from Thermtest [37]

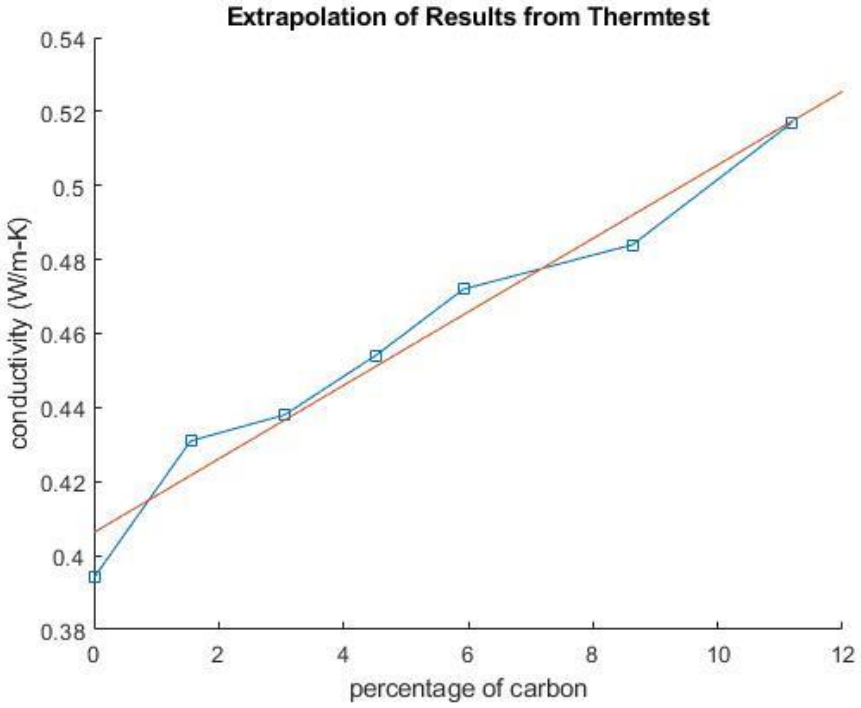

Figure 57: Extrapolated results with curve fitting

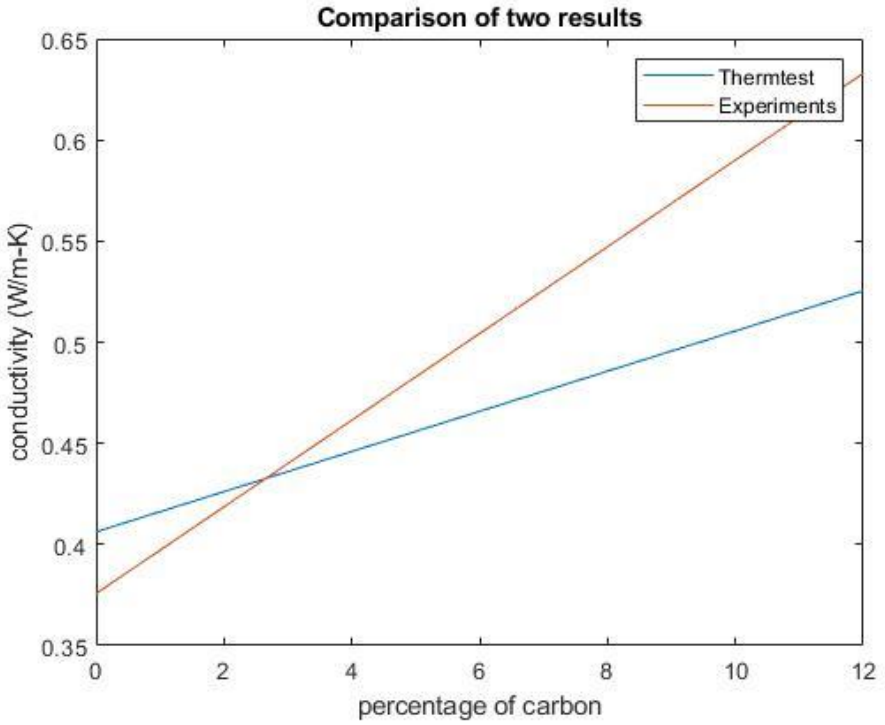

Figure 58: Comparison between Thermtest and Conductivity Experiments (Curve fitted)

Figure 58 depicts a comparison between Thermtest results and results from the conductivity experiments performed in the lab. The Thermtest results were more accurate because they had a batch of 5 experiments per sample, and the average standard deviation was 0.003 W/m-K.

5.3 Design of cooling pad

Figure 59: Design of cooling pad

Figure 59 depicts the design of the cooling pad. The inlet and outlet were on one side of the cooling pad to make a connection to the chiller easy once the cooling pad is wrapped around a leg. The cooling pad was given a flow pattern such that the coolant flows from inlet to outlet while covering the entire length of the leg. The flow channels were kept vertical to provide equal cooling for all parts of the leg because as coolant travels towards the outlet its temperature increases slightly. The dot welds were added across the surface of the cooling pad to prevent bulging of the cooling pad because bulging causes more fluid to flow into the pad and increases the pressure on parts of the pad. It also helps limit the coolant flowing in, thus a chiller with a lower reservoir capacity can be used. The length of the pad was 875 mm and breadth was 735 mm since the upper limit of thigh circumference was 55 cm, and we can wrap the leg with the cooling pad with overlap at its end, giving a firm grip on the Velcro strips.

5.4 Human limb thermal phantom

To test the performance of the cooling pad it was necessary to have something which will mimic the thermal properties of a human limb and also will have a shape like a human limb. Heat transfer characteristics may vary a lot according to the effectiveness of the skin-cooling sleeve contact. Thus, a replication of the exact shape of the human limb was necessary. To achieve that, a mannequin leg was obtained and plaster that is used for setting bone fractures was used to cover the leg. After the plaster was set it was removed by cutting into 2 pieces.

Now to replicate thermal properties, it was necessary to have similar heat holding capacity as the limb and a similar thermal conductivity as in the limb tissues. From simulations, it can be concluded that in transient performance over a long time, temperature characteristics are driven by heat holding capacity. Thus, to increase the heat holding capacity, water could be used. Since water has the highest specific heat (4186 J/kg-K), it can compensate for the low specific heat of silicone rubber (1249 J/kg-K). Average heat holding capacity of the human body is about 3500 J/kg-K. Thus, the foam was used to create an inner layer of the phantom.

Figure 60: Inner layer of the phantom

Figure 60 depicts an inner layer of the phantom which is made up of foam layers. Each layer was cut according to a corresponding cross-section in a plaster mold. The K-type thermocouples are

inserted at 8 various places, at varying depths from the skin surface to keep track of temperatures inside the phantom. Thermocouple 1-3 are just inside the skin layer while thermocouples 4-8 are the core, i.e. at the center of given cross-section plane.

The phantom was later coated with silicone rubber mixed with graphite. 5% of carbon was added to silicone to enhance its conductivity to 0.45W/m-K. The ends were given two openings that can be screwed shut with lids for adding or removing water. The thermocouple wires are attached to the DAQ when tests were carried out. Figure 61 depicts the completed phantom.

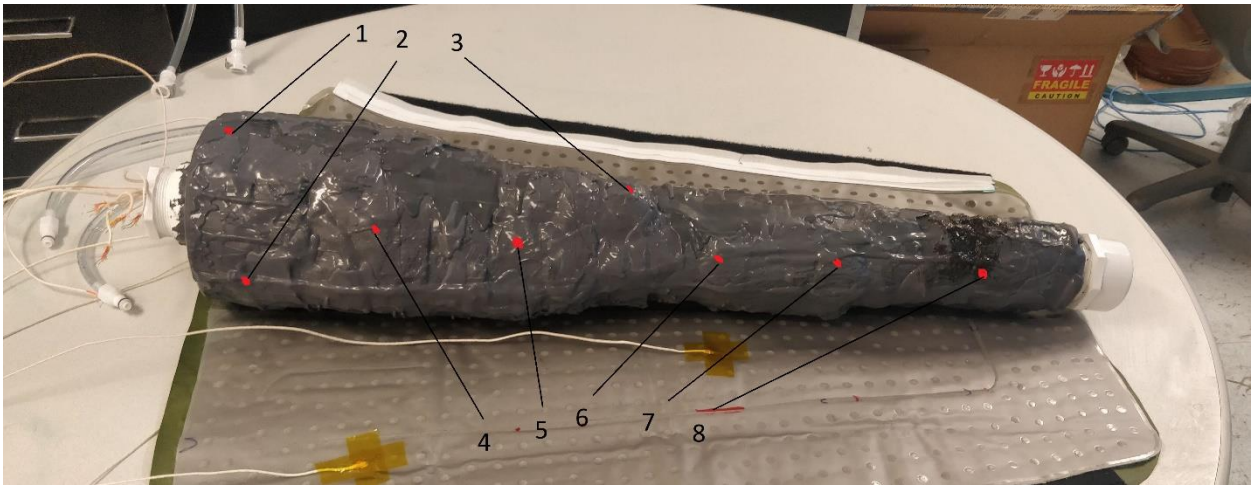

Figure 61: Human limb phantom with locations of thermocouples

This phantom could hold about 7 liters of water. Considering the average person with a weight of 80 kg and the mass percentage of a leg is 12-15% of total body mass, the mass of limb comes out as 9.6 kg. Since the average heat capacity of the human body is about 3500 J/kg-K water equivalent of the limb becomes 8.1 kg. Including the mass of silicone coating and foam, we reach heat capacity almost the same as that of the human limb.

5.5 Testing cooling pad with Human limb phantom

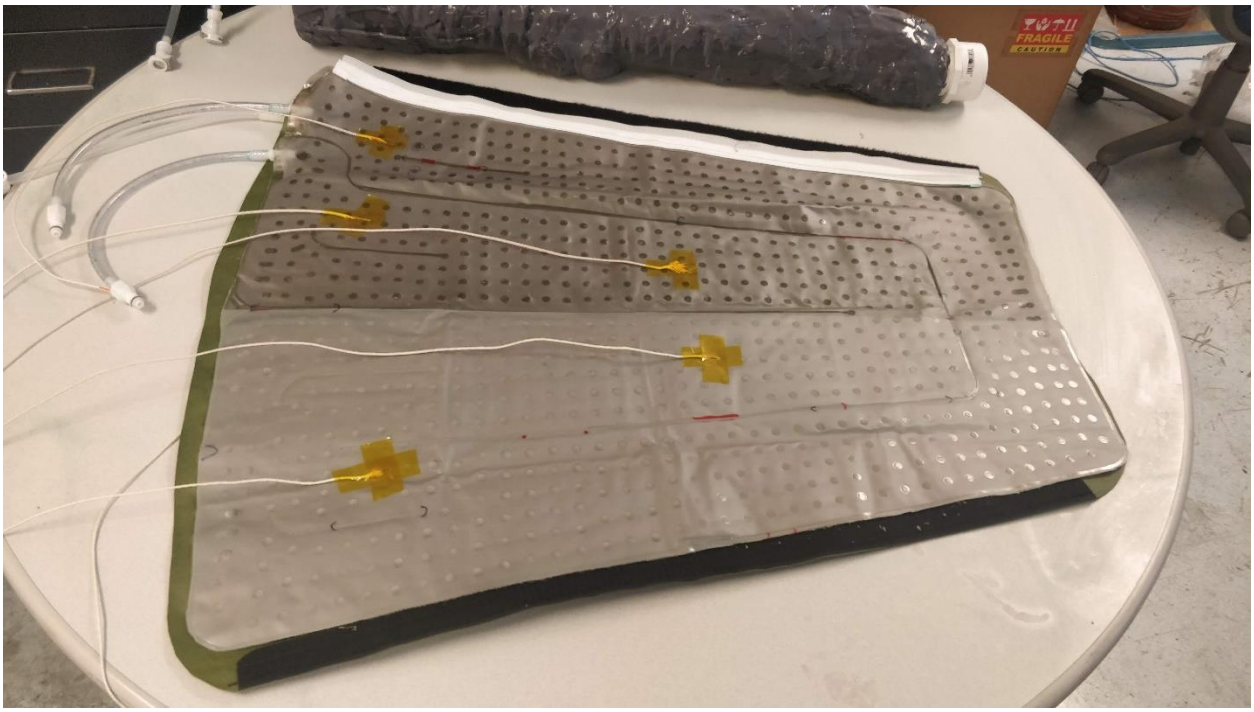

Figure 62: Cooling sleeve lined on top of air splint

The cooling sleeve was tested with the help of the phantom and a 450W chiller. Figure 62 depicts the cooling pad placed on top of an air splint (olive green). There were five thermocouples on the surface of the cooling sleeve. One thermocouple was placed outside the air splint to understand heat loss to the surrounding and one to measure the ambient temperature. Figure 63 depicts the cooling sleeve and the air splint wrapped around the phantom.

Figure 63: Cooling sleeve and air splint wrapped around the phantom

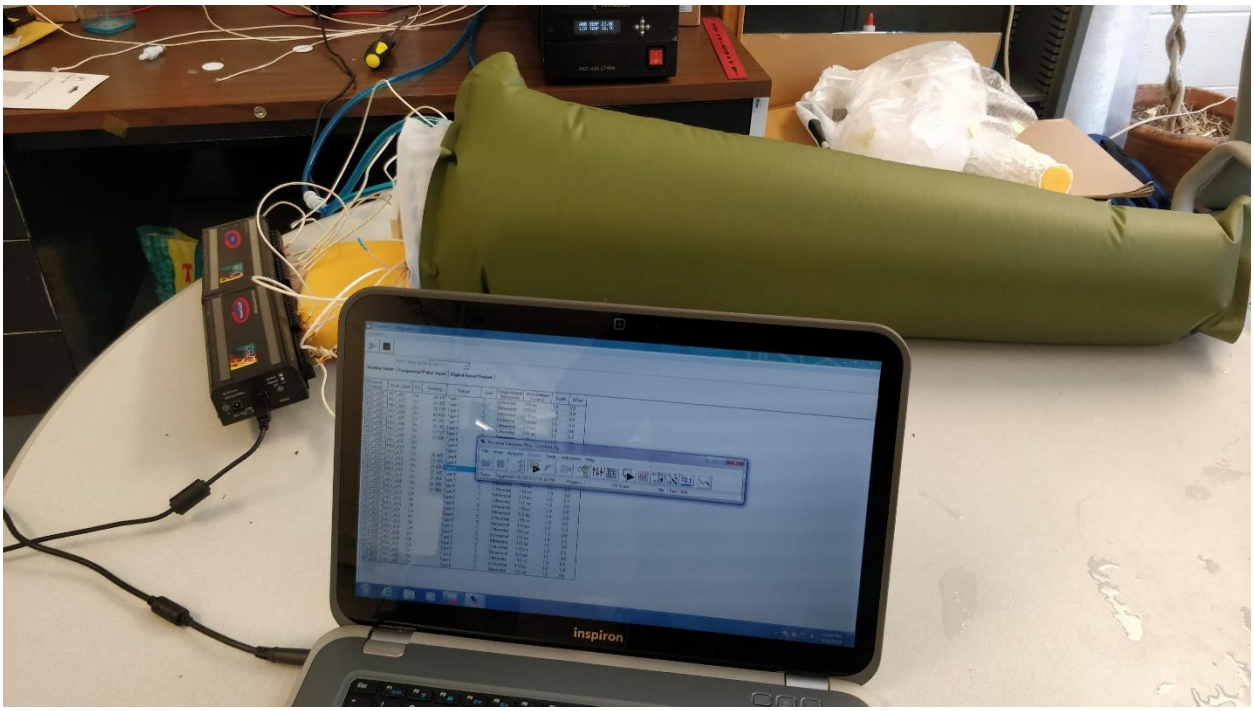

Figure 64: Experiment setup for the testing cooling sleeve

The air pressure inside the air splint was 30 mmHg. The test was run for 8 hours and the temperature histories were recorded.

5.5.1 Results

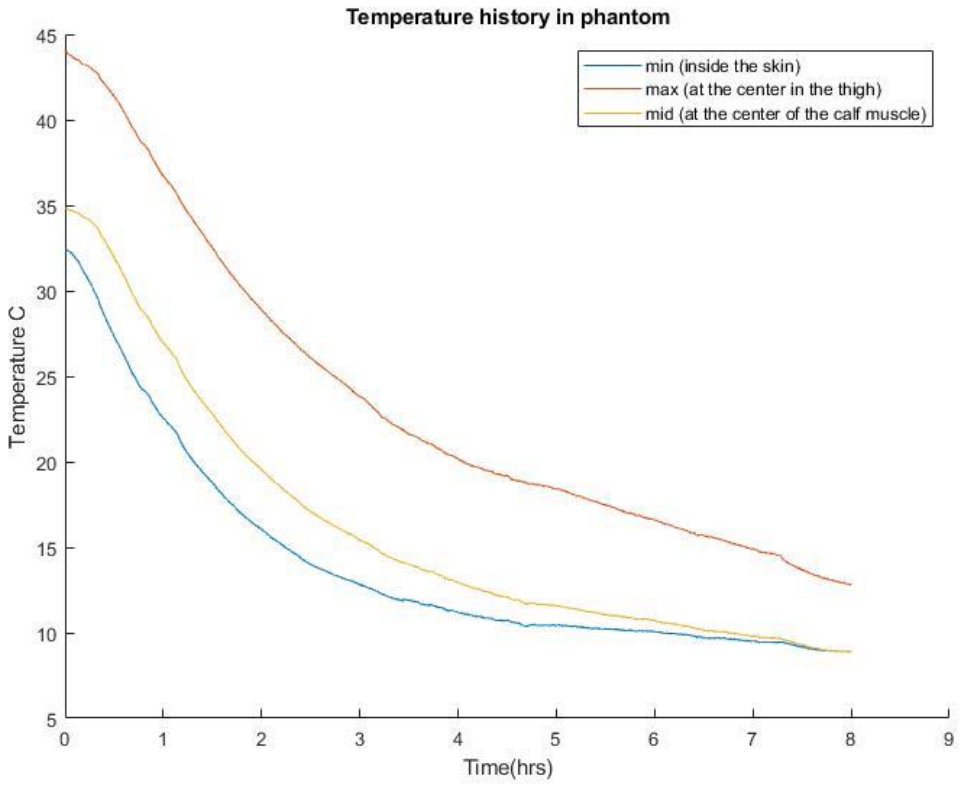

Figure 65: Temperature history in phantom

Figure 65 depicts the temperature history in the phantom under cooling using the cooling pad. Initially, the phantom was filled up with hot water and it started cooling at around 45°C. It took about an hour to reach 37°C. The minimum temperature curve was obtained from a thermocouple which was inserted just inside skin, i.e. it cools down rapidly. The mid curve represents the thermocouple in the lower limb, and as it was observed from simulation results the lower limb cools faster than upper limb because the average diameter is smaller in the lower limb and it also has a lower mass. Maximum temperature curve drops down exponentially as seen from Figure 31 of simulation. It reaches a temperature of 12.86°C in 8 hours. The minimum temperature drops down to 8.90°C at the end of 8 hours.

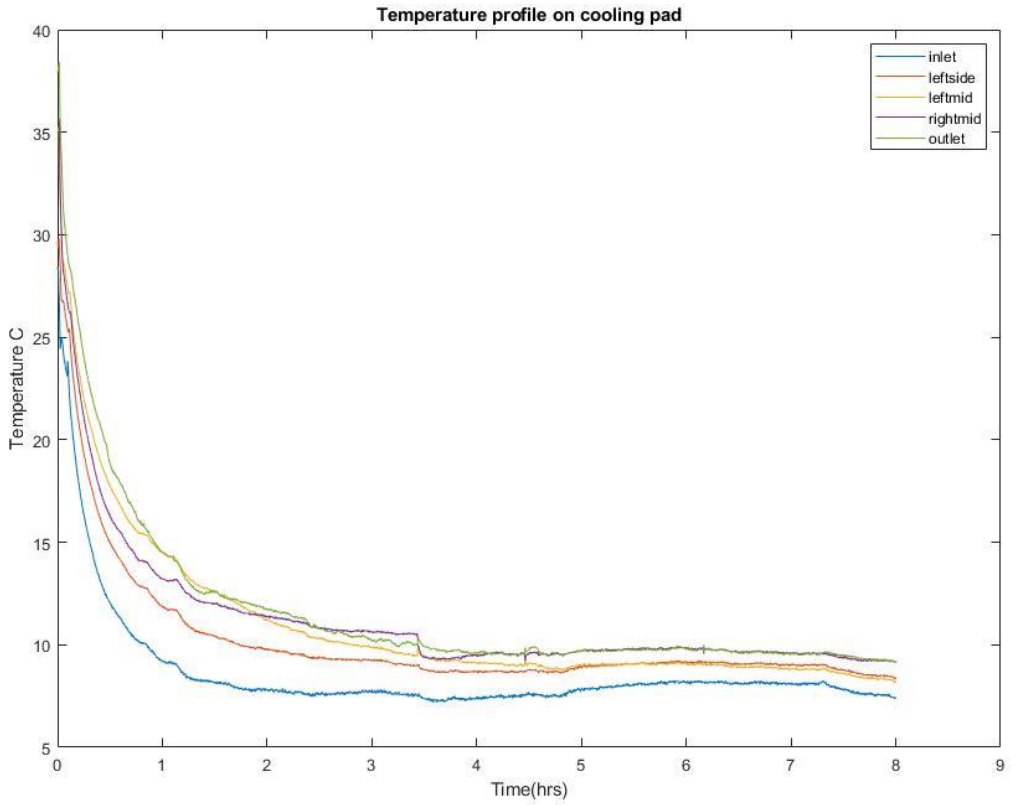

Figure 66: Temperature profiles on the cooling pad

Figure 66 depicts temperature profiles on the surface of the cooling pad. As can be seen, it takes a while for surface temperature to drop. Even when the coolant temperature is set to 0°C the temperature does not drop at the start. Initially, a lot of heat is absorbed by the coolant and thus it takes more time for the coolant to reach the set temperature as the chiller power is limited to 450W. A chiller with higher wattage can help cooling faster in the initial hour, thus increasing the cooling pace and it might need a lesser time to reach a mark of 15°C.

It takes about 4 hours to reach 20°C and it takes 7 hours for the maximum temperature curve to reach down to 15°C. The point of maximum temperature lies at the centerline on the thigh.

5.5.1.1 Comparison of results from phantom and thermal simulations of the human leg

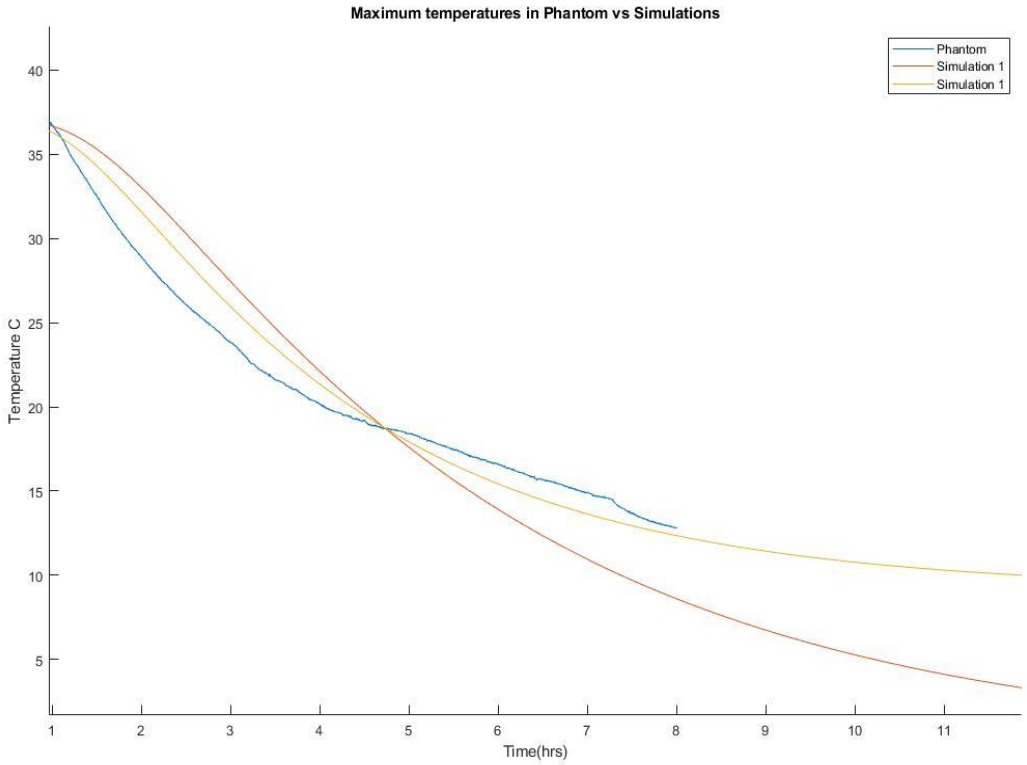

Figure 67: Comparison between results of phantom and simulations

(maximum temperature points at the center of the thigh)

Figure 67 shows a comparison between results from simulations and results from the cooling sleeve test with the phantom. The comparison was started from the 1-hour mark from where the maximum temperature reached 37°C. The temperature curves of maximum temperature in simulation 1 and simulation 2 follow the temperature curve obtained from cooling experiment with the phantom. This validates that the heat holding capacity of the phantom is roughly equivalent to actual human limb in the model. Thus this phantom could be used for the testing purpose where we could simulate thermal properties of human limb and help to improve the design of the cooling sleeve and overall device.

It can be seen that the maximum temperature curve of the phantom deviates from both simulations and does not match either of them exactly. In the first part of the phantom cooling until 5 hours, the phantom cools faster than the simulations. This can be explained with the usage of sponge and water. Because the water can flow inside the sponge, the maximum temperature hotspot cools relatively faster in phantom than in simulations where we have imparted muscle and fat layers where heat diffusion is slower. This can be solved in the next version of phantom by creating multiple compartments of sponge and water isolated from each other. However, heat holding capacity is still similar, thus the curve later represents the temperature of a phantom as a whole, i.e. closer to average temperature. Thus, after the initial drop rate of change of temperature decreases and it becomes slower than that of simulations, which are more representative of ideal case scenarios.

Chapter 6: Conclusions

The results of the thermal simulation of an animal limb model were performed and compared with the results of the study regarding the icepack cooling experiment with an animal limb ischemia. Both simulations approximate the actual situation based on the following assumptions; limb contact with the body is either adiabatic or has constant temperature contact. But the actual result of the cooling experiment lies in-between temperature histories obtained from the two simulations. So we can conclude that thermal regulation in the body with blood loss is a complex process and more experiments with animal limb cooling need to be conducted in an effort to assign more realistic boundary conditions. From simulations we can predict that 450W chiller can be effectively used for animal limb cooling experiments since the maximum power drawn by a cooling sleeve will be 190W. The first simulation reaches 15°C in 70 minutes, while simulation 2 predicts it might take about 95 minutes to reach the mark of 15°C. The actual animal experiment reached a temperature of 15°C in 84 minutes.

The thermal simulation of human limb model was performed and theoretically, it will take a minimum of 6 hours to drop the maximum temperature to 15°C with a constant temperature boundary of 0°C at the skin surface. According to simulation 2, it takes quite a long time to drop the temperature of every point in limb to 15°C, but the average temperature reaches 15°C in 52 minutes. Thus it will be interesting to understand through animal testing results if cooling the whole limb down to a given temperature is necessary or if the average temperature of limb dictates ischemic progression.

However, if we consider a case where the wound is on the lower limb and a tourniquet is applied near the knee, which happens in most limb injuries, the targeted part will be cooled way faster. It takes about 2 hours to drop the temperature of the limb to 15°C.

The 450W chiller may not give quick enough cooling performance because the initial power drawn by the cooling sleeve in simulation is about 650W. The development of custom-built chiller might be necessary for human limb cooling.

The thermal phantom with heat holding capacity equivalent to the human limb was built and the cooling sleeve was tested using the phantom. The results of cooling experiments were compared. After the first hour, the difference between maximum temperature from simulation results and the maximum temperature obtained from phantom remained under 3°C. Thus, the efficacy of thermal phantom was validated.

6.1 Future work

In the future, more simulation with models for various population demographics can be performed to understand the effectiveness of cooling on a variety of individuals. Thermal insulation can be designed for the back of the cooling pad to reduce heat losses. The thermal layer which sticks between cooling sleeve and skin to increase heat transfer efficiency can be developed. The custom-made chiller with given specifications like pressure range, fluid flow rate and power requirement to serve the purpose of human limb cooling can be designed.

References

[1] J. F. Kragh *et al.*, "Minor Morbidity With Emergency Tourniquet Use to Stop Bleeding in Severe Limb Trauma: Research, History, and Reconciling Advocates and Abolitionists," *Mil. Med.*, vol. 176, no. 7, pp. 817–823, Jul. 2011.

[2] C. P. Tountas and R. A. Bergman, "Tourniquet ischemia: Ultrastructural and histochemical observations of ischemic human muscle and of monkey muscle and nerve," *J. Hand Surg. Am.*, vol. 2, no. 1, pp. 31–37, Jan. 1977.

[3] M. Trupiano, S. Aarabi, and A. F. Emery, "Using thermoelectric cooling with tourniquets for nerve preservation," in *ASME 2016 Heat Transfer Summer Conference, HT 2016, collocated with the ASME 2016 Fluids Engineering Division Summer Meeting and the ASME 2016 14th International Conference on Nanochannels, Microchannels, and Minichannels*, 2016, vol. 2, p. Heat Transfer Division-.

[4] T. J. Walters, ; Cpt, R. L. Mabry, and M. C. Usa, "Issues Related to the Use of Tourniquets on the Battlefield," 2005.

[5] M. H. Shishehbor, "Acute and critical limb ischemia: When time is limb," *Cleve. Clin. J. Med.*, vol. 81, no. 4, pp. 209–216, 2014.

[6] A. Mowlavi, M. W. Neumeister, B. J. Wilhelmi, Y.-H. Song, H. Suchy, and R. C. Russell, "Local Hypothermia during Early Reperfusion Protects Skeletal Muscle from Ischemia-Reperfusion Injury," *Plast. Reconstr. Surg.*, vol. 111, no. 1, pp. 242–250, Jan. 2003.

[7] J. G. Wright, J. C. Kerr, C. R. Valeri, and R. W. Hobson, "Heparin decreases ischemia-reperfusion injury in isolated canine gracilis model.," *Arch. Surg.*, vol. 123, no. 4, pp. 470–2, Apr. 1988.

[8] B. V Reamy, "Frostbite: review and current concepts.," *J. Am. Board Fam. Pract.*, vol. 11, no. 1, pp. 34–40, Jan. 1998.

[9] M. Bonora *et al.*, “ATP synthesis and storage.,” *Purinergic Signal.*, vol. 8, no. 3, pp. 343–57, Sep. 2012.

[10] C. Waterhouse and J. Keilson, “Cori cycle activity in man.,” *J. Clin. Invest.*, vol. 48, no. 12, pp. 2359–66, Dec. 1969.

[11] K. Wasserman, “Coupling of external to cellular respiration during exercise: the wisdom of the body revisited.,” *Am. J. Physiol.*, vol. 266, no. 4 Pt 1, pp. E519-39, Apr. 1994.

[12] H. Stegmann, W. Kindermann, and A. Schnabel, “Lactate Kinetics and Individual Anaerobic Threshold*,” *Int. J. Sports Med.*, vol. 02, no. 03, pp. 160–165, Aug. 1981.

[13] R. M. H. Heck, A. Mader, G. Hess, S. Mucke, “Justification of the 4-mmol/l Lactate Threshold.”

[14] M. A. Creager, J. A. Kaufman, and M. S. Conte, “Acute Limb Ischemia,” *N. Engl. J. Med.*, vol. 366, no. 23, pp. 2198–2206, Jun. 2012.

[15] J. J. Earnshaw, B. Whitman, and C. Foy, “National Audit of Thrombolysis for Acute Leg Ischemia (NATALI): clinical factors associated with early outcome,” *J. Vasc. Surg.*, vol. 39, no. 5, pp. 1018–1025, May 2004.

[16] J. L. Eliason *et al.*, “A national and single institutional experience in the contemporary treatment of acute lower extremity ischemia.,” *Ann. Surg.*, vol. 238, no. 3, pp. 382–9; discussion 389-90, Sep. 2003.

[17] J. B. O’Connell and W. J. Quiñones-Baldrich, “Proper Evaluation and Management of Acute Embolic versus Thrombotic Limb Ischemia,” *Semin. Vasc. Surg.*, vol. 22, no. 1, pp. 10–16, Mar. 2009.

[18] B. C. Solymoss, P. Nadeau, D. Millette, and L. Campeau, “Late thrombosis of saphenous vein coronary bypass grafts related to risk factors.,” *Circulation*, vol. 78, no. 3 Pt 2, pp.

I140-3, Sep. 1988.

[19] “Tourniquet Conversion,” *http//www.specialoperationsmedicine.org/Documents/PFC WG/Drew JSOM Fall 2015 Ed.*

[20] “Every Second Counts - Red Cross Tourniquet.” [Online]. Available: https://redcrosstourniquet.com/. [Accessed: 28-Jul-2019].

[21] K. Kumar, C. Railton, and Q. Tawfic, “Tourniquet application during anesthesia: "What we need to know?",” *J. Anaesthesiol. Clin. Pharmacol.*, vol. 32, no. 4, pp. 424–430, 2016.

[22] “The Facts & Details About Different Types of Tourniquets - Journal of Emergency Medical Services.” [Online]. Available: https://www.jems.com/articles/print/volume-38/issue-11/2013-buyer-s-guide/facts-details-about-different-types-tour.html. [Accessed: 28-Jul-2019].

[23] “Different Types of Tourniquets: What You Need to Know.” [Online]. Available: https://scorpionsurvival.com/different-types-of-tourniquets/. [Accessed: 28-Jul-2019].

[24] “‘Game changer:’ Tourniquet for abdominal wounds is already saving lives,” *https://www.stripes.com/news/game-changer-tourniquet-for-abdominal-wounds-is-already-saving-lives-1.235791*.

[25] “Here are the details on the new combat tourniquet | Article | The United States Army.” [Online]. Available: https://www.army.mil/article/176507/here_are_the_details_on_the_new_combat_tourniquet. [Accessed: 28-Jul-2019].

[26] “Brain cooling device and method for cooling,” *https://patents.google.com/patent/US5913885A/en*, May 1995.

[27] J. N. (Junuthula N. Reddy and D. K. Gartling, *The finite element method in heat transfer and fluid dynamics*. CRC Press, 2010.

[28] R. W. (Roland W. Lewis, *The finite element method in heat transfer analysis*. Wiley, 1996.

[29] “Image to 3D Models Software | Simpleware Solutions.” [Online]. Available: https://www.synopsys.com/simpleware.html. [Accessed: 19-Aug-2019].

[30] J. Ashburner and K. J. Friston, “Why Voxel-Based Morphometry Should Be Used,” *Neuroimage*, vol. 14, no. 6, pp. 1238–1243, Dec. 2001.

[31] “Thermal Properties,” *http://users.ece.utexas.edu/~valvano/research/Thermal.pdf*.

[32] “Heat Capacity » IT’IS Foundation.” [Online]. Available: https://itis.swiss/virtual-population/tissue-properties/database/heat-capacity/. [Accessed: 11-Apr-2019].

[33] S. Kashi *et al.*, “Mechanical, Thermal, and Morphological Behavior of Silicone Rubber during Accelerated Aging,” *Polym. Plast. Technol. Eng.*, vol. 57, no. 16, pp. 1687–1696, Nov. 2018.

[34] “Types and Properties of Moldable Silicone Rubber - Albright Technologies.” [Online]. Available: https://albrightsilicone.com/types-and-properties/. [Accessed: 09-Aug-2019].

[35] “Properties: Silicone Rubber.” [Online]. Available: https://www.azom.com/properties.aspx?ArticleID=920. [Accessed: 09-Aug-2019].

[36] “Characteristic properties of Silicone Rubber Compounds,” *https://www.shinetsusilicone-global.com/catalog/pdf/rubber_e.pdf*.

[37] “Thermal Conductivity Measurement Systems and Meters | Thermtest.” [Online]. Available: https://thermtest.com/. [Accessed: 19-Aug-2019].

[38] “Thermocouple-Thermocouples-What is a thermocouple-Types of thermocouples.”

[Online]. Available: https://www.thermocoupleinfo.com/. [Accessed: 09-Jul-2019].

[39] "Thermocouple Type K | Type K Thermocouple | Chromel/Alumel Thermocouple." [Online]. Available: https://www.thermometricscorp.com/thertypk.html. [Accessed: 09-Jul-2019].

[40] "Out-of-the-Box Software for the Personal Daq/50 Series - Measurement Computing." [Online]. Available: https://www.mccdaq.com/products/personal_daqview. [Accessed: 10-Aug-2019].

Appendix

A1. Thermal Simulation of the old conductivity test setup

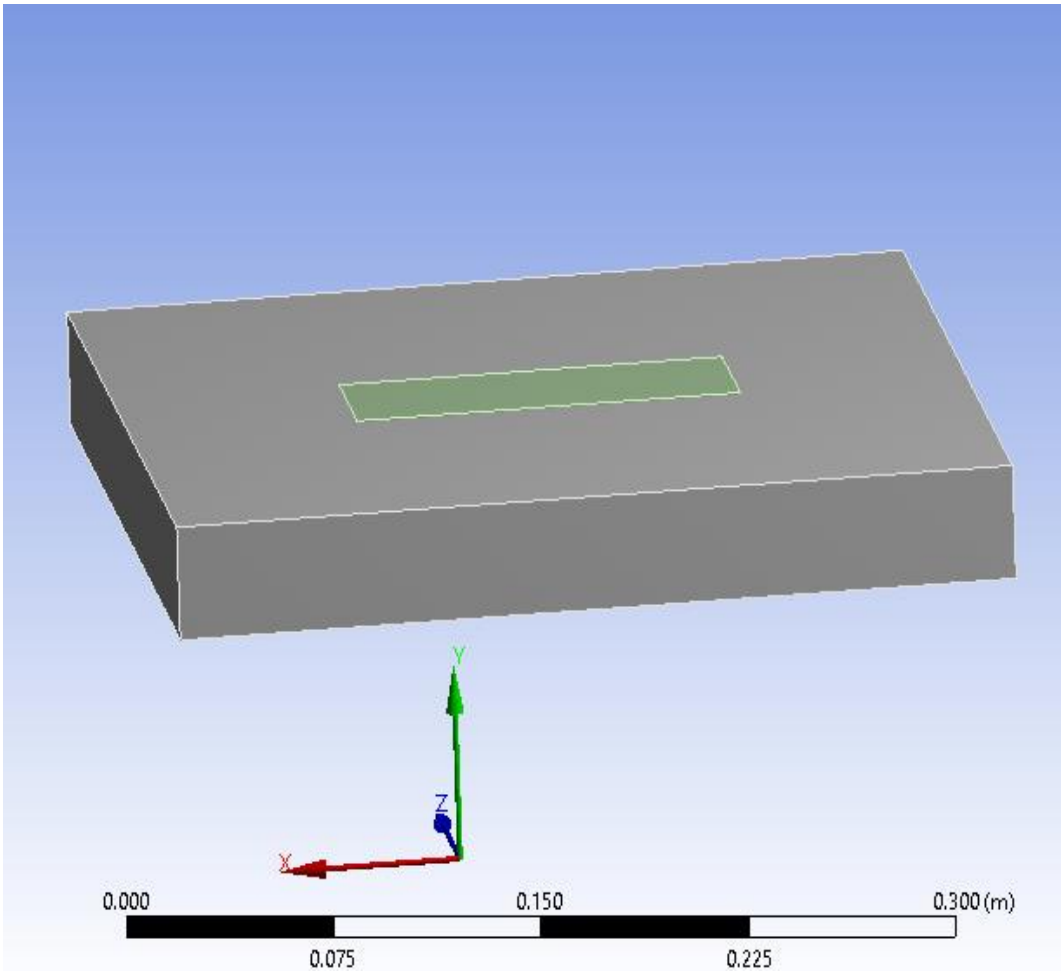

Figure 68: Testbed assembly with glass wool insulation

Figure 68 shows the testbed assembly where the grey shading region shows glass wool insulation, and 3- plate assembly. Figure 69: 3-plate assembly depicts a 3-plate assembly. The bottom plate of the 3-plate assembly was exposed to a constant temperature boundary of 50°C and the top plate was exposed to open air convective boundary.

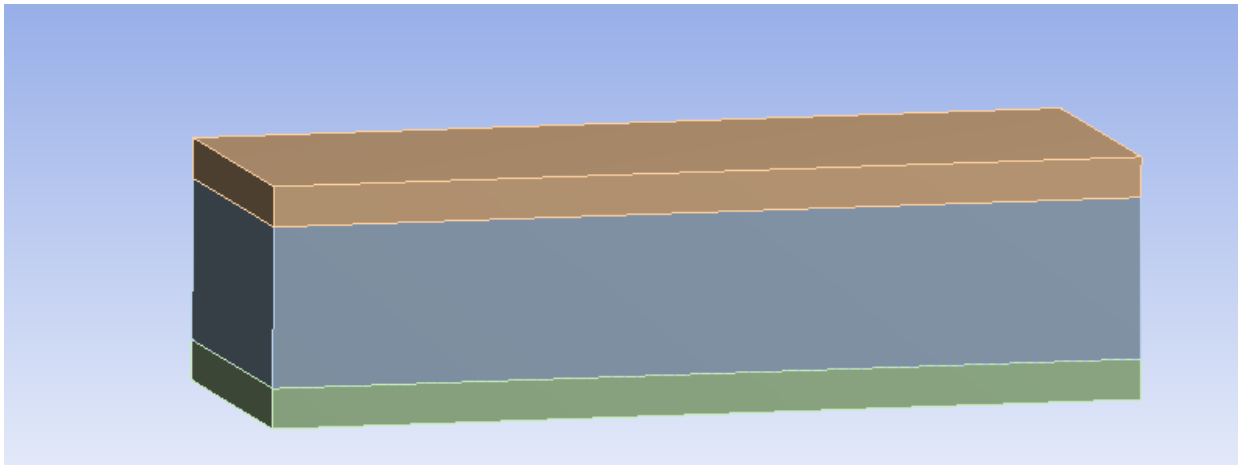

Figure 69: 3-plate assembly

Thermal simulations and results

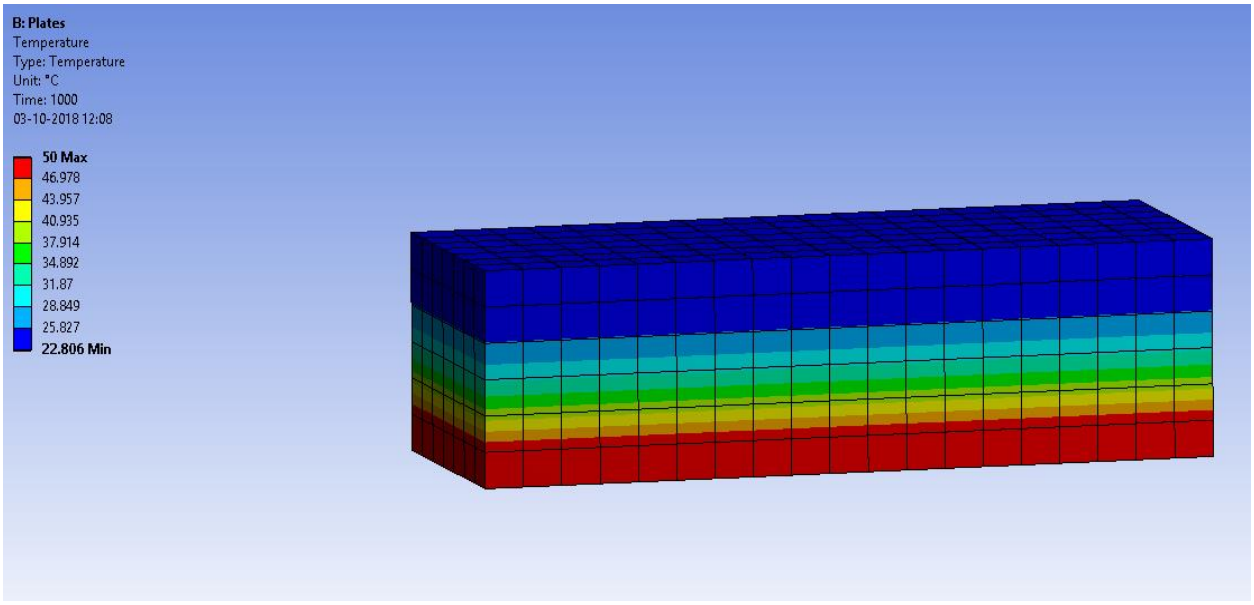

Figure 70: The temperature distribution for 3-plate assembly

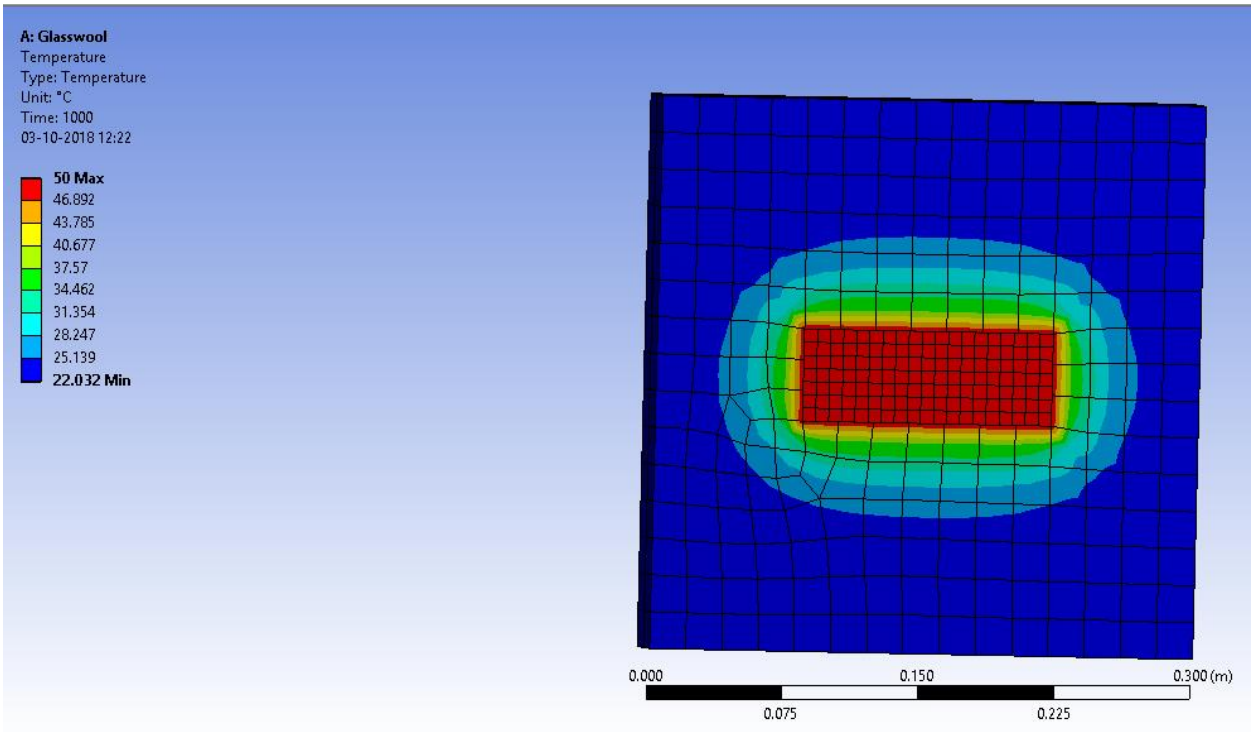

Figure 71: Temperature distribution of the entire assembly including glass wool insulation

Figure 70 shows the temperature distribution in the 3-plate assembly. Figure 71 shows the heat has been spreading through glass wool insulation. The heat loss from sides is considerably high. Thus, the second simulation where we have constant heat flux flowing in from bottom plate was carried out. The constant heat source of 200 W/m2 at bottom of the aluminum plate was used. The resulting temperature distribution can be seen in Figure 72.

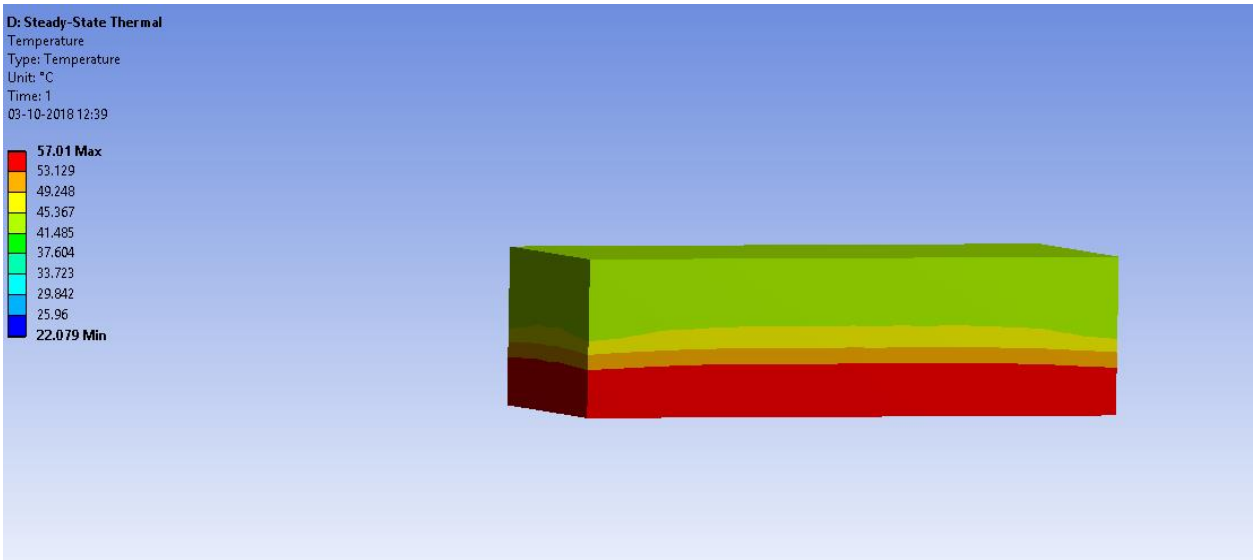

Figure 72: Temperature distribution at steady-state with a constant heat source of 200 W/m^2

A2. Least square code used to calculate thermal conductivity

```
graper='20';
ff=pwd;
cd 'DAQ';
cd (graper);


for i=1:4
   n=num2str(i);
   m=('.txt');
   rr=[n m];
   a=readtable(rr);
   t=a(end,1:6);
   for j=1:6
      T(i,j)=str2num(cell2mat(t{1,j}));
   end
end
cd(ff);

pp=[1 2 3 4];

a=8;
b=14.25;
c=23;
f=6;
e=13.5;
d=22;
r=[b/c a/b a/c f/d f/e e/d];

K=loconcal0(T,r,pp);

%K=K(:);
%x=1:24;
x=1:6;

k=lesqco0(T,r,pp);
ks=k*ones(1,6);


%figure()
plot(x,K,x,ks)
xlabel('reading number')
ylabel('conductivity')
%legend('local conductivities','least squares')
y=[graper ' grams of carbon'];
title(y)

function h=loconcal0(T,r,pp)
   t=zeros(4,6);
   for i=1:4
      for j=1:6
         val=j;
         switch val
```

```
            case 1
                t(i,j)=T(i,j)-T(i,j+1);
            case 2
                t(i,j)=T(i,j)-T(i,j+1);
            case 3
                t(i,j)=T(i,j)-T(i,j-2);
            case 4
                t(i,j)=T(i,j)-T(i,j+2);
            case 5
                t(i,j)=T(i,j)-T(i,j-1);
            case 6
                t(i,j)=T(i,j)-T(i,j-1);
        end
      end
   end
   p=pp;
   t=abs(t);
   %r=[7/15 15/22 7/22 7/22 7/15 15/22];

   con=zeros(4,6);

   for i=1:4
      for j=1:6
         %mod(i,j)=abs(kg*2*pi*0.083*t(i,j)/log(r(j)));
         con(i,j)=abs(p(i)*log(r(j))/(2*pi*0.083*(t(i,j))));
      end
   end
    h=con;
end

function h=lesqco0(T,r,pp)
   t=zeros(4,6);
   for i=1:4
      for j=1:6
         val=j;
         switch val
            case 1
                t(i,j)=T(i,j)-T(i,j+1);
            case 2
                t(i,j)=T(i,j)-T(i,j+1);
            case 3
                t(i,j)=T(i,j)-T(i,j-2);
            case 4
                t(i,j)=T(i,j)-T(i,j+2);
            case 5
                t(i,j)=T(i,j)-T(i,j-1);
            case 6
                t(i,j)=T(i,j)-T(i,j-1);
        end
      end
   end

   t=abs(t);
   %r=[7/15 15/22 7/22 7/22 7/15 15/22];
   %r=[15/22 7/15 7/22 7/22 7/15 15/22];
```

```
    conv=1;
    tol=1.e-4;
    %k=pow*log(radratio)/2*pi*0.083*dt
    kg=1;%guess K

    p=pp;
    while(conv>tol)
       s=zeros(4,6);
       mod=zeros(4,6);
       res=zeros(4,6);
       for i=1:4
          for j=1:6
             x=abs(kg*2*pi*0.083*(t(i,j))/log(r(j)));
             mod(i,j)=x;%model=power
             res(i,j)=p(i)-mod(i,j);
             s(i,j)=2*pi*0.083*t(i,j)/log(r(j)); %sensitivity of k
          end
       end
       s=s(:);
       res=res(:);
       %s=s';
       g=inv(s'*s);
       cor=g*s'*res;
       kg=kg-cor;
       conv=norm(cor);
       kg;
    end
    h=kg;
end
```

A3. Thermocouples

Thermocouples are sensors which measure temperature. Thermocouples are active sensors, i.e. they convert nonelectrical input to electrical output. They are made up of two dissimilar metal strips and at a junction, they generate a voltage difference depending on the temperature difference. The thermoelectric effect is the reason behind this temperature-voltage relation. For a given pair of metals, the same temperature difference gives the same voltage difference, i.e. there is one to one relation for temperature and voltage difference generated across a junction. This is usually a linear relation and thus can be used to measure the temperature by calibrating its one end with known temperature such as an ice bath.

There are various types of commercially available thermocouples. Depending on the pair of alloys that are used in thermocouples we get different sensitivity and different temperature sensing ranges. Some of the commercially available thermocouples are listed in Table 9 [38]:

Sr. no.	Type	Metal alloys	Range low °C	Range High °C	Tolerance °C
1	K	NiCr-NiAl	0	1100	±1.5
2	J	Fe-Constantan	0	750	±1.5
3	N	Nicrosil-Nisil	0	1100	±1.5
4	R	PtRh13-Pt	0	1600	±1
5	S	PtRh10-Pt	0	1600	±1
6	B	PtRh30-PtRh6	200	1700	±1
7	T	Cu-Constantan	-185	300	±0.5
8	E	NiCr-Constantan	0	800	±61.5

Table 9: Types of thermocouples

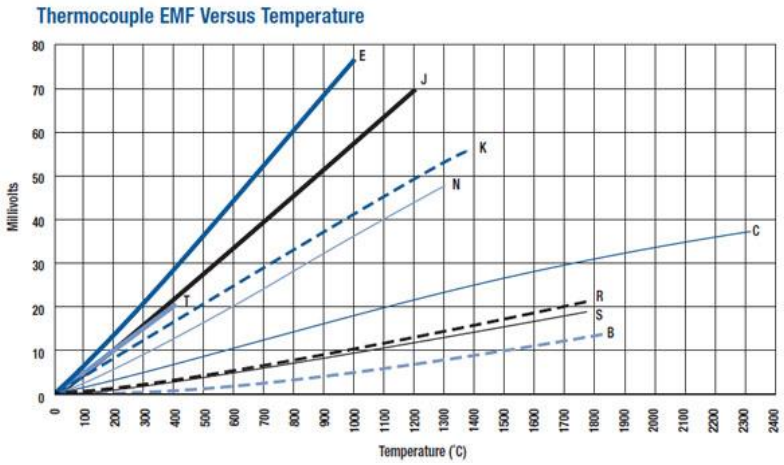

Figure 73: Sensitivity of various types of thermocouples

Figure 73 gives us an idea about the sensitivity of various thermocouple types.[39] The sensitivities of thermocouples are expressed in V/°C or mV/°C. The signal from thermocouples is usually fed to a data acquisition system which encompasses the conversion of voltages to corresponding temperatures for each type of thermocouples. The noble metal thermocouples have a longer life and are immune to a change of sensitivity over time and thermal cycles.

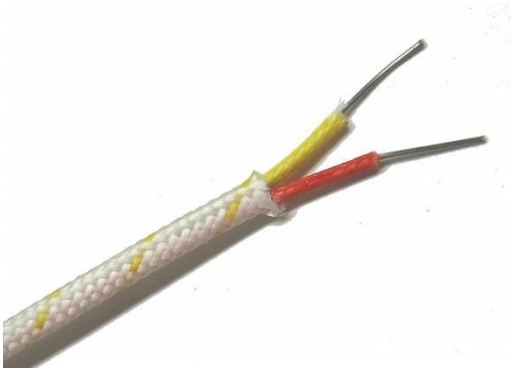

Figure 74: Thermocouple wire-positive and negative end

Figure 74 shows a typical thermocouple wire. The yellow wire is the positive end and the red wire is the negative end. The ends of the wire are welded together to create a junction. There are two qualities of wires available. Thermocouple grade wire and extension wire. The first kind is used as thermocouple probes and to create junctions, which actually does help measure temperature

accurately. On the other hand, extension grade wire is lower grade and typically used to extend probe wire to data acquisition systems. In industries, extension grade wires are very important because the control or data acquisition unit might be quite far from the point where the temperature sensing is being done. Since the extension grade wire is cheaper than thermocouple grade wires, we need them for an extension.

K-type Thermocouple

In the thermal conductivity experiments K- type thermocouple wires were used. It has a range of 0-1100 °C. The yellow lead is positive and non-magnetic. The red lead is negative and non-magnetic. The thermocouple leads are made up of *Chromel* (90% Nickel 10% Chromium) and *Alumel* (95% Nickel 2% Manganese 2% Aluminum 1% Silicon) which are positive and negative end respectively. It comes in two variants, one with a lower tolerance of ±1.5 °C and other class with slightly higher tolerance of ±2.5 °C.

K-type thermocouples can be used in multiple environments like aqueous solutions, dry areas, hot parts of the vehicle like engine, exhausts, even high pressure and temperature environments like boilers. This versatile nature of K-type makes it favorite choice in the industry. It has good linearity in range it operates in, it is chemically stable and inexpensive compared to other thermocouple types. The only drawback is it has aging of emf characteristic as time passes which do not happen with noble metal thermocouples like B, R or S type.

It has a quite big range and gives the linear output of -6.4 to 54.9 mV of output over the range. The sensitivity of K-type thermocouples is approximately 41µV/°C. Thus, this makes it a better choice than other temperature- electric transducers like thermistors or resistance temperature detectors.

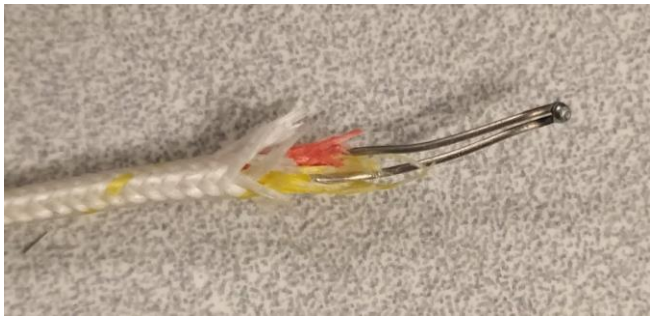

Figure 75: Welded K type thermocouple

There are several different types of K-type thermocouple junctions. In the first grounded type, the wires are grounded by welding sheath and thermocouple wires together. This gives a very good response time, but because of grounding may introduce interference. In the second ungrounded type, the welded wires are insulated from the sheath and thus reducing the interference. This introduces latency in readings. The third method is directly welding the wires to form a junction without a sheath. See Figure 75 In this method the response time is good because of the direct connection and the noise level is not that high because of the absence of sheath. This method is, however, is not recommended at the places where junction can be exposed to chemicals and solutions because this method does not shield thermocouples junction in any way and thus the corrosion rate can be high at the junction, requiring frequent replacement of thermocouple probes. [39]

A4. Data Acquisition Systems (DAQ)

In both cases, in the thermal conductivity tests and the thermal phantom thermocouples were used to sense the temperature. Thermocouples measure temperature by converting temperature to a potential difference. So, we need a system which will correlate temperature with a potential difference. The data acquisition system does that. Figure 76 depicts a general block diagram of the DAQ system.

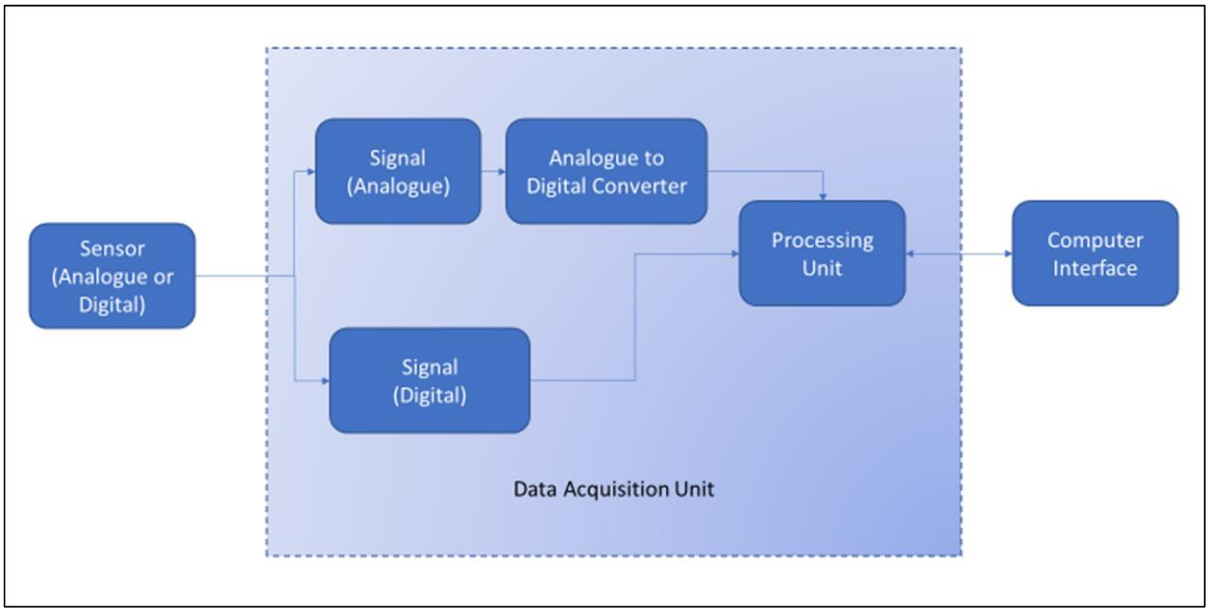

Figure 76: Block diagram of the DAQ system

DAQ has a number of input channels, either configured for analog or digital inputs. Analog inputs pass through A/D (Analogue to Digital) converters. The processing unit processes the data and relays the data to the computer. Usually, various DAQ systems have Graphical User Interfaces (GUIs) as computer applications. We can set a channel configuration where we can select channels that are going to be active. We can select the type of inputs, for example, if we set channel type as K-type thermocouple then it automatically converts potential difference to corresponding temperatures and displays data in °C. We can set the frequency of readings so that we can choose

the interval between two readings. Figure 77 shows the Personal DAQ View GUI that comes with the series Personal DAQ/50 series device that was used with all tests.

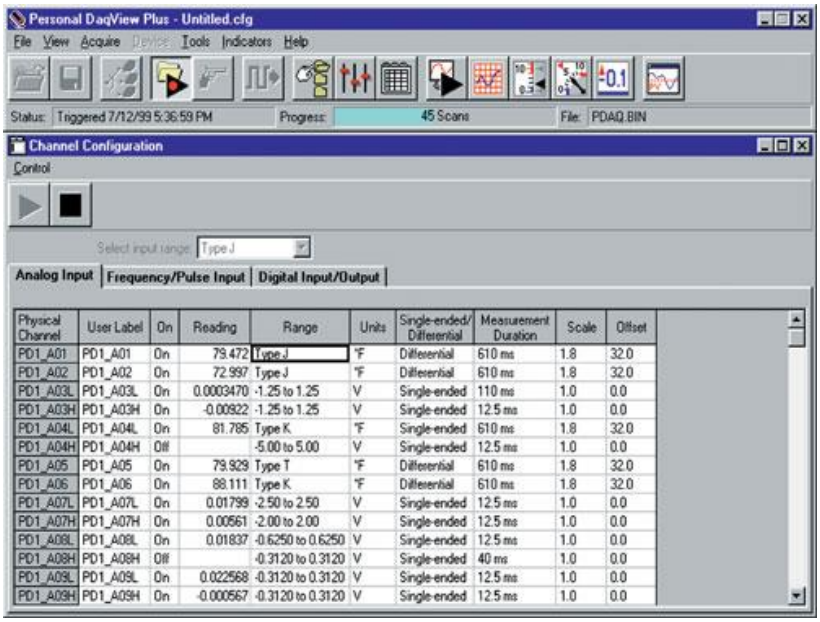

Physical Channel	User Label	On	Reading	Range	Units	Single-ended/ Differential	Measurement Duration	Scale	Offset
PD1_A01	PD1_A01	On	79.472	Type J	°F	Differential	610 ms	1.8	32.0
PD1_A02	PD1_A02	On	72.997	Type J	°F	Differential	610 ms	1.8	32.0
PD1_A03L	PD1_A03L	On	0.0003470	-1.25 to 1.25	V	Single-ended	110 ms	1.0	0.0
PD1_A03H	PD1_A03H	On	-0.00922	-1.25 to 1.25	V	Single-ended	12.5 ms	1.0	0.0
PD1_A04L	PD1_A04L	On	81.785	Type K	°F	Single-ended	610 ms	1.8	32.0
PD1_A04H	PD1_A04H	Off		-5.00 to 5.00	V	Single-ended	12.5 ms	1.0	0.0
PD1_A05	PD1_A05	On	79.929	Type T	°F	Differential	610 ms	1.8	32.0
PD1_A06	PD1_A06	On	88.111	Type K	°F	Differential	610 ms	1.8	32.0
PD1_A07L	PD1_A07L	On	0.01799	-2.50 to 2.50	V	Single-ended	12.5 ms	1.0	0.0
PD1_A07H	PD1_A07H	On	0.00561	-2.00 to 2.00	V	Single-ended	12.5 ms	1.0	0.0
PD1_A08L	PD1_A08L	On	0.01837	-0.6250 to 0.6250	V	Single-ended	12.5 ms	1.0	0.0
PD1_A08H	PD1_A08H	Off		-0.3120 to 0.3120	V	Single-ended	40 ms	1.0	0.0
PD1_A09L	PD1_A09L	On	0.022568	-0.3120 to 0.3120	V	Single-ended	12.5 ms	1.0	0.0
PD1_A09H	PD1_A09H	On	-0.000567	-0.3120 to 0.3120	V	Single-ended	12.5 ms	1.0	0.0

Figure 77: Personal DAQ view, GUI for DAQ [40]